6-2019

Assessing Infrastructure Elements using Automated Object Detection Technique in Smart City Applications

Majid Mastali
Western Michigan University, mastali.majid@gmail.com

ASSESSING INFRASTRUCTURE ELEMENTS USING AUTOMATED OBJECT DETECTION TECHNIQUE IN SMART CITY APPLICATIONS

by

Majid Mastali

A dissertation submitted to the Graduate
College in partial fulfillment of the requirements
for the degree of Doctor of Philosophy
Civil Engineering
Western Michigan University
June 2019

Doctoral Committee:

Jun-Seok Oh, Ph.D., Chair

Osama Abudayyeh, Ph.D.,

Alvis Fong, Ph.D.

DEDICATION

To my wife, Elnaz, and my parents.

ACKNOWLEDGEMENTS

First and foremost, I want to sincere thanks my advisor Prof. Jun Seok Oh, the chair of my dissertation committee, for his fundamental role in my doctoral work. Dr. Oh provided me guidance and assistance, without whom I may never have discovered my passion for data processing. His supervision and guidance helped me in all the time of my research work to the success of my work.

I would also like to specially thanks Prof. Osama Abudayyeh, my dissertation committee member and chair of Civil and Construction Engineering Department, for his kind and supportive remarks, which always made me feel comfortable all the time of my research work. I would also like to thank Dr. Alvis Fong, my committee member, for his guidance and valuable comments in my research.

I am deeply thankful to my family for their love and support. I would also like to acknowledge and thank my brother and Tolu for helped and guidance when I needed, and my wonderful sister for her support. I would like to thank my parents, which would not have been possible for me to complete my study without their relentless prayer and support throughout my study. I don't have enough words to thank my wife for her understanding and unconditional support throughout my study. She has been there many times with all ups and down.

I would like to acknowledge the U.S. Department of transportation (USDOT) and Transportation Research Center for Livable Communities (TRCLC) for their financial support.

Majid Mastali

ASSESSING INFRASTRUCTURE ELEMENTS USING AUTOMATED OBJECT DETECTION TECHNIQUE IN SMART CITY APPLICATIONS

Majid Mastali, Ph.D.
Western Michigan University, 2019

Nowadays, road features are becoming more complex leading to more complicated complaints regarding urban environments. Point Cloud Data (PCD) processing is an essential element for detecting objects and analysing human driving behavior to identify the variables defining challenging objects and maneuvers in smart cities. PCDs include a range of processing, including indirect processing (e.g., data converting, cleaning process) and direct process (e.g., pass through elevation filter, statistical outlier removal, normal estimation as well as classification).

Static and dynamic object detection and analysis are typically considered the most sophisticated options subsumed under PCDs. They involve direct evaluation of both static and dynamic objects of maneuvers variables for people who use the road with and without a vehicle in line with American with Disability Act (ADA) and trajectory variables of passing distance law for challenging scenarios.

The results of point cloud data evaluations allow government agencies to provide communities with the information necessary to strategically plan transportation infrastructure improvements for people using roads and sidewalks. This two-part study identifies the essential components of sidewalk evaluation, and driver behaviors and reports the degree to which object and driver analysis are aligned with the expert recommended components of the ADA and passing distance law.

The first study explores the feasibility of using both terrestrial laser scanner and open source processing algorithms to develop an approach to automate the evaluation of the alignment of transportation infrastructure with public rights of way. In the second study, a new approach of LIDAR data processing is developed to determine the speed and distance of vehicles approaching and entering the passing zone for bicycles. The model develops a technique for analysing the motorist passing behavior in the natural driving environment using the data collected from real vehicle and bicycle maneuvers.

TABLE OF CONTENTS

Table of Contents—Continued

Table of Contents—Continued

LIST OF TABLES

List of Tables - Continued

LIST OF FIGURES

List of Figures - Continued

List of Figures - Continued

List of Figures - Continued

List of Figures - Continued

1 INTRODUCTION

1.1 Overview of the Study

Government agencies have made attempts to employ remote sensing to detect and analyze static and moving objects to provide communities with the information necessary to strategically planned transportation and infrastructure improvements for individuals using roads and sidewalks. High-resolution data could be a primary source of data for many complex dynamic urban environments. A high-resolution dataset not only can be used to extract and assess static objects such as sidewalls but also can evaluate vehicles passing maneuvers. Remote sensing sensors such as Light Detection and Ranging (LiDAR) and laser scanners can be adopted as an integral component in an accurate measurement and assessment process.

LiDAR and laser scanner sensors supply a high-resolution source of data which can synchronize and generalize data with an Inertial Measurement Unit (IMU). The LiDAR continuously measures and captures the data and integrates data with the IMU. Detecting and generalizing the complex objects and maneuvers can be enhanced using LIDAR and laser scanner in point cloud data (PCD). Mobile and static objects such as sidewalks and vehicles can be detected and evaluated in PCD shaped by three-dimension LIDAR and laser scanner information. Furthermore, the LIDAR data also provide an opportunity to track the speed and distance of motorists and bicyclists while passing maneuvers; however, laser scanner data mostly can be used to detect fixed objects such as sidewalk, curbs, and ramps.

Remote sensing analysis is beneficial; however, it generates big size data. Manual object extraction and evolution is time-consuming; therefore, automated algorithms are essential in the trajectory detection process. A comprehensive set of data would help the city officials in utilizing the interaction of static and mobile objects features. The accessibility of individuals with

disabilities has been taken into consideration, whereas the focus was on the assorted variables, including topography (ramps, slopes), accessible routes, curbs, alternate routes, boards, signage, facility maintenance, social barriers, and access to the public transportation services such as buses or taxies.

1.2 Scope of the Study

Object detection, clustering, and analysis are significant factors in analyzing the behaviors of drivers, bicyclists, and pedestrians. This dissertation addresses the static and dynamic object detection problem using LiDAR and Laser Scanner. Laser scanner data was analyzed to provide facilities for individuals with a disability in accordance with the ADA regulation. Obje To some extent, autonomous vehicles must have a comprehensive algorithm to detect and analyze obstacle detection, recognition, and analysis. They must also examine vehicles and bicycles as well as infrastructure elements such as sidewalks, ramps, and curbs. Laser scanner as a fix scanning device produces massive point cloud data with high accuracy, which can be used to detect fix and complex objects such as ramps and curbs. LiDAR can be used as fixed and moving devices, which supplies point cloud data with a smaller number of points and is most efficient in object detection.

The methods proposed in the present study focused on point information for laser scanner data as well as point and pixel information for LiDAR data classifications. For object detection in both LiDAR and laser scanner, PCD point based detection is common in order to use point information-based detection. In LiDAR data processing, however, pixel boundary is used to limit the object's relevant points. After detecting and recognizing objects in laser scanner data, objects will be analyzed based on the ADA regulation. Moreover, with the detection and recognition of objects in LiDAR data, the driver's behavior toward objects in different frames can be further

distinguished.

Operating speed and moving vehicle speed, as well as moving distances, further impose requirements on maximum detection distance and reading frequencies. In LiDAR data processing, detection box was developed to analyze the driver's behavior. Detection box was limited to 18ft longitude and 33ft in latitude distance from the LiDAR. A semi-automated method was developed to meet the object tracking requirements.

1.3 Americans with Disability and Limitations

Individuals with disabilities have rights, according to the movement laws to defend their equality with all society members. The Americans with Disabilities Act (ADA) advocates for the rights of individuals with disabilities and provides excellent services for those with disabilities to live within the community. The ADA 1990 is a civil right statute, prohibiting discrimination against individuals with disabilities (Americans with Disabilities Act 1990, 1991). As a necessary step to provide accessibility under the ADA, the local public entities are required to perform inventories for their current facilities. Among other cases, the ADA requires access to the roadway paths such as sidewalks and curbs. The information developed through the inventory (or self-evaluation) process must be quantified and presented as a baseline so that the progress can be monitored and measured. The ADA Application Guideline (ADAAG) is a primary set of laws dealing with the disabled individuals' needs for technical requirements in planning and designing, including the construction facilities tailored to the conditions of individuals with disabilities. The primary goal of this study is to provide an automated process solution as one of the fastest and securest ways of checking the accessibility of the existing facilities for ADA. Since there are numerous incentives to complete an ADA transition plan to act as valid defenses in ADA-related

legal actions, there have been a lot of measures adopted to foster more walkable, attractive, and livable communities. The overall completion of an inventory of the physical barriers can be a daunting task for municipal budget and staff constraints.

Stakeholders are responsible to provide accessibility for individuals with disabilities, particularly access to route facilities such as sidewalks and curbs. This includes individuals concerned with transportation and construction projects. In 2000, the analysis conducted by the US Congress showed that 20% of Americans have disabilities. Moreover, the number of individuals with disabilities increases as the population ages. Obviously, individuals with disabilities are more concerned with the use of public facilities, especially sidewalks (Kockelman et al., 2000).

A series of demanding compliances are required to evaluate the facilities at various levels. New constructions need to consider ADA or ADAAG and the Uniform Federal Accessibility Standards (UFAS) (as long as it is applicable) in the design and construction phases (Kockelman et al., 2000). For the existing facilities, however, the ADA requirement checklist needs to be observed. The ADAAG provides a list of the vital features to be checked in numerous steps from planning to construction in the new and existing transportation and construction projects. On the other hand, the conventional methods of checking the roadway facilities are usually time-consuming and costly, and it is hard to maintain the facilities in a convenient timeframe (Ai & Tsai, 2016). The most essential guideline regarding the accessible design is the UFAS, which should be observed in all construction phases (Steven Winter Associates, 2017).

ADA is one of the first comprehensive civil right laws to support individuals with disabilities and to protect them against discrimination imposed by their disabilities. The ADA is divided into five sections addressing different areas of public life such as employment, programs,

and activities of state and local government entities (design criteria for the environment, transportation, communication, medical diagnostic equipment, and information technology), private entities considering the places with public accommodation.

As a necessary step to provide the accessibility under the ADA, the state and local entities are required to evaluate their current facilities according to the accessibility requirements of this act. Further, these public entities are required to develop a transition plan, which describes the accessibility act for non-compliances within the public right of way. Accordingly, the accessibility act of non-compliances will be modified, scheduled, budgeted, and monitored for progress and compliance. The evaluation process for accessibility can help communities to solve problems and leads to positive changes benefiting those with disabilities (Jacobs Engineering Group, 2009).

In the long term, improving the accessibility for individuals with disabilities may reduce paratransit demand response services. Enhancing accessibility is especially important in terms of the high costs of demand-response transit services (which can be four times as much per as fixed-route bus service (Fei & Chen, 2015)) and aims at a rapidly growing older and limited mobility population. For instance, the US Census Bureau estimates that 19.5% of the Michigan population will be 65 and older by 2030— 38.1 % increase in comparison to 2015—whereas the total population of Michigan is estimated to grow by less than 1% within the same period (State Population Projections by 2030, Michigan Department of Technology, Management, and Budget, 2016).

It should also be noted that improved accessibility via ADA compliance brings the benefits not only to individuals with disabilities but also to the whole community at a large scale (McCann, 2013). Recent investigations regarding transportation have revealed that the public

right-of-way accessibility brings a more livable community (Burden, 2000).

The ADA was passed almost unanimously by US Congress and signed by President George H.W. Bush on July 26, 1990. The Department of Justice was settled in Toledo, Ohio, where it was agreed to remove the barriers for individuals with a disability (Settlement Agreement Between the United States of America and Toledo, Ohio, 1999). Since then, the Disability Rights Section (DRS) of the Department's Civil Rights Division monitored several other local and state governments to develop technical assistance checklists. The checklists of local agents could be immediately used to become fully compliant with the requirements of the ADA (Project Civic Access Fact Sheet, 2018).

The above project now includes more than 222 settlement agreements with localities in all 50 states, including four Michigan communities (Burton [2004], Detroit [2004], Mount Pleasant [2001], and Muskegon [2010]). In most of these cases, the compliance reviews were undertaken for the Department's initiatives under the authority of Title II Section 504 of the Rehabilitation Act of 1973. Hence, the governments receive financial assistance from the Department and are prohibited by the Act from discrimination against disability. In other cases, reviews were undertaken in response to complaints filed against the localities in cases which the communities had inaccessible programs or facilities and lacked an up-to-date transition plan (CMAP, 2012).

The first step in preparing an ADA transition plan is to conduct an inventory of the existing physical barriers to accessibility (i.e., a self-evaluation process). Different deficiencies were frequently reported in an inventory of the pedestrian facilities in public rights-of-way, including sidewalks, pedestrian paths, and curb ramps, etc. The information developed through the inventory process should be quantified and presented as a baseline so that the progress can be

monitored and measured.

Since more compelling incentives for a comprehensive ADA transition plan are implemented, the completion of such a plan and the inventory of existing the physical barriers, in particular, can be a daunting task. The combination of budget and staff insufficiencies make the inventory process extremely challengeable to be completed. For instance, a survey sponsored by the National Cooperative Highway Research Program showed that the budgetary constraints on staffing and supporting ADA programs were significant factors to complete the tasks of the transition plan (Jacobs Engineering Group, 2009). As a result, many transition plans tend to stall in the inventory phase, either awaiting a full completion of self-evaluation activities or unable to collect data and develop priorities for remediation.

1.4 ADA and Technology

The explosion of new technology in data processing has changed the automated analysis and assessment conditions. This research presents a new-brand of algorithm analysis to assess the accessibility compliance of the current facilities based on the PCD analysis technique. A set of data points are needed as a database to begin the analysis. Raw data were collected in X, Y, and Z coordinates referring to PCD to represent the surface, which preserves the flexibility and accuracy within the new and existing transportation facilities.

1.5 Cyclist and Limitations

In 2016, the National Highway Traffic Safety Administration (NHTSA) reported more than 11 bicyclists being killed in a total of 2000 traffic fatalities from 2015 in the United States. In 2016, there were 840 bicyclists killed in traffic crashes, and this number had steadily increased from 628 in 2009. The numbers represent a 34 percent increase in accidents from 2009. Seventy-one percent of pedal cyclist's fatalities have occurred in urban areas. Additionally, more than 50 bicyclists were killed on shoulder/roadside, more than 33 of whom were killed using the bicycle lane. Kay et al. (2014) study show that motorists do not share the road fairly with the pedal cyclist (Kay. et al., 2016).

The detection and evaluation of the motorist and pedal cyclist's interactions are essential to facilitate a better understanding of overtaking in the metropolitan areas. Thus, the overtaking analysis of motorist and bicyclists is one of the main factors that could affect interactions. The set of speed and distance data for vehicles which overtaking bicyclists would generate a valuable dataset to be used in a micro traffic level analysis of the motorist and bicyclist interactions. However, the accurate speed and distance of overtaking measurements are vital for overtaking analysis; therefore, the feature data from bicyclists and motorists are needed to analyze different road types at the highest possible accuracy to have an overview of bicyclist and motorist interactions.

Transportation agencies are to use remote sensing to detect and analyze the trajectories of mobile objects' such as cars and bicycles to generate the bicyclist's perceived level of clearance. It is desirable to have an automated platform to detect vehicles and bicycle maneuver in order to measure passing characteristics based on the high-resolution datasets in the complex urban environment. Furthermore, high-resolution data could be a primary solution for many complex

dynamic urban environments. A high-resolution dataset can be used to extract and assess passing maneuvers automatically. Remote sensing sensors such as Light detection and ranging (LiDAR) and laser scanners can be used as an integral component in an accurate measurement and assessment process.

LiDAR technology supplies a high-resolution source of data which can synchronize and generalize data with an inertial measurement unit (IMU). LiDAR continuously measures and captures the data and then integrates data with the IMU. Detecting and generalizing the complex maneuvers could promote the use of the LIDAR data. Objects such as vehicles and pedestrians are extracting from data processing phases which are shaped by three-dimension LIDAR information. LIDAR data also provide an opportunity to track the speed and distance of motorists and bicyclists during passing maneuvers. Remote sensing analysis is beneficial; however, it generates big size data. Manually interrogating overtaking maneuvers information is time-consuming; therefore, automated algorithms are essential in the trajectory detection process. A comprehensive set of data would help city officials in utilizing the features of interactions between motorists and bicyclists such as bicyclists and motorists for the speed and distance analysis.

1.6 Cyclist and Technology

U.S. Department of Transportation (U.S. DOT) in 2003 introduced the vehicle-infrastructure integration (VII) systems such as remote sensing in vehicle and infrastructure communication systems to improve mobility and safety (Farradyne, 2005). Most recent remote sensing instruments can be employed to detect objects, make a classification, and provide tracking data. Data collection of advanced remote sensing instruments have been developed over time. LIDAR is classified as a high-resolution sensor that can operate to achieve the defined research goals (Antonellis, 2017).

For instance, A Velodyne V16 LIDAR can generate up to 600000 coordinate positions of the surrendering conditions. In addition, LIDAR has a 360-degree horizontal and a 15-degree vertical field of view (Velodyne, 2018). However, in the way of contrast individuals have an approximate front-horizontal view field of 210-degrees (Traquair, 1927).

Kidono (2011) defined light detection and ranging as a horizontally scanning laser scanner, which generates the point cloud data. The dataset generated by LIDAR provides high-resolution environmental perception opportunities. Remote sensing sensors such as the LIDAR and laser scanner which are usually set up in the stationary or mobile mode can supply a three-dimension dataset and would be used in the object detection procedure. The LIDAR produces an accurate measurement of object characteristics in the PCD environment. The point cloud data are used to extract different surfaces of the motor vehicles and bicycles in overtaking maneuver detections. There are many techniques to detect and measure objects in the point cloud data, including grouping methods or segmentation methods which are used in the first stage of this research. In a three-dimension trajectory detection method, data directly retrieved from LIDAR are converted to PCD. However, processing large sets of data such as point cloud data processing is time-consuming. An automated algorithm was developed to overcome the discussed limitations.

The LIDAR and laser scanner technology are affected by machine learning technique (e.g., autonomous cars and automated measurements) accompanied by many advances having been achieved in the field. In general, the integration of LIDAR data and machine learning techniques have brought many benefits to the users in terms of reducing the time consumption and increasing the accuracy of data processing. Many powerful algorithms have been developed for the classification and regression of the data such as the k-Nearest Neighbors (KNN) at least squares, k-Nearest Neighbors, and Support Vector Machine (SVM). Vehicle and bicycle feature detection

is a primary goal in this investigation. In object detection, the determination of a smooth and reasonable boundary is required to track the mobile objects.

Pucher's (2017) research showed that cycling is one of the most rapidly developing sustainable transportation modes (Pucher 2017); therefore, state agencies have become interested in providing a safe and comfortable bicycle infrastructure. Reviewing previous studies generally shows that geometric road information and speed limits can affect the drivers and bicyclists' behaviors considering different transportation's infrastructures (Evans et al., 2018; Parkin et al., 2010; and Mehta et al., 2015). Studies indicate that many states have passed laws to provide adequate clearance for motorists passing bicyclists when the drivers are overtaking a cyclist. According to this legislation, drivers must pass cyclists at a lateral distance of more than three feet (Burbidge et al., 2018). The interaction between speed and safe passing distance, however, is not empirically determined. Marco 2016 has broken down the behavior of drivers' overtaking cyclist in a 4-step model. These four steps encompass the vehicle approaching bicycle, steering away, passing zone and returning mode (Dozza et al., 2010). Moreover, different overtaking strategies considered in previous studies are the flying strategy, the accelerate strategy, and the piggy backer's strategy (Wilson et al., 1982).

This technology offers an integrated solution to implement complex issues in a sustainable way in megacities, called "smart cities." Smart cities use different types of technology to integrate all data and platforms to provide a higher quality of life (Van der Hoeven et al., 2017). Smart cities need to develop a bicyclist infrastructure monitoring system to provide safe and comfortable bicycle facility in order to increase the bicyclist's perceived level of comfort. Real-time data processing facilitates the use of big data (Malik et al., 2017). Smart algorithms play an important role in improving service quality through accelerating and coordinating data processing in smart cities.

1.7 The Impact of Measurement Equipment on an Analytical Process

Efforts have been made in developing the measurement systems that combine sensing technologies with a mobile platform to explore a cost-effective approach for data collection in the self-evaluation step. LiDAR is a survey technology that collects spatial information based on the distance traveled by a laser beam; thus, it is also called laser scanner. LiDAR is widely used in surveys and 3D model creation for many industrial sectors because of its high accuracy (i.e., millimeter level accuracy). In the construction industry, each project includes many different tasks, which could benefit from new visualization and automation measurement-interfacing techniques. Recent developments in terrestrial LiDAR, GPS, and inertial measurement unit provide the grounds to collect 3D point clouds with high frequency and accuracy, which in turn lead to high accountability and high quality of city model reconstruction and road feature extraction. Identifying accessibility compliance is the main goal of our attempts in developing an automatic analysis approach. The collected datasets need to be segmented to check the compliances. Each segment represents an object in the PCD.

PCD is used to generate a 3-dimension surface with particular coordinate information for each segment, which may be used in facility's evaluation process to analyze the accessibility of the new and existing public facilities for ADA compliance. The laser scanner is one of the most stable and accurate measurement equipment that can provide X, Y, and Z coordinates.

These scanners are significantly developing these days. In 2000, laser scanners could approximately collect around 1000 points per second, and they can now collect around a million points per second (Geosystems, 2017). This increase provides more precise and clear observation to record the surrounding environment.

In this research, a Leica C10 laser scanner with the capability of reading up to 50000 points per

second was used. Laser scanner collected point cloud data employed for surface modeling of as-built objects in an accurate mensuration of the objects (Argüelles-Fraga et al., 2013). Such laser scanner data is also widely used to detect static and moving objects in the fields (Sun et al., 2018).

In this research, a Leica C10 laser scanner was used, which can read up to 50,000 points per second. Laser scanner collected point cloud data has been employed for surface modeling of as-built objects for an accurate mensuration of the objects (Argüelles-Fraga et al., 2013). Such laser scanner data is also widely used to detect static and moving objects in the fields (Sun et al., 2018).

1.8 Object Detection in PCD

Nowadays, road features are getting more complicated, leading to more complex complaints regarding urban environments. Commonly, PCD produces a rich source of data, which needs to undergo a PCD processing to identify and detect the objects in the target. It is essential to extract objects such as edges, pedestrians, curbs, and ends from the PCD. Over the past few years, many efforts have been made for the detection of objects such as buildings, doors, etc. from the PCD (Wang et al., 2014). Cluster analysis, which is a massive PCD processing that contributes to the recognition of different naturally clustered groups or structures, is one of the primary methods for massive data analysis to detect objects. In other words, clustering can create a set of meaningful subclasses of data, which makes it easier to detect different objects (e.g., Curbs, Ramps) in comparison to the direct detection in the whole dataset (Ankerst et al., 1999). Figure 1 shows the PCD data processing that would be essential for high-level sensing tasks such as simultaneous localization and mapping to detect an object (Wang et al., 2003). Wang et al. (2003) evaluated a mathematical framework that integrated simultaneous localization and mapping to detect an object and to help with detecting and tracking moving objects.

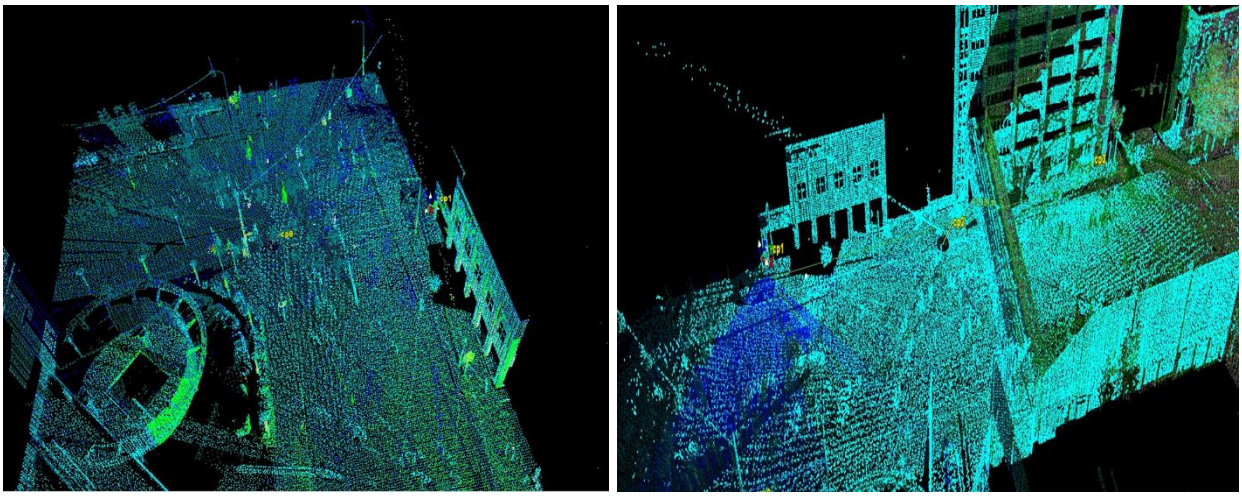

Figure 1 3D laser scanner point cloud data

1.9 The Role of Automation in the Analysis Process

The automation in accessibility assessment facilitates the realization of compliance through the following steps:

1. Conducting automatic data analysis and reviewing as the best practice, which allows more time for interpretations. It facilitates the federal or state agencies' self-evaluation process;

2. Boosting productivity through automation of the calculation process by using the algorithms, where the PCD processing would, otherwise, be time-consuming; and

3. Improving the efficiency and accuracy of ADA evaluation in the same way as most automated systems.

The manual evaluation methods faced different problems, which need to be considered in this automated method, including the classification of ground surfaces, intersections, cars, pedestrians, vegetation, poles, sidewalks, and construction options (Bisio, 2016).

Completely different scopes –like ground surfaces, intersections, cars, pedestrians, vegetation, poles, sidewalks, and building options—need to be considered in the automated method. Isolating the noise and eliminating the number of errors in the data and unnecessary points to layers is one of the foremost and vital benefits of the automated method. In addition to classifying planes and ground surfaces, it also extracts edges, pedestrians, curbs, and ends. The advantages of automated modeling and identification are significant. In scanning a public environment with many intersections and a thousand miles of sidewalks and curbs of various classifications and styles, the automatic identification and modeling would save the cost and time (Bisio, 2016).

1.10 Contribution of the Study

This dissertation presents several methods and approaches for Laser scanner and LiDAR-based fixed and dynamic object detection in a complex urban environment. One approach classifies point clouds from a laser to detect objects such as curb ramps and sidewalks, while another approach classifies point cloud data from a LiDAR to detect moving vehicles. The proposed methods and their experimental results are summarized in the following chapters. The presented data, collected data, and proposed approach in the urban environment to analyze fixed and moving objects encompass some contributions and novelties. This dissertation addresses two core problems in laser scanner and LiDAR-based object detection and analysis. The main contributions of this study are as follows:

- A multi-model dataset for static objects in accordance with the ADA regulation.
- An automated procedure to detect, cluster, and save object analysis and data
- A multi-corridor dataset for dynamic objects in order to conduct driver's behavior analysis.

A semi-automated procedure to detect, cluster, and analyze object analysis in order to produce trajectories and driver behaviors.

2 STATIC OBJECT DETECTION

2.1 Overview

The ADA 1990 includes the civil right laws that require the same general protection for individuals with disabilities as those given to other individuals on the basis of race, sex, national origin, and religion under the Civil Rights Act 1964. Ramps and curb ramps along accessible routes in public are required. These requirements are applicable wherever the sidewalks meet. The ADA intends to address all public facilities in the long term to provide services to the public. The public facility ought to be made accessible to individuals with disabilities through an endless unobstructed pedestrian circulation of networks. Therefore, once altered, most streets (except for rural roads associated with highways) need to construct an accessible pathway wherever possible (Pölzlbauer et al., 2012).

An accessible route is a roadway specifically designed to provide access for people with disabilities, including those who need a particular width and require passing areas for their wheelchairs or other mobility devices. The accessible routes are required wherever a circulation of ways is altered or designed. The allocation of the public facility to individuals with disabilities will contribute to cities and turn into various structures.

The main ADA checklist for the existing facilities includes:

1. Travel route, stair, stable, firm and slip-resistant, 36 inches wide, protruding into the circulation paths.

2. Ramps with a slope of 1:12 (i.e., one-inch height increases per 12 inches of the ramp). For a 1:12 slope, at least one foot of ramp length is required. Ramps longer than 6 feet (1.83 m) should have railings on both sides, railings sturdy. The railings should mostly be between 34 (0.86 m) and

38 (0.96 m) inches of height, and the width between railings or curbs must be at least 36 inches.

3. Parking and Drop-Off Areas should be 8 feet wide for the car plus 5-foot access aisle, 8-foot-wide spaces, with minimum foot wide access aisles, and 98 inches of vertical clearance available for lift-equipped vans).

4. Building Entrances (If there are stairs at the main entrance).

Table 1 shows the accessibility guidelines for accessible routes according to different regulations. The following values indicate the necessity of measuring different aspects of path accessibility.

Table 1 Accessibility guidelines for accessible routes

Source	Maximum Allowable Running Grade without Handrails	Maximum Allowable Running Cross Slope	Maximum Allowable Vertical Change in Level
ADA Standards for Accessible Design 1 (US DOJ, 2010)	5.0%	2.0 %	6.4 (mm) 

In Table 2, the guidelines for curb ramps for ADA and ADAAG are presented. The requirements for curb ramps apply just to the ramps that go through curbs or are constructed up to the ramp (Figure 2).

Table 2 Accessibility guidelines for curb ramps (CR)

Source	Maximum Slope of Curb Ramps	Maximum Cross-Slope of Curb Ramps	Maximum Slope of Flared Sides
ADA Standards for Accessible Design (US DOJ, 2010)	8.33 %	2.0 %	10.0 %

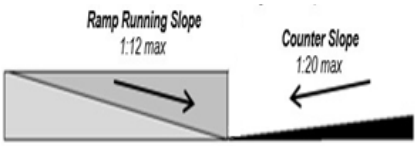

Figure 2 Curb ramps (CR) of the slope

According to the literature review, the accessibility for individuals with disabilities has been attended, whereas the focus has been on the assorted variables, including topography (ramps, slopes), accessible routes, curbs, alternate routes, boards, signage, facility maintenance, social barriers, and access to the public transportation services such as bus or taxi. In this research, a new-brand analysis technique is proposed based on unorganized PCD measurements. This approach can measure existing facility components by employing a Leica C10 laser scanner to scan the case study area. The automated algorithm will provide reliable analysis measurements and results for evaluating ADA compliance of the infrastructure facilities. This study aims to assess the reliable routes for those who need to have access and use federal or state roadway facilities through an automatic measuring technique for ADA roadway users.

2.1.1 Proposed Approach and Algorithm

Manually checking the compliance of roadway's infrastructures with ADA requirements is time-consuming, costly, and error-prone (Thi & Helfert, 2017). The primary aim of this study is to develop an approach and corresponding algorithms using the manipulated standard algorithm to automatically evaluate the compliance of transportation and construction infrastructures/facilities (i.e., ramps, curbs, and alternate routes) with ADA based on the analysis of the PCD. Detecting the status of route accessibility is essential in this analysis, which is carried out by analyzing quantitative features (e.g., width, depth, and the slope of curb ramps, and sidewalks) of the roadway infrastructure and comparing the results with the regulated requirements. A critical step in this research was to classify the infrastructure/facility components (e.g., for the curb ramp and sidewalk). In the present study, two significant steps were adopted: (1) detecting the normal surface of planes; and (2) segmenting the point cloud into separate datasets to represent potential objects. The following four steps describe the fully automated segmentation and tracking of transportation infrastructure:

Data acquisition and pre-processing: Scanning the environment with the laser scanner. The PCD data collected from the laser scanner is pre-processed by importing into PCD platforms (e.g., Microsoft Visual Studio, Cloud Compare, and Cyclone). PCD will be thus cleaned up and organized;

Data processing: In this step, the PCD data is filtered with respect to the point coordinates information, outlier removal (K-nearest point), and normal estimation;

Classification: Enormous information (such as points coordinates and colors) was captured in PCD by the laser scanner. After preprocessing and processing steps, PCD still has random objects,

which need to be classified based on their features. In this step, plane normal vector information was used to extract different surfaces such as roads, sidewalks, and ramps;

Feature extraction: PCD is classified based on the plane vectors. Each surface has some unique information used to classify objects. After such a classification, each object has geometric information such as slope, width, and length. This information was employed to analyze the ADA requirements such as sidewalk width or ramp slope.

A summary of the proposed methodology is depicted in Figure 3.

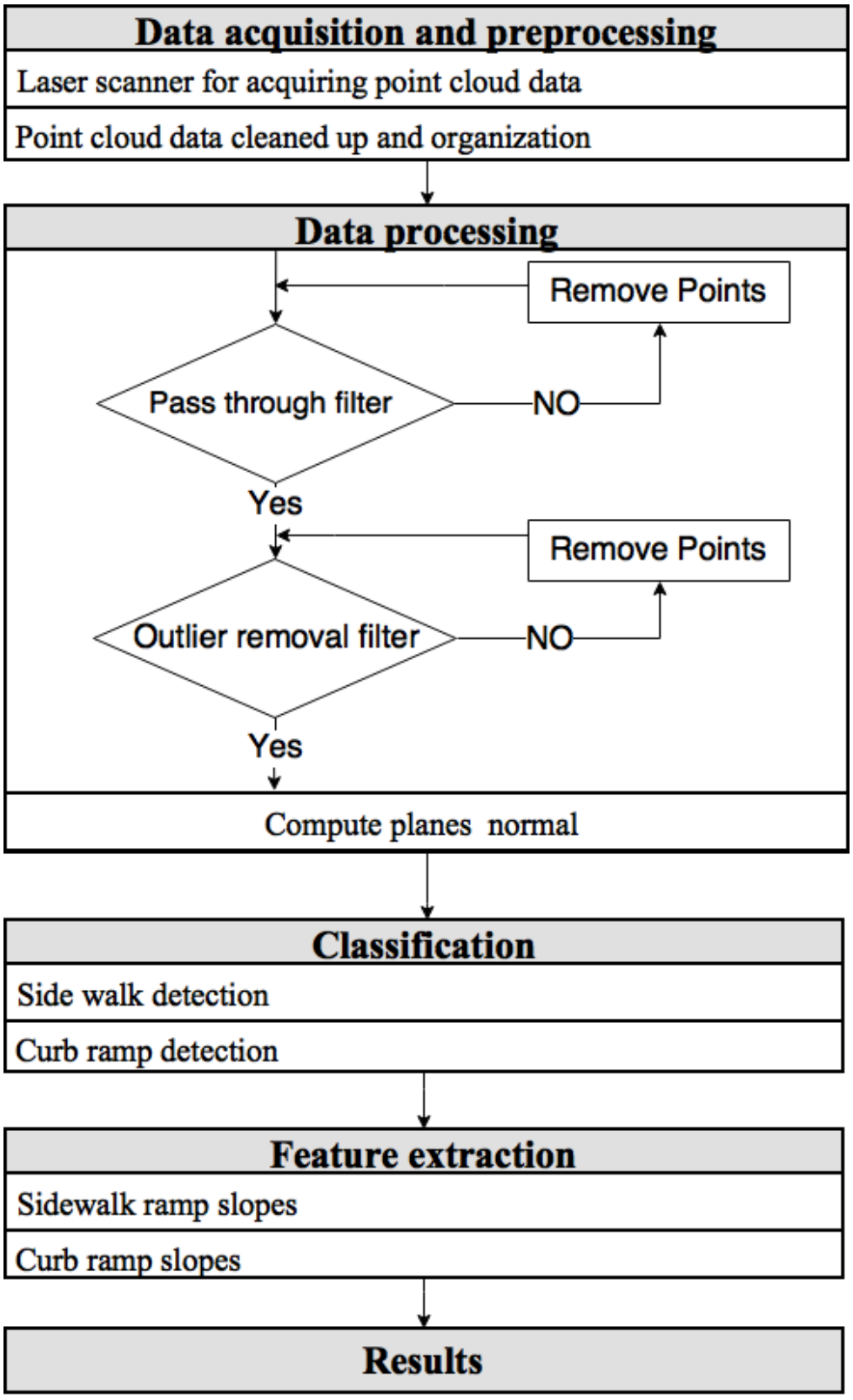

Figure 3 The proposed methodology

2.1.2 Data Acquisition and Pre-Processing

The laser scanner produces a large number of points with their coordinate information. In this study, about 70 million points were collected. High-quality data is required to process the PCD data (Rusu et al., 2008). An automated algorithm was developed in a preprocessing step to produce high-quality information, which improves the operational processes. Before any PCD processing (Figure 4), noises and errors need to be filtered (Figures 5 and 6) and then be organized as meaningful patterns.

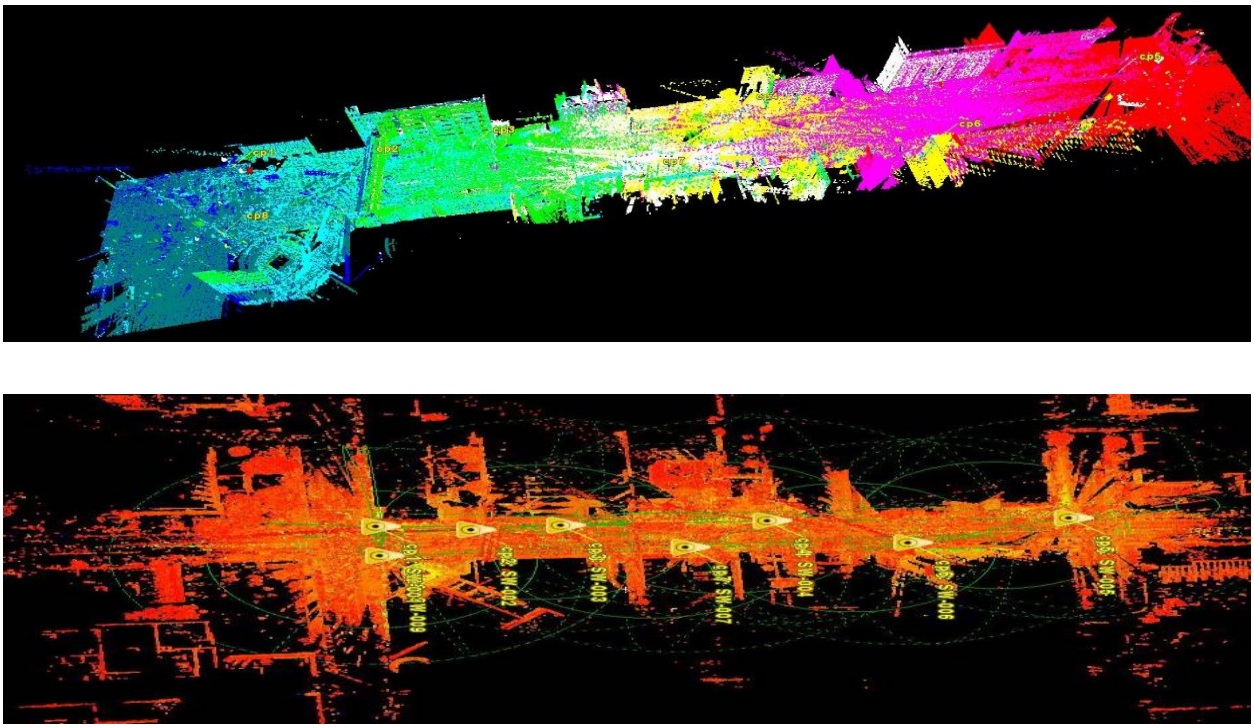

Figure 4 PCD before data processing

In the PCD data, each point contains X, Y, and Z coordinates along with its color intensity. Figure 5 shows the distribution of the points along the X, Y, and Z dimensions and the color intensity by individual points. The frequency of PCD error range in the point cloud data distribution is shown

in figure 6. Figure 6a illustrated X range point data distribution while 6b shows Y range point data distribution and Z data distribution has is presented in 6c. On the other hand, Figure 6d illustrate the color distribution of the point.

The plot matrix of the point cloud data distribution is shown in Figure 7.

X	Y	Z	Rf	Gf	Bf
-16.97142982	149.055542	-1.83205605	1	0.984314	0.694118
-17.40548134	149.3778076	-1.82924902	1	0.980392	0.537255
-17.02037239	149.3696747	-1.83608496	1	0.980392	0.94902
-31.09266853	153.6121979	-1.78347397	1	0.984314	0.156863
-31.22300339	152.2851105	-1.804775	1	0.984314	0.478431
-31.15230179	152.1466675	-1.80657601	1	0.984314	0.521569
-31.14230347	152.2229767	-1.80526304	1	0.984314	0.501961
-31.10012245	152.179596	-1.80596495	1	0.984314	0.439216
-31.11326408	152.1891937	-1.80572104	1	0.984314	0.513725
-31.11257935	152.2046509	-1.80541599	1	0.984314	0.247059
-31.00472069	152.0660858	-1.80657601	1	0.984314	0.321569
-31.05157852	152.0063629	-1.80816305	1	0.984314	0.290196

Figure 5 PCD X, Y and Z coordinates and color intensity (Red, Green, Blue)

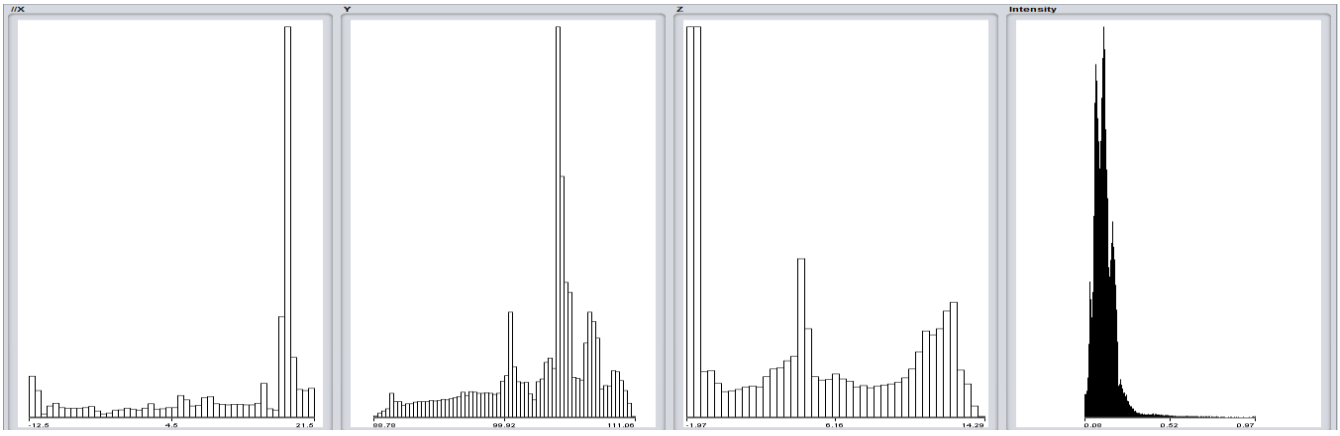

(a) (b) (c) (d)

Figure 6 PCD error range frequency

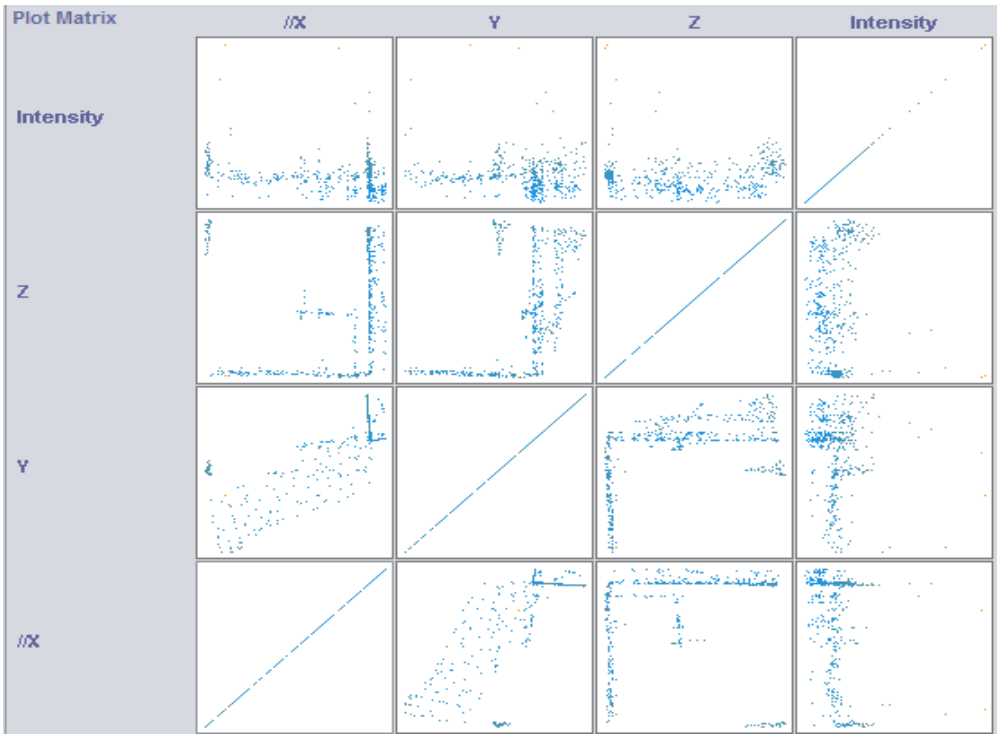

Figure 7 PCD plot matrix of the case study

2.1.3 Data Processing

After pre-processing the PCD, the information is ready to be used in the process and analysis steps. In the processing step, elevation and outlier removal filter was applied to the points to exclude the outlier by Descriptive Statistics method (e.g., mean and standard deviation) and to outrange the points based on their coordination information (Figure 8).

This step processes the PCD using normal estimation and data segmentation. In this step, the surface normal of planes is calculated by the point cloud data information. The segmentation of the PCD by normal estimation calculations would generate a compact representation for robust model fitting. This step has three subtasks: (1) passing through the elevation filter; (2) statistical

outlier removal; and (3) normal estimation.

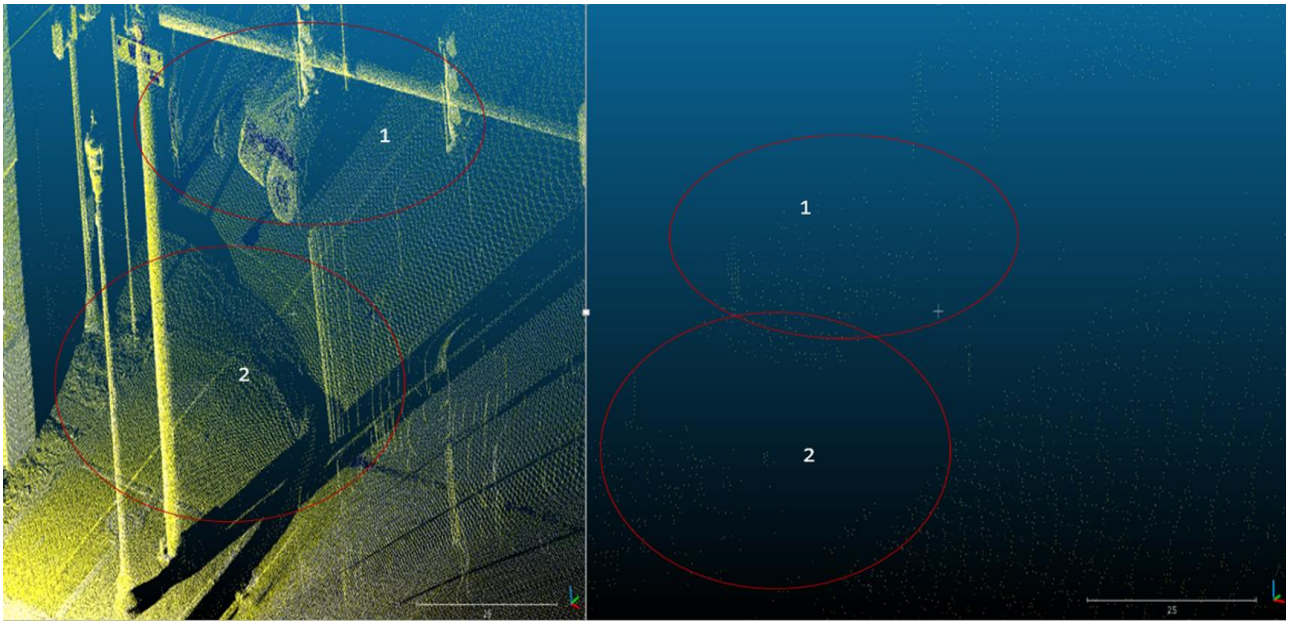

Figure 8 The effect of applied filters on point cloud data

2.1.3.1 Pass through Elevation Filter

The first step of PCD processing is to use a pass-through elevation filter to filter the points based on their assessment information (Z). The points placed beyond the boundary of the dense PCD environment were removed. In this case, those points required to build facades, trees, electrical poles, etc. were also removed. The boundary distance was set to be from ground zero to 6 ft.

2.1.3.2 Statistical Outlier Removal

The laser scanner generates point cloud datasets with varying point densities, which makes erroneous results if it is directly used to determine the normal surface as the points belong to different surfaces. This process is generally conducted in descriptive statistics, which can modify these irregularities by a variety of statistical methods such as the mean, median, and standard deviation. The sparse outlier removal is one of the most commonly used methods in normalizing the points in the PCD. The sparse outlier removal is computed by standard deviations (σ), sample distributions (S), and the mean values (μ) of the nearest neighbor distances (N) (OuYang & Feng, 2005). The distance (D) between points P1(x1, y1, z1) and P2 (x2, y2, z2) is calculated by Eq. (1).

$$D(P1, P2) = \sqrt{(x_2 - x_1)^2 + (y_2 - y_1)^2 + (z_2 - z_1)^2} \quad \text{Eq. 1}$$

The data will be trimmed if the calculated distance is out of the boundary $Z = \mu \pm \alpha * \sigma$. Aligned with the goal of this research, Equations (2) and (3) were used to normalize the PCD in this research.

$$Z = \mu \pm \alpha * \sigma \quad \text{Eq. 2}$$

$$\sigma = S/\sqrt{K} \quad \text{Eq. 3}$$

In this research, we have $\alpha = 1$ and $k = 100$ to provide the right balance between accuracy and efficiency in the proposed algorithm (Figure 3). As indicated in Figures 9 and 10, experiments

with multiple PCD segmentations from the collected PCD confirmed that μ ± σ thresholds would eliminate noise in PCD.

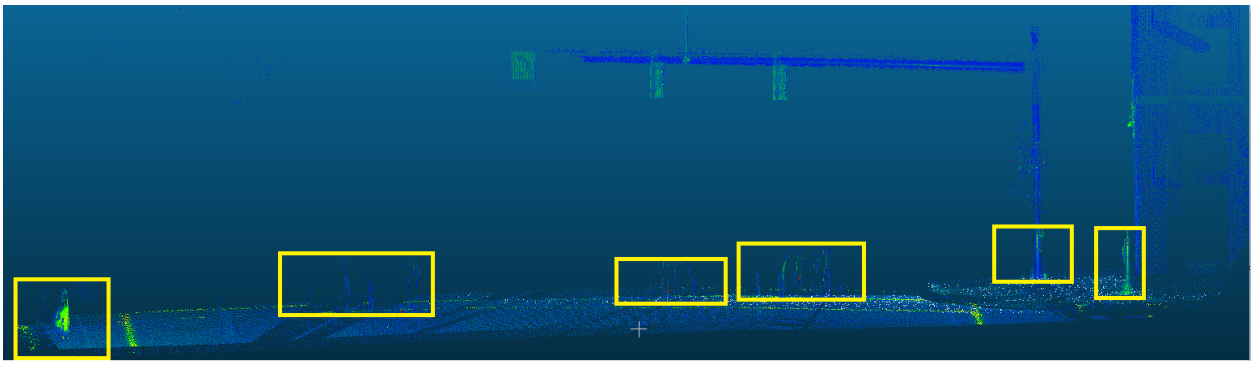

Figure 9 Noises and errors in PCD

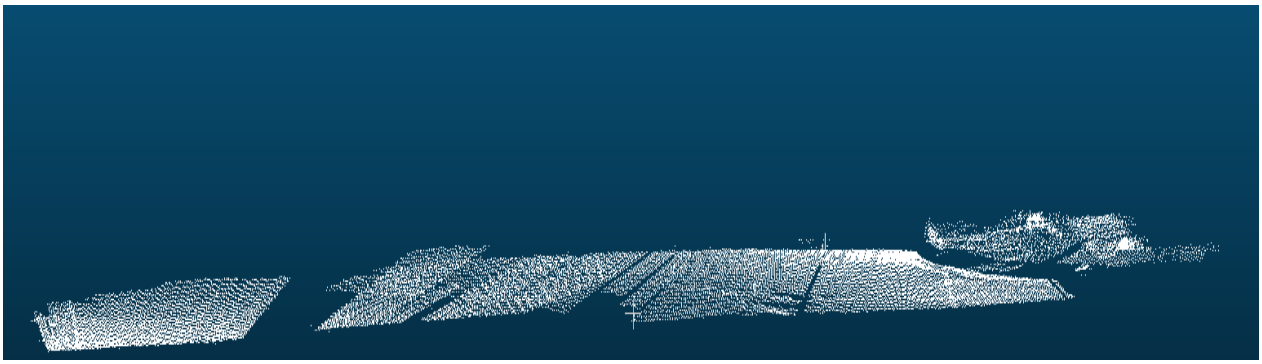

Figure 10 PCD after pre-processing

2.1.3.3 Normal Estimation

After a series of sequential steps such as pass-through elevation and outlier removal filter, the data were prepared to be processed for pattern identification and normalization. These steps prepare the PCD for planes/surface fitting. Planes/surface fitting is a process, through which the points would

fit in an estimated surface in the PCD with an angular direction. For angular direction estimation, 100 neighbor point needs to be calculated. Uniform PCD data have better estimation results of the normal vectors from the same surface compared to non-uniform data (Trevor et al., 2013). Figure 11 indicates the magnitude and direction of the vectors that describe the normal surface of planes. The left part shows the normal surface of planes fitted to non-uniform points in the PCD. The right part depicts the surface normal of planes fitted to the points using the normal estimation technique.

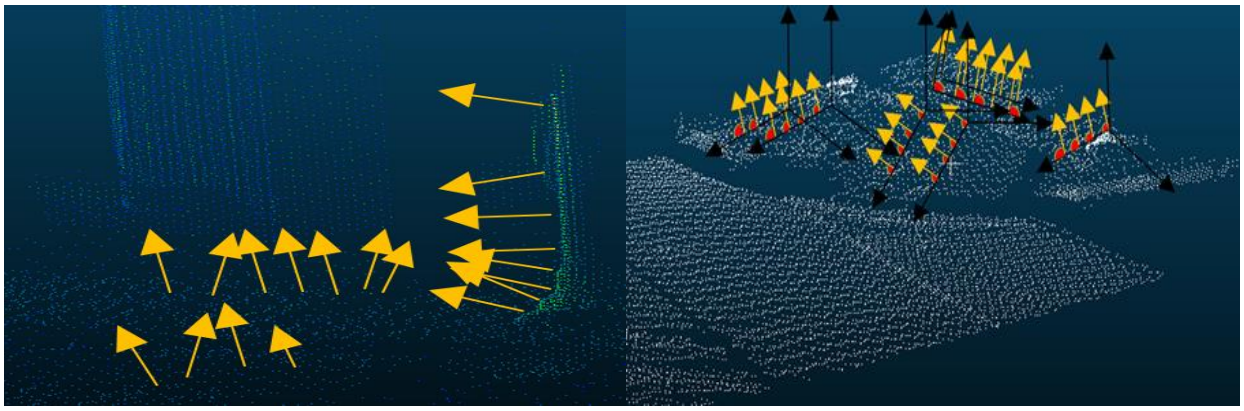

Figure 11 Non-uniform and uniform PCD after normal vector estimation

The ground plane is not to be recognized right after the data pre-processing. The proposed approach to detect the plane is to compute the plane equation for a set of data in Euclidean space. The plane equation was used to find the normal planes in the planar segmentation process. The hessian's normal form was employed to describe planes. Four coefficients of the plane are normal x, normal y, normal z, and the constant d shifts the plane so that it does not pass through the origin. As shown in Eq. (4).

$$ax + by + cz + d = 0 \quad \text{Eq. 4}$$

The equation for a plane with nonzero normal vector n= (a, b, c) through the point x0= (x0, y0, z0) can be described as a set of points (x, y, z) meeting the Eq. (4) in data processing (Hara et al., 2013).

2.1.3.4 Classification

The boundary points in the automated segmentation provide numerous benefits for the evaluation of road facilities such as the facility's edge detections (Miraliakbari et al., 2015). Boundary points make a higher accuracy in the plane normal calculation process in a massive PCD to detect objects with similar geometric information. For example, Miraliakbari (2015) successfully extracted a curbstone and road surface by using the jump detection method to detect height differences and height data histograms (El-Halawany et al., 2011). Using the elevation gradient with the normal surface of the local neighborhood can isolate the curbs from the rest of the objects in a scene (Fischler & Bolles, 2011).

In an attempt to improve the efficiency and accuracy of the classification step, an automated curb ramp and sidewalk detection method was established based on the plane vectors. Each plane has a specific angular direction, which produces a unique normal vector. The characteristics of the plane normal vector were used to extract each object automatically and to organize points. The points were organized according to their characteristics in different data sets for the further calculation process.

Several techniques (e.g., Naïve Bayes Classifier Algorithm, K Means Clustering

Algorithm, and Support Vector Machines Algorithm) can be used to fit a parametric model into the data (Wu X. et al., 2008). Random sample consensus (RANSAC) is selected to estimate the residual of the objects in a model based on the distance threshold (Veichtlbauer et al., 2011) because of the robust approach used in this method to estimate the matrix. In the algorithm, RANSAC was employed to determine if a point was an inlier or an outlier in an object.

Object segmentation is another step in our automated classification process. In this step, point cloud data are broken down into different objects based on their characteristics and contextual information about neighboring points. Figure 12 depicts the results of segmentation of the PCD.

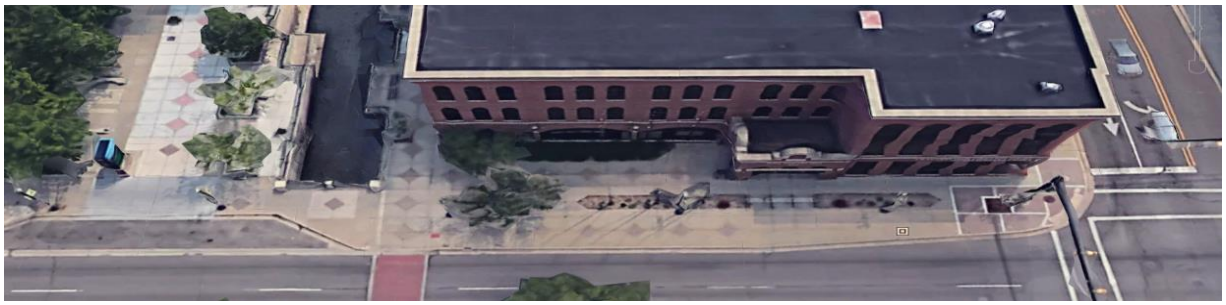

(a)

(b)

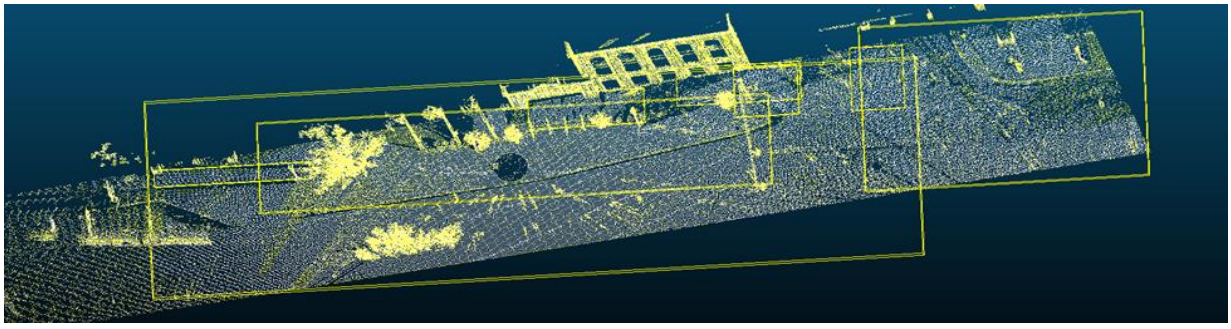

(C)

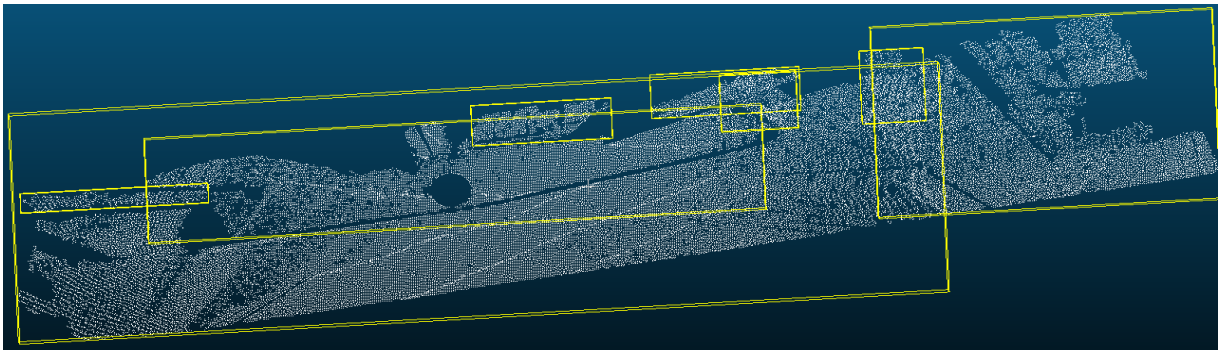

(d)

Figure 12 Sidewalk and ramp detection flow in the automated PCD (top view (a), front view (b), top PCD view (c), surface top PCD view(d))

2.2 Case Study for Static Object Detection

2.2.1 Overview

Individuals with different disabilities face different barriers to have access to public and commercial services (Park & Subeh, 2018). The Business district of Kalamazoo, Michigan, is a useful case study to investigate the disability barriers according to the ADA. The case considered in this study was located on Ross Street between West Michigan Ave. and East Kalamazoo Ave. in the downtown of Kalamazoo. This area is located in a business district with various public and commercial buildings (e.g., a museum, university campus buildings, public parking facilities, banks, and hotels), which cause high pedestrian traffic. It is a residential-commercial area with a wide variety of residents as road users (Figure 13).

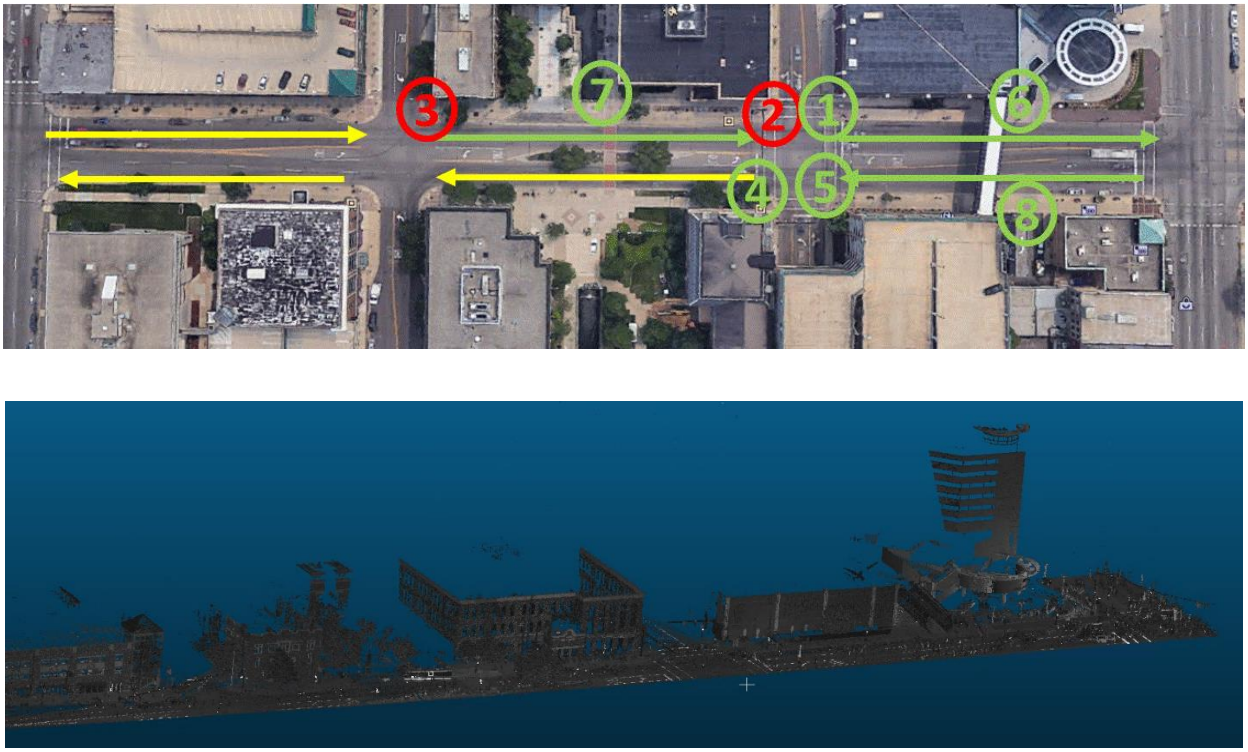

Figure 13 The bird-eye-view image of the case study area and its PCD (Green color passed ADA and red color rejected)

Some constraints affecting the data collection through laser scanning (e.g., the Leica C10 laser scanner used in this study scans 50,000 pts/s) were detected, and it took 2 to 5 minutes to finish each scan (Figure 14).

Figure 14 laser scanner in data collection

Moving vehicles and pedestrians may block the laser beams, while the laser scanner scans areas; therefore, the noise needs to be analyzed and removed from the PCD (Figure 15).

Figure 15 Laser scanner view image of the case study area (Sources of errors)

2.3 Data Collection of Static Object Detection

Bascom and Christensen (2017) showed that 70% of those with a disability need to balance their accessibility requirements with their life, indicating the significance of the measurement accuracy in their life quality (Bascom & Christensen, 2017). Through having accurate detection and analysis of sidewalks and ramps, automatic measurements of different object elements could subsequently be conducted. The experiment was conducted to assess the accuracy of the proposed approach. The sidewalk and curb ramp features (Figure13) were manually registered by measuring tape to obtain a ground truth for curbs and sidewalks. Tables 3 and 4 compare the results of two sets of object features detected for measurements. Tables 3 and 4 present the performance of the proposed algorithm for essential features of the sidewalks and ramps in the case of compliance checking.

Table 3 Comparison of the selected curb ramp slopes

Results of Curb Ramp Slopes			
Number	By manual measurements (%)	By proposed approach (%)	The difference (%)
1	8.17	7.99	0.18
2	10.42	10.21	0.21
3	10.42	10.60	-0.18
4	7.11	6.45	0.66
5	7.62	7.64	-0.02

Table 4 Comparison of the selected sidewalk slopes

Results of Sidewalk Ramp Slope			
Number	By manual measurements (%)	By proposed approach (%)	The difference (%)
6	1.23	0.95	0.28
7	2.00	1.67	0.33
8	1.14	1.57	-0.43

The proposed approach and algorithms were tested by different experiments with different curb ramp and sidewalk data sets. The measurements derived from the proposed approach were

close to the ground truth data. Checking the requirements of ADA regulations should be continued to ensure the accessibility of the public facility for the ones with limited mobility (Oh et al., 2017). As shown in Figure 13, the green color represents sidewalks and ramps meeting the ADA regulation, and the red color represents curbs not meeting the ADA regulations. Table 2 shows the results of the curb ramp slope data by comparing the physical measurements and the results obtained from the proposed automation method in five different ramps across the studied area. The mean absolute error of the selected curb ramps data is 0.22%, which indicates the accuracy of our proposed method. Three out of five selected curb ramps met the ADA requirements in terms of the maximum slope of curb ramps (8.33%).

2.4 Limitations in Static Object Detections

This study is one of the few investigations on the use of a comprehensively automated algorithm in assessing the compliance of roadway features with ADA. The primary motivation was to prepare a comprehensive evaluation method for the public infrastructure facilities (such as curb ramps and sidewalks) according to the ADA requirements. To achieve this aim, the PCD was collected by laser scanning. ADA maintains the design criteria for safe and accessible roadways for individuals with disabilities. Data acquisition and 3D modeling facilitated the evaluation process of the local facilities according to the ADA requirements. Point cloud data is a high-quality 3D modeling data collected by laser scanners.

Different research methods were used to investigate the accessibility checking. Alghamdi. et al. (2017) used a simulation technique to check compliance (Alghamdi et al., 2017) and Ai. et al. (2017) reported an accurate measurement technique of the sidewalk cross slope and grade by using LIDAR and camera data (Ai, and Tsai, 2016); however, they reported different appearance

challenging to implement a fully automated curb ramp extraction method, so they used a semi-automatic approach.

In the present research, an automated assessment methodology was proposed for ADA compliance to adopt various types of point-based measurement technology using LIDAR. Standard data format from these measurements are in the form of PCD, and this study addresses the steps to identify critical features that constitute ADA compliances of these measurements. Although a variety of sensors are available to measure different maneuvers, only a few sensors can provide comprehensive data.

2.5 Static Object Detection Summary

The PCD data is required to process and interpret various techniques to be used. Different data processing techniques such as normal estimation, surface fitting, and segmentation can be used to analyze and categorize road features. This helps the automated detection of road elements such as sidewalk and curb ramp, and the automated measurement of their dimensions, including slopes. We proposed a new approach to use LiDAR data to automatically detect different objects such as curb and sidewalk and calculate different object characteristics such as slope, length, and width. Experimental testing was conducted to evaluate the proposed technique in a real case study on Ross Street in Kalamazoo, Michigan. The results showed that the mean absolute error of the selected curb ramps data was 0.22% and this value was 0.13% for the sidewalks when compared to other manual measurements. The proposed method and algorithms were expected to help the local authorities in assessing their infrastructure facilities and identify accessibility problems based on the ADA requirements.

3 DYNAMIC OBJECT DETECTIONS

3.1 Overview

Nowadays, bike riding is considered as an expanding sustainable mode. Transportation modes are getting more sophisticated, particularly in megacities, and this leads to more complicated interactions between vehicles and bicycles; hence, it is necessary to generate a reliable design and plan to facilitate safe interactions between vehicles and bicycles.

Analyzing drivers' behaviors is one of the most important and critical topics in traffic engineering and management. The effect of the drivers' behaviors has been studied in a few different methods which were developed by other researchers. For example, Wang, et al. 2014 developed an instrument to measure the driver behavior in the different scenarios.

Most of the remote sensing techniques used for vehicle detection and vehicle tracking are based on fixed sensors installed along the roads (Yang &Rong, 2009).

Nonetheless, analyzing vehicle and bicycle maneuver is still exposed to many problems. An accurate analysis of data of the passing maneuver is critical to address the central problems of overtaking research. Safe interaction between cyclists and drivers consistently arises in a broad spectrum of real-life applications.

Most of the previous studies, for example, those by Dozza et al. (2016) _ and Debnath et al. (2018) only focused on passing distance as the main factors to analyze the vehicle overtaking trajectories. However, Sun et al. (2018) used LiDAR to analyze speed as one of the vehicle trajectory factors. As discussed, the drivers' overtaking a bicyclist behavior has long been studied; however, it has never been investigated in terms of highly accurate speed and distance. The speed and distance are

considered as important factors before and after the adaptation of an approach in vehicle-bicycle passing interactions. The data was collected from two and three-lane roads with or without a shoulder for the bicycle, which were equipped with a LiDAR. One of the significant limitations of the existing vehicle and bicycle feature analysis is access to the comprehensive database to be used for analyzing the data. The general concept of LiDAR object detection can be used to generate object features for the motor vehicle and bicycle trajectories after data processing.

In this study, a new analysis algorithm is presented to assess the speed and distance transformation of the vehicles approaching and entering the passing zone of the bicycles in the micro level transportation systems. Data collected from X, Y and Z coordinates that are referred to as PCD to represent the surface of objects in the transportation facilities. For the purpose of this research, the definition of data gathering and post-processing would involve complex calculation challenges. The entire recognition process was implemented by a single algorithm. The recognition process was implemented by a semi-automated point-wise classification process by using an adaptive neighborhood in the region of interest (ROI) within a complex urban environment. Points were classified as either vehicle or others, which would store vehicle information for further data processing.

According to the literature review, data processing methods and corresponding algorithms were developed to detect vehicles automatically. Most of the publications used data obtained from the controlled environments and did not consider the relationship between distance and speed measurements as overtaking-related parameters; however, our data collection method represents the real vehicle and bicycle maneuvers. In this study, there was a vehicle detection, and tracking based on the length, height, intensity and pulse reflections is developed to classify the vehicles and extract trajectories in order to analyze drivers' behavior.

Two significant measures were adopted to accurately evaluate and assess vehicles overtaking a bicycle: (1) detecting vehicles by preprocessing and processing raw data in this step from multiple sensors such as GPS and IMU to produce a point cloud information; and (2) segmenting extracted vehicles and then evaluating vehicles overtaking bicycle's characteristics data. At the same time, the region of the study was detected, and the data was extracted from the concerned study area. Based on our study, the objects are within the boundary are extracts and other data will be discarded. The details of our proposed method to accomplish the automated evaluation and extraction of vehicles overtaking a bicycle are shown in the following figure (Fig. 16):

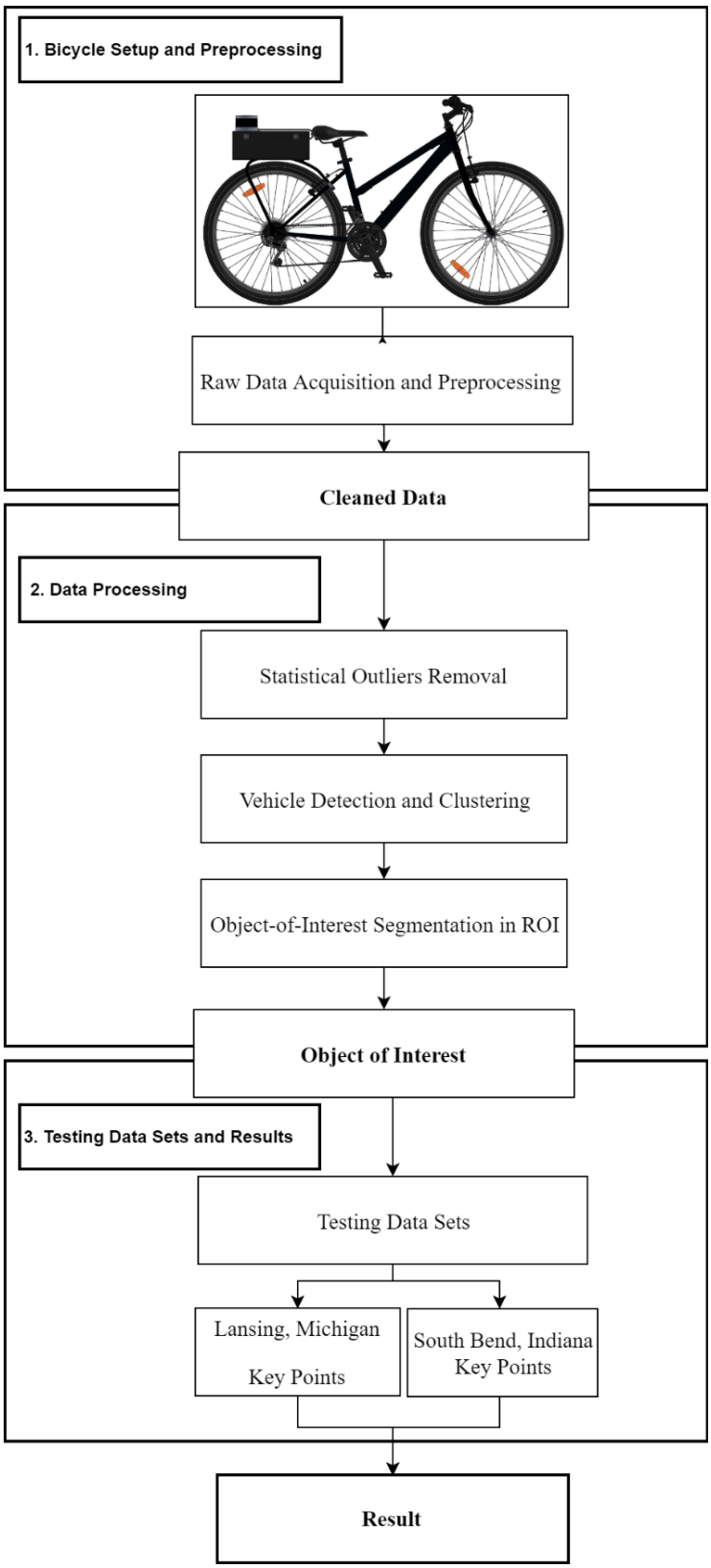

Figure 16 Proposed methodology flow chart

3.2 Raw Data Acquisition and Preprocessing for Dynamic Object Detection

The LiDAR sensor used in this study was Velodyne's VLP-16 model, and it was mounted on the back side of the bicycle. The LiDAR view is 360 degrees to be installed vertically on the bicycle. The LiDAR usually collected distance and reading deliver distance in a 3D point cloud environment.

Moreover, the LiDAR serves as a 3-dimension (3D) scanner recording the range and direction of each point around the bicycle. The LiDAR frame is a set of 3D point information about distance, integrity, and pulse. The 3D data information in the data frames allows the measurement of speed and distance. The LiDAR is a sensor which can generate up to 30,000 points with their coordination information in each data frame. Figure 17 shows a 3D data frame. In the frame, the X and Y respectively are the vertical and horizontal distance of the points from the LIDAR and Z is the height of the points based on the LiDAR height.

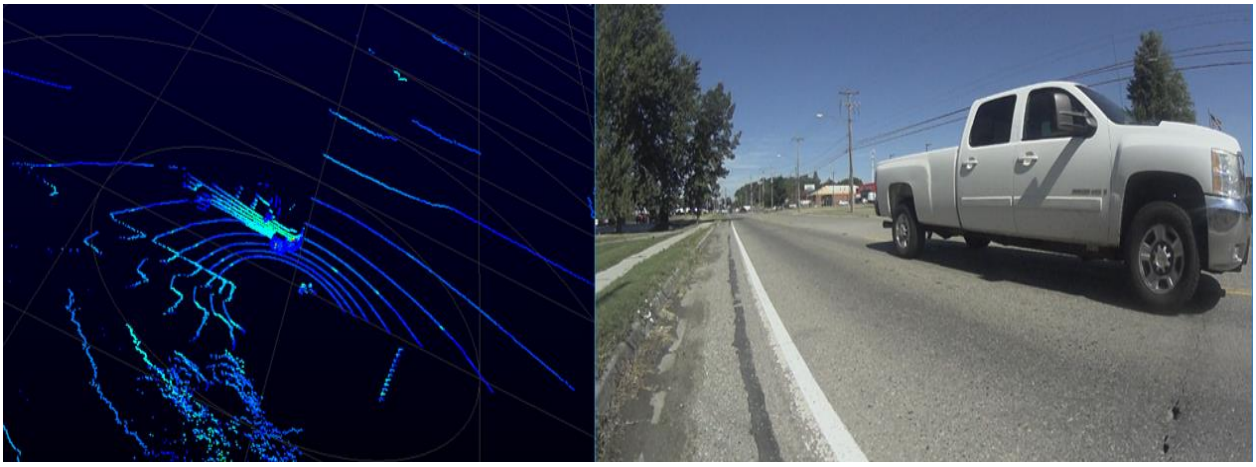

Figure 17 Raw data of a vehicle (left) and the camera view of the same vehicle (right)

The first step in drivers' behavior information analysis is to improve data quality. The first key factor considered in this study was a boundary limit for our Region of Interest (ROI). The second key factor was cleaning the noises and errors in this step to construct an automated algorithm to extract vehicle and bicycles trajectory information with high-resolution. Finally, the integrated data frames were in the format settled for the next step.

The LiDAR data was used to acquire data points from the object's surface such as the vehicle, trees, building surfaces, etc. When the outliers were removed, the objects such as traffic signs, trees, and others that are noise in our dataset should be filtered out within the range of 16 feet.

3.3 Dynamic Object Detection Procedures

3.3.1 Smart Segmentation in ROI (Statistical Outlier Removal)

When the dataset is clean, the noise and inconsistent noise data points near the Object of Interest (OOI) will be removed. This process is carried out by using a descriptive statistic method in a machine learning process. The sparse outlier removal is one of the most commonly used methods to trim data out of the research ROI dataset. This step is needed to calculate standard deviations (σ) and the mean values (μ) of the nearest neighbor distances (N) (NND) (Rusu et al., 2008). The object of the research in ROI it would define the dataset. Three main phases were executed to perform segmentation based on the existing ROI to define dataset. The first step was to limit the boundary based on timestamps in each LiDAR frame. The second step was to restrain longitudinal and lateral distance to the bicycles (X and Y dimension). And the last step was to have distance calculations. The distance (D) between the points was calculated by the following Eq. (1).

$$D(P1, P2) = \sqrt{(x_2 - x_1)^2 + (y_2 - y_1)^2 + (z_2 - z_1)^2} \quad (1)$$

Where, X, Y, and Z represent X-dimension, Y-dimension, and Z-dimension of the LiDAR (Bicycle), respectively. The following algorithm was also used in all steps.

If the distance between the points is taken from the boundary $Z = \mu \pm \alpha \times \sigma$, the obtained data is removed. In accordance with the research ROI, the following equation was used.

$$Z = \mu \pm \alpha * \sigma \quad (2)$$

$$\sigma = S/\sqrt{K} \quad (3)$$

In this algorithm, $\alpha = 1$ and $k = 100$. The experiment shows that the adoption of $\mu \pm \sigma$ eliminates the objects with the highest outlier properties.

3.3.2 Segmentation in the Time Stamp, X and Y Dimensions

The key point is to keep the information belonging to the vehicles in the segmentation process for each frame and to keep tracking the same segmentations in the following frames. The LiDAR scans and collects data for all surrounding objects such as trees, buildings, vehicles, bicycles, etc. In our complex urban environment, there were multi-corridors for the vehicles moving on one-way or two-way paths. In order to extract objects, it is thus necessary to exclude the points belonging to the vehicles moving in the opposite directions. Accordingly, the primary objective in the vehicle and bicycle trajectory detection is to define the ROI, which is a portion of a data-limited based on the road and vehicle geometry. In this study, the data analysis was run for the considered

area. Based on Dozza et al. (2016), the vehicles which maneuver more than 12 feet on the side of bicycle and 16 feet before and after leaving the bicycle are not significant in determining the overtaking trajectory of the overtaking vehicle (10). In the present research, a threshold distance was required to differentiate the points belonging to the other side vehicles. It is therefore assumed that vehicles pass the left side of bicycles and their longitudinal distance is less than 18 ft. In addition, the ROI was defined for a lateral distance of 33 feet, indicating that all points with distance above 33 feet are removed from the LiDAR (Figure 18).

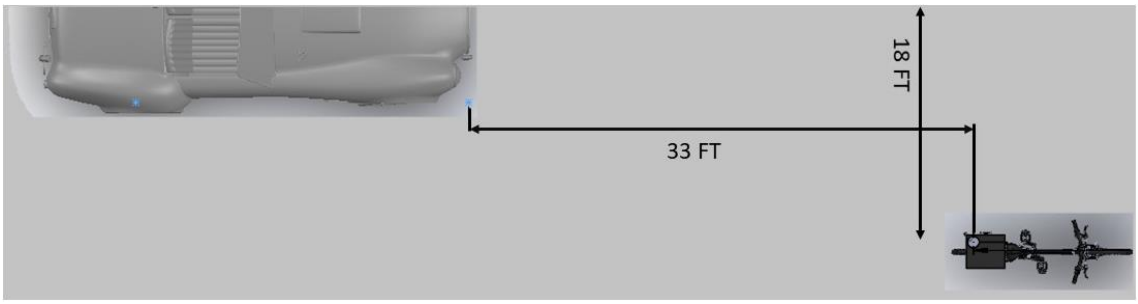

Figure 18 ROI schema for a vehicle trajectory detection

3.3.3 Vehicle Detection and Clustering

The general vehicle detection applications involved in developing an algorithm to filter out the noises clean unrelated objects automatically, build the models such as Random Sample Consensus (RANSAC), and finally assess the model in the format finalized for the ground plane detection and segmentation. In RANSAC, a mathematical model needs to be developed for each targeted surface. The data is explored using an iterative process to fit the object's surfaces. The RANSAC model was developed to analyze the relationship between various variables fitting the surfaces. These procedures should be adopted for each individual surface. Finally, each unfit surface is

removed from the dataset. Although this method works, it is time-consuming when applied to the big size datasets.

The authors present a new solution for processing the vehicle's surface detection in a high-frequency vehicle detection environment. In this phase, the author developed an automated method for mobile trajectory detection by using the developed algorithm. The LiDAR builds a 3-D map of an object's surroundings surfaces by firing thousands of laser pulses at a second. LiDAR fires laser pulses to collect the reflections from various target surface's density. Each surface has a specific density which can be calculated based on the laser pulses. Some surfaces such as vehicles, however, may return more or fewer pulses than the local density; therefore, each object's surface can be detected by calculating the pulse data (Watershed Sciences, 2009). The reflection time is measured for round-trip travel from LiDAR to the target surface by the laser pulse. Distance is also measured based on the flight time principle. Furthermore, surface angle and coordination information are measured and recorded in the data frames. Accordingly, data frames not only present surface coordination values, but also target the surface intensity, vertical angle, and other point attributes (Fernandez-Diaz et al., 2014).

In our proposed method, instead of a complicated mathematical model such as RANSAC, an algorithm was developed to extract and cluster object's range measures by using the vertical angles, distances, and the coordination of each vehicle's surface in the data frame. Figure 19 indicates the effect of the developed algorithm to detect vehicle processing in a noisy data frame. Furthermore, the developed algorithms help users to define another specific ROI in the detected object, as it will be discussed later.

The X- Y- T- I (X, Y dimension, timestamp, and integrity) plane was developed to divide the data frames into several small pieces. Each piece will be associated with one object; therefore, any other

point might also be removed. Since the number of objects in one frame is unknown and varying in different frames, the data frames should be broken down into the different regions with similar features such as distance and intensity.

Equation. 4 shows the relationship between the X- Y- I- T plane and the data frames.

$$(i, j) \leftrightarrow \{(X, Y, I, T), \left[\begin{array}{l} Y_{max} - j * \Delta y \leq y \leq Y_{max} - (j-1) * \Delta Y \\ X_{max} - j * \Delta X \leq x \leq X_{max} - (j-1) * \Delta X \end{array}\right], t=t_i\} \quad (4)$$

$$0 \leq I \leq 5$$

Where, (i ; j) show a piece of an object in the data frame; the sets on the right side of the curly brackets are the corresponding area in the X, Y, I, T space; Xmax and Ymax are the conversion range of the Y and X dimensions, which are set to be 33 and 18ft, respectively. ΔY is the length of the rectangular area, Δx is the width of the rectangular area, "I" is the integrity of the points, and ti is the timestamp of the corresponding LiDAR frame.

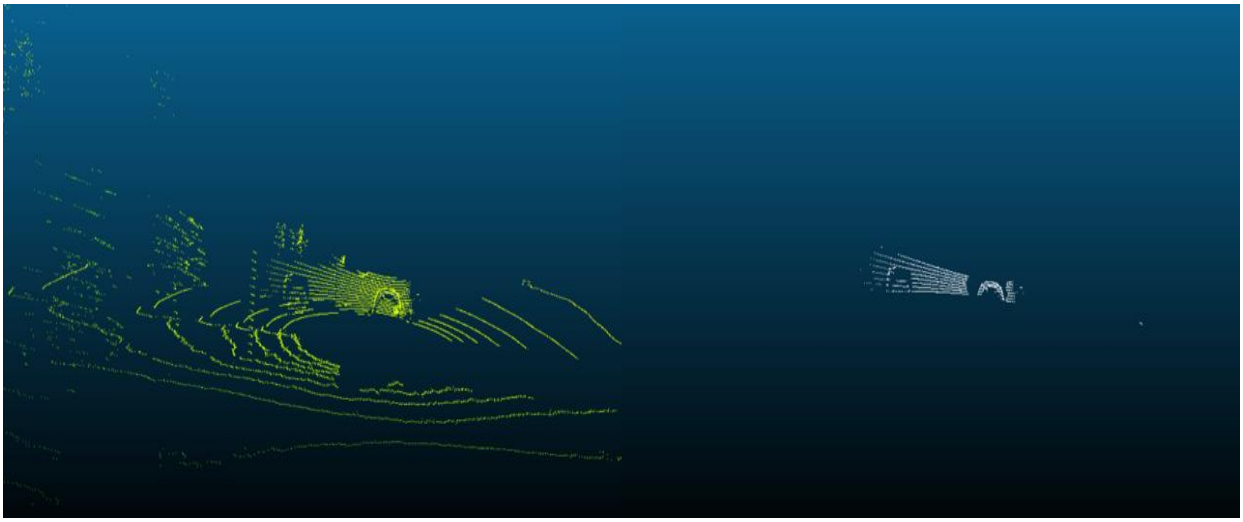

Figure 19 The results of the proposed method: noisy data frame (left) before processing and vehicle points (right) after processing.

3.3.4 Point Cloud Classification (Smart Segmentation in ROI)

The automated approach in point cloud classification was adopted in vehicle detection by measuring range data. Accurate identification of a vehicle approaching and entering the passing zone in point cloud is one of the most critical steps in vehicle trajectory processing. As discussed, the LiDAR produces a 3D point cloud of the surrounding objects, which is ideal for object detection; however, massive data filtering, as well as the cleaning of unrelated points in the data frames, are required to reduce the size of the data based on the research ROI boundary. Using our advanced algorithm, we managed to detect just vehicle information in 2016 for the National Highway Traffic Safety Administration in our ROI boundary. There was still a big size of datasets generated. In this step, we suggested a smart approach technique for the segmentation. The algorithm would limit the points to the detected part of the OOI in the ROI data frames to reduce the number of dataset points before bringing them into the analysis. The smaller size of the final dataset points would reduce the processing time through clustering the OOI to multiple segmentation and analysis just for the specific segments of the OOI in a data frame. The yellow boundary in Figure 20 shows the smartly detected segmentation of the OOI.

Equations 5 and 6 show the relationship between the object and the OOI.

$$\text{Strat maneuvering bicycle } (i, j) \leftrightarrow \{(D, t), D_i - D_j = Z, Z = \mu \pm \alpha * \sigma, \sigma = S/\sqrt{K}, t = t_i\} \quad (5)$$

where, (i; j) express a piece of an object in the data frame; D is the distance of the object from LiDAR and $\alpha = 1$ and $k = 5$. The experiment shows that $\mu \pm \sigma$ eliminates the objects with the highest heterogeneous properties.

While passing bicycle:

$$(i, j) \leftrightarrow \{(x, y, t), Y_{min} - j * \Delta y \leq |y| \leq Y_{min} - (j - 1) * \Delta Y, 0 \leq X \leq 18, t = t_i\} \quad (6)$$

where (i; j) express a piece of an in the data frame; ΔD is the distance of the object and Ymin is the conversion range of the Y-dimension; Δy is the length of the rectangular area and ti is the timestamp of the corresponding LIDAR frame.

Figure 20 shows the detected steps required for detecting a vehicle trajectory in different data frames. In Figure 20 (a), Vehicle (a) enters to the approaching zone of the bicycle. Vehicle (b) enters to the bicycle passing zone. Vehicle (c) passes the bicycle.

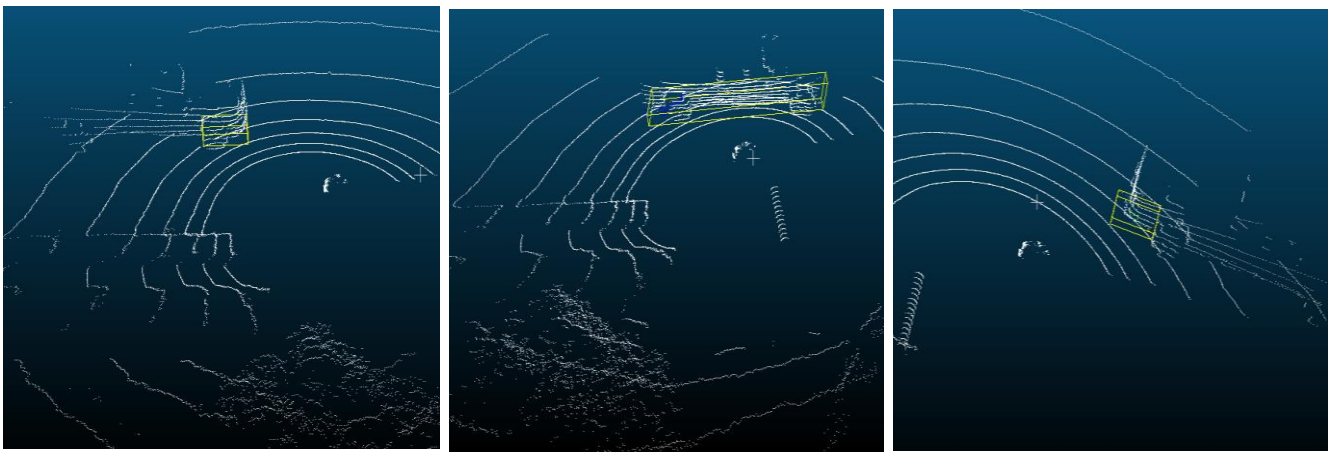

a b c

Figure 20 Smart detect at the Front-end of the vehicle (a) whole vehicle (b) and the rear-end of vehicle segmentation in ROI (c)

3.3.5 Overtaking Maneuver

According to Rasch (2018), overtaking and passing definitions are not the same. Overtaking is defined as any maneuver through which one vehicle passes another object such as a car or a bicycle when they are in the same direction. Rasch (2018) also notes that the overtaking maneuver is a special situation in the passing.

On the other hand, a driver passes a bicycle or a pedestrian or any vehicle which is in front of the vehicle either through increasing speed or traffic condition. Overtaking starts at the moment when a driver changes the lane and increases the speed to pass another object. Overtaking is completed whenever the vehicle moves back in the same direction in front of another moving object. The overtaking maneuver should occur in a sufficient longitudinal direction for a safe maneuver. Overtaking by a cyclist is dangerous because of different relative speeds. Different variables affect overtaking maneuvers scenarios, including geography conditions, speed limitation, vehicle speed, and bicycle speed. In the following section, we will analyze vehicle trajectories while passing a bicycle. Overtaking happens in five phases. The first phase is approaching phase, i.e., the driver observes a bicyclist and makes a decision about his next act. The second phase is steering away, i.e., the driver starts to change the speed and changes the lane. The third phase is passing, i.e., the vehicle is passing a cyclist at a higher relative speed. The fourth phase is steering back to the same lane and direction. The last step is to continue driving in the same path and direction. Our proposed algorithm can be used to accurately detect the trajectory to understand better human behaviors at different road conditions, including different lateral and longitudinal scenarios involving different speeds for both drivers and cyclists.

The key elements of overtaking are the time of observation of the cyclist which is related to the speed of the bicyclist and vehicle. Based on the proposed algorithm, all variables could be

extracted from LiDAR data object extraction at a high standard level.

3.3.6 Maneuver Detection in Time Series

As we discussed in the previous section, the maneuver information needs to be extracted from LiDAR frames. For the moving LiDAR, two speed needed to extract, Bicycle speed from IMU and vehicle speed which extracted from LiDAR Data. Vehicle speed and bicycle speed are not constant and change during the drivers and bicyclists' maneuvers. Moreover, the LiDAR can collect data at the rate of 5-10 HZ which altogether will contort the vehicle detection process in a complex urban environment with multiple objects at one frame. Speed of the bicycle will extract based on IMU information. Moreover, the distance between the two frames can be calculated via the following formula.

$$x_V = \sum_{i=1}^{n-1} (T_i - T_{i-1}) * V_i$$

Where, T and V represent the time differences between frames ith and (i-1) th and speed of the bicycle, and x_V is the bicycle's traveling distance during the data collection process.

3.4 Data Collection for Dynamic Object Detection

3.4.1 Overview

In 2016, the NHTSA report indicated that 58 percent of pedal cyclist's fatalities did not occur at intersections and that 71 percent of pedal cyclists' fatalities occurred in urban areas. The procedure of the developed algorithm was tested by the data collected at two cities with different road geometrics and speed limit information in Lansing, Michigan, and South Bend, Indiana.

3.4.2 LiDAR and Bicycle Setup

This research employs a bicycle equipped with different sensors such as LiDAR and GPS and a data acquisition system to integrate all data. To meet the data collection needed, a Velodyne LiDAR system was installed at the top of the case. The Sony X3000 4K camera was installed on the left corner of the case viewed passing motorists from it is concealed location within the case. The configuration of the system was not likely to attract the attention of passing vehicles as it was inserted within the typical outline of the bicyclist. The LiDAR, Sony camera, Garmin GPS receiver, and accelerometer equipment (SBG sensor) were all powered by a pair on onboard batteries (Figure 21).

Figure 21 LIDAR and bicycle set-up

The overall weight of the system installed on the bike was not an impedance to the rider and never impacted its normal operation. The resulting point cloud data was used to extract vehicles and analyze the drivers' behaviors. In addition, Table 5 shows more details of the devices installed on the bikes.

Table 5 LiDAR data setup package

Sensor type	**Sensor Name**	**Data Provided**	**Resolution**	**Sample frequency**
LIDAR	Velodyne V-16	Point Cloud	Angular resolution (vertical): 2°	5 – 20 Hz
Camera	Sony X3000	Video Frames	1920*1080 Pixel	30 fps
GPS	Garmin 18x LVC	Latitude and Longitude	1 MS	1 Hz

3.4.3 Data Validation for Vehicle Detection

The experiment was conducted to evaluate the accuracy of the proposed method. The overtaking distance was manually measured by using a fixed measuring tape to obtain the ground truth for the overtaking distance.

The proposed method and algorithms tested in the experiments by using different datasets and 28 vehicles passing distances, which were measured manually and compared with the database. The measurements derived from the proposed method were close to the ground truth data.

Table 6 LiDAR data collection package

Measuring Results				
	Number of samples	**Mean**	**standard Deviation**	**Standard Error**
Manual Measurements	28	68.18	20.98	3.96
C3FT	28	64.54	19.29	3.65
Proposed Method	28	69.79	21.01	3.99

Table 6 shows the results of overtaking pass distances for the vehicle and bicycle data, obtained from physical measurements and C3FT. The results were obtained by using the proposed automated method for 28 different interactions. The standard error of the overtaking test distance data was 3.96 inch for manual measurements, 3.65 for C3FT, and 3.99 inches for the proposed method, indicating the accuracy of the proposed method.

3.5 City Selection

Study areas should be selected based on different factors such as population, number of bicyclists, the traffic condition, and passing distance regulations. Different cities were analyzed, and two cities were selected: Lansing in Michigan, and South Bend in Indiana. During the data collection period, South Bend had passed 3 feet passing distance law but not Lansing. Three different types of roads were analyzed: Roads with a bike lane, roads with a shoulder, and roads without bike lane and shoulder (Figure 22). In South Bend, even though, four types of roads were analyzed: roads with a bike lane, shoulder, and sharrow and roads without a shoulder, sharrow, and bike lane (Figure 23)

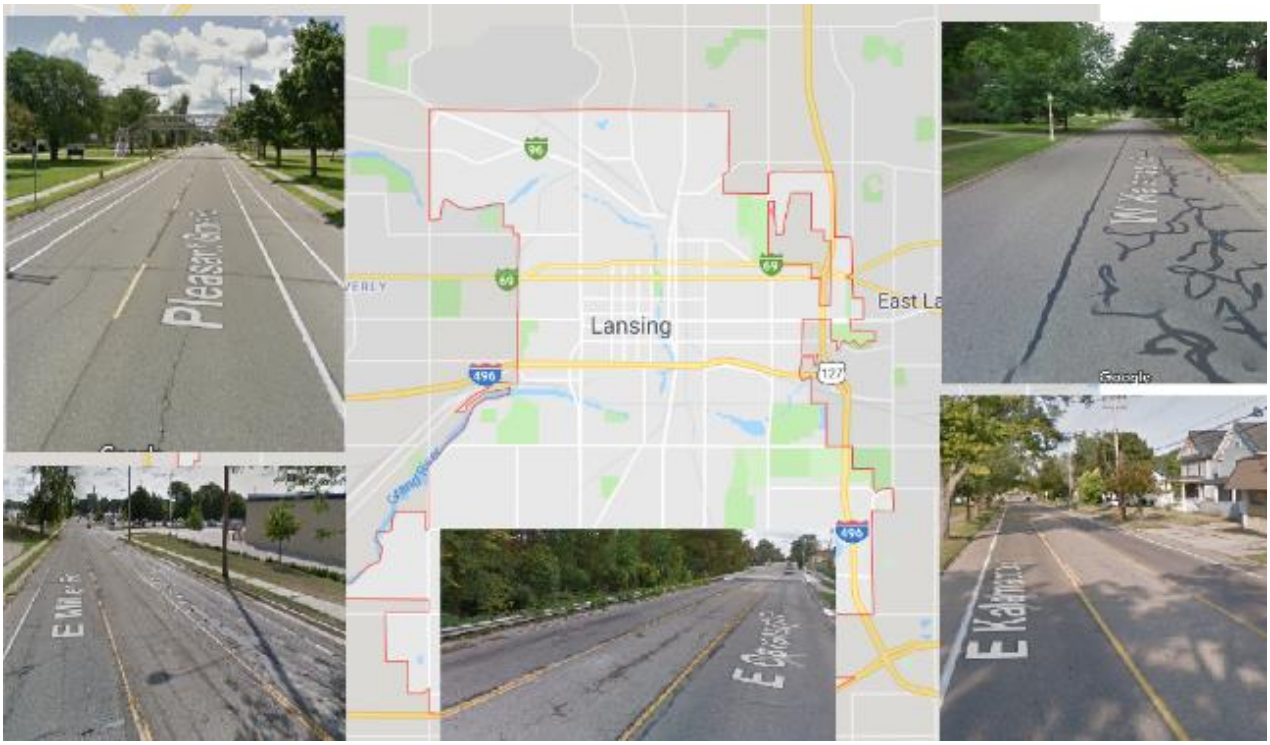

Figure 22 Selection of routes in Lansing, Michigan

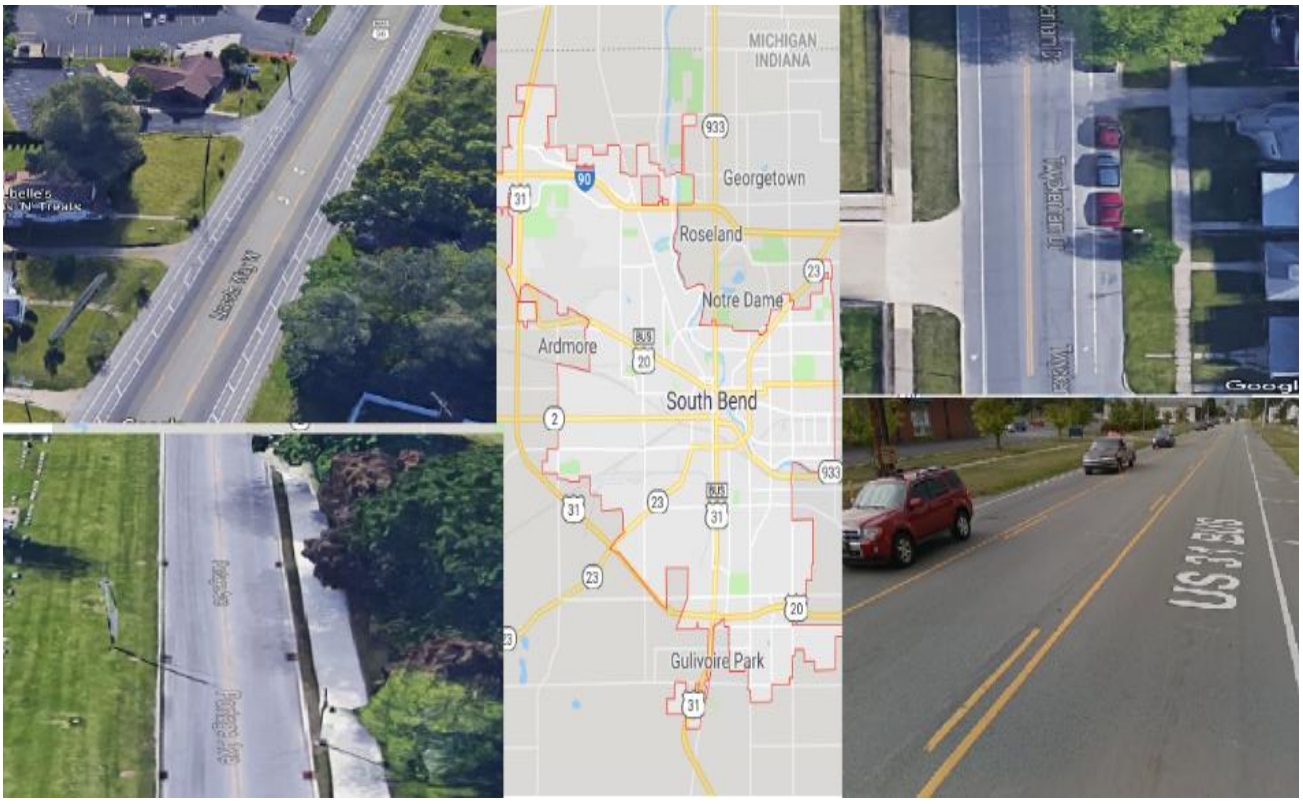

Figure 23 Selection of routes in Lansing, Michigan

3.6 Data Measured from LiDAR Data

After data collection, LiDAR data was processed by the proposed algorithm. Passing distance was detected for each individual vehicle, and 304,000 data frames were analyzed. A total of 830 vehicles were detected in the studied area. The data was limited to 12 feet from the bicycles. Table 7 shows a summary of the collected data in Lansing and South Bend.

Table 7 Bike speed data in approaching and passing zone

Feature	City	Road	Vehicle position	Mean	Standard Error	Median	Standard Deviation	Sample Variance	Minimum	Maximum	Count
Bike Speed	Lansing	West Kalamazoo	vehicle in approaching zone	16.09697	0.75514752	15.877	3.699452209	13.68594665	9.451035	21.35424	24
			vehicle in the passing zone	16.76843	0.528644908	16.731	2.589820559	6.707170527	12.54326	21.335853	24
		East Kalamazoo	vehicle in approaching zone	22.46351	0.492662187	22.9615	2.872689515	8.252345051	14.67552	26.982184	34
			vehicle in the passing zone	22.09692	0.535069989	22.2715	3.07374307	9.447896462	14.52422	27.672126	33
		Pleasant Grove Road	vehicle in approaching zone	20.35747	0.461408003	20.8657	3.915176731	15.32860884	9.564625	26.672857	72
			vehicle in the passing zone	20.29449	0.446687234	20.5449	3.790266866	14.36612291	9.583785	25.917294	72
		East Miller Road	vehicle in approaching zone	19.82562	0.348688913	20.1523	3.62368148	13.13106747	13.21844	26.839178	108
			vehicle in the passing zone	19.6091	0.349838714	19.9148	3.635630558	13.21780955	11.66567	27.661278	108
		East Cavanaugh road	vehicle in approaching zone	22.46351	0.492662187	22.9615	2.872689515	8.252345051	14.67552	26.982184	33
			vehicle in the passing zone	22.09692	0.535069989	22.2715	3.07374307	9.447896462	14.52422	27.672126	33
		Martin Luther king	vehicle in approaching zone	20.35747	0.461408003	20.8657	3.915176731	15.32860884	9.564625	26.672857	72
			vehicle in the passing zone	20.29449	0.446687234	20.5449	3.790266866	14.36612291	9.583785	25.917294	72
	South Bend	Lincoln Way	vehicle in approaching zone	23.02656	0.276817155	23.3932	2.299415982	5.287313858	17.04745	27.820289	69
			vehicle in the passing zone	22.83232	0.277011029	23.1144	2.301026428	5.29472262	16.46792	28.451266	69
		Portage Avenue	vehicle in approaching zone	21.77876	0.252647839	22.2974	3.361260877	11.29807468	12.6447	27.74256	177
			vehicle in the passing zone	21.47809	0.241428495	21.9388	3.211997217	10.31692612	13.49856	27.209239	177
		Twyckenham Drive	vehicle in approaching zone	20.08889	0.441718404	20.6549	3.721985432	13.85317556	3.377464	26.392604	71
			vehicle in the passing zone	19.89819	0.372395876	20.0825	3.137863425	9.846186877	12.63797	25.265304	71
		South Main Street	vehicle in approaching zone	21.7917	0.279628053	21.891	2.810227152	7.897376644	10.96991	29.388784	101
			vehicle in the passing zone	21.54958	0.276470937	21.6471	2.778498532	7.720054091	12.23766	27.334933	101

Table 8 Relative speed data between bicycle and vehicle in approaching and passing zone

Feature	City	Road	Vehicle position	Mean	Standard Error	Median	Standard Deviation	Sample Variance	Minimum	Maximum	Count
Relative Speed	Lansing	West Kalamazoo	vehicle in approaching zone	2.521711	0.185033669	2.49299	0.90647615	0.82169901	1.034215	4.712038	24
			vehicle in the passing zone	0.912393	0.065463483	0.89179	0.320704262	0.102851224	0.505319	1.776925	24
		East Kalamazoo	vehicle in approaching zone	3.105782	0.126052042	3.06291	1.241468633	1.541244366	0.198824	7.6882915	97
			vehicle in the passing zone	1.349377	0.063999833	1.29018	0.630325255	0.397309927	0.158005	3.0881332	97
		Pleasant Grove Road	vehicle in approaching zone	3.643323	0.164320981	3.63436	1.304257355	1.701087248	0.947404	7.4757806	63
			vehicle in the passing zone	1.553983	0.091880705	1.47639	0.729280487	0.531850028	0.321527	3.9480053	63
		East Miller Road	vehicle in approaching zone	3.303867	0.127377089	3.24468	1.323741537	1.752291657	0.486252	7.5653103	108
			vehicle in the passing zone	1.405616	0.078135222	1.27293	0.812005049	0.659352199	0.226835	3.6462416	108
		East Cavanaugh road	vehicle in approaching zone	2.491594	0.131965706	2.44308	0.769485681	0.592108213	0.907887	4.0738303	34
			vehicle in the passing zone	1.452196	0.115179275	1.37163	0.671604811	0.451053022	0.569581	3.5283833	34
		Martin Luther king	vehicle in approaching zone	2.380966	0.119065962	2.25286	1.010308187	1.020722632	0.593804	4.8222003	72
			vehicle in the passing zone	2.380966	0.119065962	2.25286	1.010308187	1.020722632	0.593804	4.8222003	72
	South Bend	Lincoln Way	vehicle in approaching zone	2.581997	0.148311256	2.34696	1.231965815	1.517739769	0.621568	7.4683926	69
			vehicle in the passing zone	1.381193	0.08146518	1.39923	0.676700604	0.457923708	0.221789	3.1065871	69
		Portage Avenue	vehicle in approaching zone	3.18115	0.127223177	2.90164	1.692594284	2.86487541	0.227838	9.2082363	177
			vehicle in the passing zone	1.821196	0.074532196	1.70617	0.991586379	0.983243547	0.266321	5.2057308	177
		Twyckenham Drive	vehicle in approaching zone	3.388507	0.155533128	3.37746	1.310545432	1.71752933	1.230526	7.5631084	71
			vehicle in the passing zone	1.435885	0.078163218	1.26315	0.658614978	0.433773689	0.407725	2.9098473	71
		South Main Street	vehicle in approaching zone	3.347146	0.152226135	3.20015	1.529853719	2.340452402	0.503352	8.1227046	101
			vehicle in the passing zone	1.575861	0.080008922	1.4363	0.804079713	0.646544185	0.12078	4.7939582	101

Table 9 Latitude distance data between vehicle and bicycle in approaching and passing zone

Feature	City	Road	Vehicle position	Mean	Standard Error	Median	Standard Deviation	Sample Variance	Minimum	Maximum	Count
Latitude Distance	Lansing	West Kalamazoo	vehicle in approaching zone	31.13492	0.246935572	31.3914	1.209732304	1.463452247	26.41919	32.382481	24
		East Kalamazoo	vehicle in approaching zone	30.22663	0.676535339	31.4478	6.663100356	44.39690636	17.09377	32.388879	97
		Pleasant Grove Road	vehicle in approaching zone	29.66376	0.811180399	31.3759	6.43854481	41.45485927	16.68957	32.42697	63
		East Miller Road	vehicle in approaching zone	28.42219	0.413287322	30.4121	4.295007838	18.44709233	16.35961	32.124246	108
		East Cavanaugh road	vehicle in approaching zone	28.00947	0.639061326	29.017	3.726335847	13.88557885	21.14843	32.341865	34
		Martin Luther king	vehicle in approaching zone	29.50482	0.415714915	30.6858	3.527458025	12.44296012	14.32205	32.724017	72
	South Bend	Lincoln Way	vehicle in approaching zone	30.73468	0.216369598	31.3059	1.797300863	3.230290393	20.47034	32.163813	69
		Portage Avenue	vehicle in approaching zone	29.61589	0.264879951	31.2236	3.523998549	12.41856578	16.21887	32.653708	177
		Twyckenham Drive	vehicle in approaching zone	30.795	0.298276427	31.5007	2.513321849	6.316786716	19.00725	32.365749	71
		South Main Street	vehicle in approaching zone	29.6192	0.377889635	31.1557	3.797743834	14.42285823	16.00551	32.461057	101

3.7 Limitation in Dynamic Object Detection

There were some limitations to this research. They can be eliminated in future studies to improve the performance of driver behavior detection. We used Velodyne V16 as the data collection device; however, its accuracy sharply decreased after 15-20 ft away from the LiDAR. Velodyne V-16 was equipped with 16 laser beams, which had a Field of View with a +15 to -15 vertical degrees. Furthermore, based on the LiDAR website, each of the 16-laser beams was directed about two degrees apart which means is for every 10 ft different between each channel would be 0.35 ft away. Another limitation of this study was object detection based on the distance. At 33ft far from the LiDAR, we had just two channels out of 16 channels to read the data.

3.8 Dynamic Object Detection Summary

This study used an automated method to extract and smartly assess the data of vehicles overtaking bicycles. This research introduces a reliable and straightforward vehicle trajectory extraction method regarding the LiDAR point clouds preprocessing. The proposed method has been tested by moving vehicle trajectory detection procedures for massive data processing. This procedure encompasses four main steps: (1) Organizing point clouds by preprocessing the raw data, e.g., filtering and cleaning the defined RON and OOI; (2) Filtering raw point clouds using a statistical outlier removal method to trim nearby object points; (3) Introducing our new vehicle detection and clustering method by using surface angles collected based on laser pulse in a novel way through extracting the initial features; (4) Projecting initial ROI features onto the OOI.

The developed algorithm method relies on the 3D coordinate and angle values of point clouds. The dataset was applied to the two datasets. A total of 260,000 data frames was collected and analyzed. The algorithm was applied to Lansing, Michigan and South Bend, Indiana. The

trajectories were then plotted.

The developed algorithm could also be applied to different transportation road facilities to analyze the vehicle and bike trajectories. This algorithm would also be applied to the variety of traffic applications to provide safe interaction between vehicles and bicycles in smart cities. Moreover, this algorithm can be used in autonomous car applications for automated overtaking procedures. It should be stated that the effects of different transportation facilities were not considered in this study.

4 CONCLUSION

This dissertation demonstrated that a LiDAR and Laser Scanner can be used for fix and dynamic object detection and classification. In this study in section 2, the road features were distinguished from off-road features based on the object detection and boundaries and the features were analyzed based on the ADA regulation. This study is one of the few investigations using a fully automated algorithm to assess the compliance of roadway features with the ADA. To achieve this aim, the PCD was collected by laser scanning. The ADA maintains design criteria for safe and accessible roadways provided to individuals with disabilities. Data acquisition and 3D modeling facilitated the evaluation process of the local facilities with regard to the ADA requirements. Point cloud data is a high-quality 3D modeling data collected by laser scanners. The PCD data is required to process and interpret various techniques to be used. Different data processing techniques such as normal estimation, surface fitting, and segmentation can be used to analyze and categorize road features.

Data processing helps the automated detection of road elements such as sidewalk and curb ramp, and the automated measurement of their dimensions, including slopes. Experimental testing was conducted to evaluate the proposed technique in a real case study on Ross Street in Kalamazoo, Michigan. The results showed that the mean absolute error of the selected curb ramps data was 0.22% and this value was 0.13% for the sidewalks when compared to other manual measurements.

In Section 3, the LiDAR was equipped with GPS and IMU, and a camera was mounted on the top of the bicycle to provide drivers' maneuver behaviors. Every single object that is possible to be a vehicle was extracted from the LiDAR frames using a combination of the smart segmentation and object of interest detection. Furthermore, after detecting all possible vehicles, the vehicles were tracked in each individual frame, the trajectory was created, and the driver's behaviors were analyzed. The approach finds the possible vehicles and differentiates the on-road objects and other

objects based on their features. The IMU and GPS were also used to implement both relative and absolute speeds of mobile vehicles. The IMU and LiDAR data implemented to the developed vehicle detection method empowers data processing applications to extract objects and differentiate them from background information effectively.

As future research, the analysis of both directions while passing a bicycle is suggested. The new data processing would provide a comprehensive set of information for both path traffic while one vehicle is passing a bicycle.

It is unlikely that a single LiDAR can acquire all the necessary information required to perform acceptable and accurate detection, recognition, analysis, and prediction; therefore, it would be more visible to combine laser scanner's massive point cloud data as a database data for autonomous vehicles are using LiDAR to detection and recognition object. Merging both point cloud data and LiDAR could the information in a cloud environment would supply a novel opportunity for autonomous vehicles to have a human maunder prediction.

REFERENCES

Ai, C., and Tsai. Y., 2016. Automated Sidewalk Assessment Method for Americans with Disabilities Act Compliance Using Three-Dimensional Mobile LiDAR. Transportation Research Record: Journal of the Transportation Research Board. pp.25-32.

Alghamdi, A., Sulaiman, M., Alghamdi,A., Alhosan, M., Mastali, M., Zhang, J., 2017. Building Accessibility Code Compliance Verification Using Game Simulations in Virtual Reality. Computing in Civil Engineering 2017. pp. 262-270.

Americans with Disabilities Act of 1990, 1991. 101-336 § 2.

Ankerst, M., Breunig, M.M., Kriegel H.P., Sander, J., 1999. OPTICS: ordering points to identify the clustering structure. ACM Sigmod record, Vol. 28, No. 2, pp. 49-60.

Antonellis, R.A., "Progress Towards LiDAR Based Bicycle Detection in Urban Environments." Ph.D. diss., Northeastern University Boston. 2017.

Argüelles-Fraga, R., Ordóñez, C., García-Cortés S., Roca-Pardiñas J., 2013. Measurement planning for circular cross-section tunnels using terrestrial laser scanning. Automation in construction. pp.1-9.

Bascom, G.W., Christensen, K.M., 2017. The impacts of limited transportation access on persons with disabilities' social participation. Journal of Transport & Health. pp.227-234.

Bisio, R., 2016. http://www.pobonline.com/blogs/23-geodatapoint-blog/post/100664-automation-in-point-cloud-processing-the-bar-moves-up.

Burbidge, S. K., and M. S. Shea, and Active Planning. Measuring Systemic Impacts of Bike Infrastructure Projects. No. UT-18.03. Utah. Dept. of Transportation. Research Division, 2018.

Burden D., 2000. Streets and Sidewalks, People and Cars: The citizens' guide to traffic calming.

CMAP, 2012. ADA Transition Plans for Your Community Accessibility for People with Disabilities: A Step Toward Continuing Compliance with the Americans with Disabilities Act and the Rehabilitation Act.

Debnath, A. K., N. Haworth, A. Schramm, K. C. Heesch, and K. Somoray. Factors influencing noncompliance with bicycle passing distance laws. Accident Analysis & Prevention 115, 2018. 137-142.

Dozza, M., R. Schindler, G. Bianchi-Piccinini, and J. Karlsson. How do drivers overtake cyclists?. Accident Analysis & Prevention 88, 2016. 29-36.

El-Halawany, S., Moussa, A., Lichti, D.D., El-Sheimy, N., 2011. Detection of road curb from mobile terrestrial laser scanner point cloud. In Proceedings of the ISPRS Workshop on Laser scanning, Calgary, Canada (Vol. 2931).

Evans, I., J. Pansch, and L. Singer-Berk. Factors Affecting Vehicle Passing Distance and Encroachments While Overtaking Cyclists. Institute of Transportation Engineers. ITE Journal 88, no. 5. 2018, 40-45.

Farradyne, P. Vehicle Infrastructure Integration (VII) Architecture and Functional Requirements, Version 1.1. FHWA US Department of Transportation, 2005.

Fei, D., Xueming, X., 2015. The Americans with Disabilities Act of 1990 (ADA) Paratransit Cost Issues and Solutions: Case of Greater Richmond Transit Company (GRTC), 3 CASE STUDY. TRANSP. POLICY 402.

Fernandez-Diaz J. C., W. E. Carter, R. L. Shrestha, C. L. Glennie. Now you see it… now you don't: Understanding airborne mapping LiDAR collection and data product generation for archaeological research in Mesoamerica. Remote Sensing. 2014 Oct 20;6(10):9951-10001

Fischler, M.A., and Bolles, R.C., 1981. Random sample consensus: a paradigm for model fitting with applications to image analysis and automated cartography. Communications of the ACM. pp.381-395.

Geosystems, l., 2017. Leica ScanStation P40 / P30. http://leicageosystems.com/products/laser-scanners/scanners/leica-scanstation-p40--p30,.

Hara, K., Sun, J., Chazan, j., Jacobs, D., Froehlich, J.E., 2013. An initial study of automatic curb ramp detection with crowdsourced verification using google street view images. First AAAI Conference on Human Computation and Crowdsourcing.

Jacobs Engineering Group, 2009. ADA Transition Plans: A Guide to Best Management Practices (National Cooperative Highway Research Program, National Academy of Sciences. pp.20–27.

Kay, J.J., Savolainen, P.T., Gates, T.J. and Datta, T.K., 2014. Driver behavior during bicycle passing maneuvers in response to a Share the Road sign treatment. Accident Analysis & Prevention, 70, pp.92-99.

Kockelman, K., Zhao, Y., Heard, L., Taylor D., Taylor, B., 2000. Sidewalk cross-slope requirements of the Americans with Disabilities Act: Literature review. Transportation Research Record: Journal of the Transportation Research Board., pp.53-60.

Kong, X., Li, M., Ma, K., Tian, K., Wang, M., Ning, Z. and Xia, F., 2018. Big trajectory data: A survey of applications and services. *IEEE Access*, *6*, pp.58295-58306.

Malik, F., and M. Ali Shah. "Smart city: A roadmap towards implementation." In Automation and Computing (ICAC), 2017 23rd International Conference on, pp. 1-6. IEEE, 2017.

McCann B., 2013. Completing our streets: The transition to safe and inclusive transportation networks. Island Press.

Mehta, K., B. Mehran, and B. Hellinga. "Evaluation of the passing behavior of motorized vehicles when overtaking bicycles on urban arterial roadways." Transportation Research Record: Journal of the Transportation Research Board 2520, 2015. 8-17.

Miraliakbari, A., Hahn, M., Sok, S., 2015. Automatic extraction of road surface and curbstone edges from mobile laser scanning data. The International Archives of Photogrammetry, Remote Sensing and Spatial Information Sciences. p.119.

NHTSA's National Center for Statistics and Analysis, Available online: https://crashstats.dot.gov/Api/Public/ViewPublication/812507 (accessed on 26 February 2019).

Oh, J.S., Kwigizile, V., Ro, K., Feizi, A., Kostich, B.W., Hasan, R.A.H., Mousa, F.A. 2017. Effect of Cycling Skills on Bicycle Safety and Comfort Associated with Bicycle Infrastructure and Environment (No. TRCLC 15-01). Western Michigan University. Transportation Research Center for Livable Communities.

OuYang D., Feng H.Y., 2005. On the normal vector estimation for point cloud data from smooth surfaces. Computer-Aided Design. pp.1071-1079.

Park, J., Subeh C., 2018. Investigating the barriers in a typical journey by public transport users with disabilities. Journal of Transport & Health.

Parkin, J., and C. Meyers. The effect of cycle lanes on the proximity between motor traffic and cycle traffic. Accident Analysis & Prevention 42, no. 1, 2010, 159-165.

Pölzlbauer, F., Bate, I., Brenner E., 2012. Efficient constraint handling during designing reliable automotive real-time systems. International Conference on Reliable Software Technologies, pp. 207-220.

Project Civic Access Fact Sheet, 2018. http://www.ada.gov/civicfac.htm.

Pucher, J., and R. Buehler. Cycling towards a more sustainable transport future. Transport Reviews 37, no., 2017, 6:689–694. doi:10.1080/01441647.2017.134-0234

RASCH, A., Modelling driver behaviour in longitudinal vehicle-pedestrian scenarios. Master Thesis, 2018, http://publications.lib.chalmers.se/records/fulltext/255829/255829.pdf

Rusu, R.B., Marton, Z.C., Blodow, N., Dolha, M., Beetz, M., 2008. 3D point cloud based object maps for household environments. Robotics and Autonomous Systems, pp.927-941.

Settlement Agreement Between the United States of America and the City of Toledo, Ohio: Department of Justice Complaint Number 204-57-35,1999.

State Population Projections to 2030, (Michigan Department of Technology, Management and Budget), 2016.

Steven Winter Associates, Inc., 2017. Best practices for accessibility compliance. https://www.wbdg.org/resources/best-practices-accessibility-compliance.

Sun Y., Xu, H., Wu, J., Zheng, J., Dietrich, K.M., 2018. 3-D Data Processing to Extract Vehicle Trajectories from Roadside LiDAR Data. Transportation Research Record. https://doi.org/10.1177/0361198118775839.

Thi, T.T.P., Helfert, M., 2017. A review of quality frameworks in information systems. arXiv preprint arXiv:1706.03030.

Traquair HM. An Introduction to Clinical Perimetry. St Louis, MO; CV Mosby; 1927,58–77.

Trevor, A.J., Gedikli, S., Rusu, R.B., Christensen, H., I., 2013. Efficient organized point cloud segmentation with connected components. Semantic Perception Mapping and Exploration (SPME).

Veichtlbauer, A., Dorfinger, P., Schrittesser, U., 2011. Live Data Acquisition for Situation Awareness in Traffic Management Systems Using. The Fifth International Conference on Sensor Technologies and Applications. Nice/Saint Laurent du Var: IARIA XPS Press. pp.268-273.

Van der Hoeven, D. "Unfolding the Smart City Label: Definition and Application of Performance Measurement System for Smart Cities". 2017: https://pdfs.semanticscholar.org/0e08/5870dd884114ccbf846e6354fbdeef61a3ed.pdf

Velodyne LIDAR, Inc. Products. Available online: http://velodyneLiDAR.com/products.html (accessed on 27 January 2018).

Wang, C.C., Thorpe C., Thrun, S., 2003. Online simultaneous localization and mapping with detection and tracking of moving objects: Theory and results from a ground vehicle in crowded urban areas. ICRA, Vol. 1, pp. 842-849.

Wang, H., Wang, C., Luo, H., Li, P., Cheng, M., Wen, C., Li, J., 2014. Object detection in terrestrial laser scanning point clouds based on Hough forest. IEEE Geoscience and Remote Sensing Letters. pp.1807-1811.

Wang, J., K. Li, and X.-Y. Lu, Effect of Human Factors on Driver Behavior. 2014.

Watershed Sciences, inc. LiDAR remote sensing data collection: Lake Billy Chinook, Oregon. 2009. Available online: http://www.oregongeology.org/pubs/ldq/reports/Billy_Chinook_LiDAR_Report.pdf (accessed on 28 July 2018).

Wilson, T., and W. Best. "Driving strategies in overtaking." Accident Analysis & Prevention 14, no. 3 (1982): 179-185.

Wu X, Kumar V, Quinlan JR, Ghosh J, Yang Q, Motoda H, McLachlan GJ, Ng A, Liu B, Philip SY, Zhou ZH. Top 10 algorithms in data mining. Knowledge and information systems. 2008 Jan 1;14(1):1-37.

APPENDICES

A. Data Distribution

In this appendix collected data from Lansing and South bend analyzed. Data distributions plotted in a 3 dimensions contour model which express relations between vehicle and bike speeds with longitude distances. This section, Mu represents Mean of the normal distribution. In addition, sigma represents the standard deviation of normal distribution.

West Kalamazoo

- A 2 and 3-lanes road with bike lane and shoulder
- The speed limit of 25 mph

Table 10 Normal data distribution in approaching zone in West Kalamazoo

	Distribution	Parameter	Estimate	Lower 95%	Upper 95%
Bike Speed	Normal	Location mu	16.09697	14.61691	17.57703
		Scale sigma	3.69945	2.76215	4.95481
Vehicle Speed	Normal	Location mu	18.61868	16.9593	20.27807
		Scale sigma	4.14768	3.09682	5.55514
Longitude Distance	Normal	Location mu	8.0924	7.31935	8.86544
		Scale sigma	1.93224	1.44269	2.58792

Table 11 Normal data distribution in the passing zone in West Kalamazoo

	Distribution	Parameter	Estimate	Lower 95%	Upper 95%
Bike Speed	Normal	Location mu	16.76843	15.7323	17.80455
		Scale sigma	2.58982	1.93366	3.46864
Vehicle Speed	Normal	Location mu	17.68082	16.61389	18.74775
		Scale sigma	2.66682	1.99115	3.57176
Longitude Distance	Normal	Location mu	6.69327	6.09301	7.29352
		Scale sigma	1.50035	1.12022	2.00948

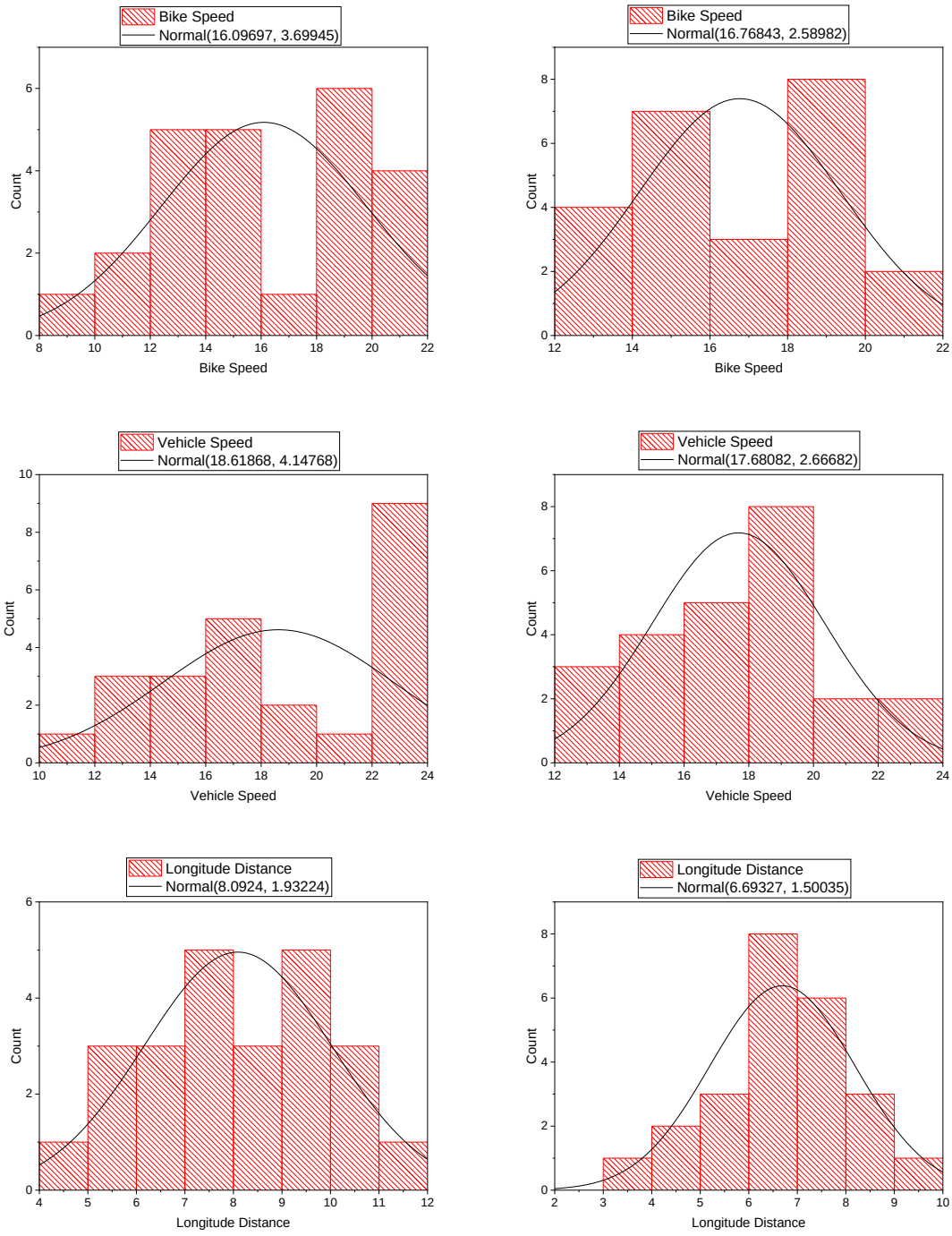

Figure 24 Vehicle, bicycle speed and longitude distance distribution in West Kalamazoo

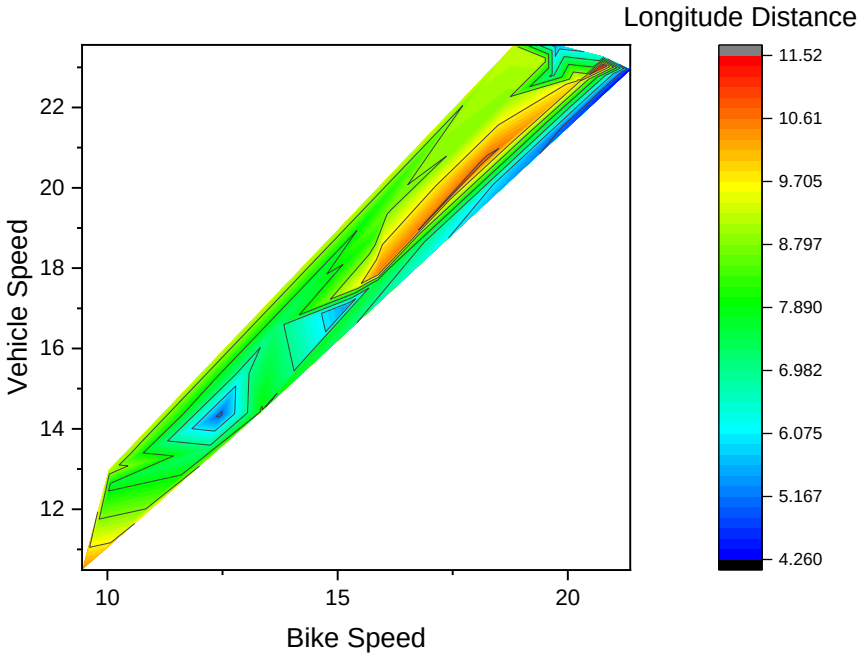

Figure 25 Maneuver analysis in approaching zone in West Kalamazoo

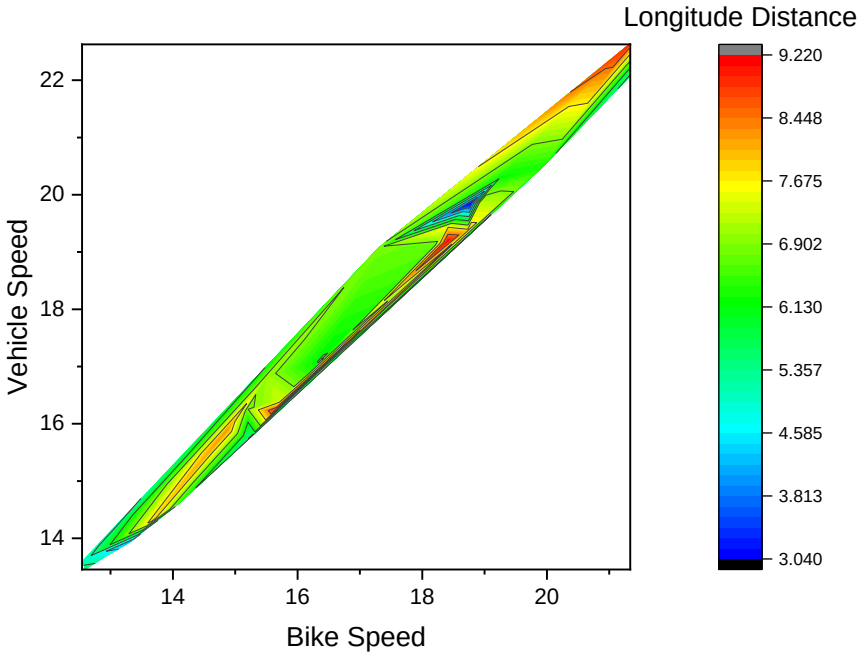

Figure 26 Maneuver analysis in the passing zone in West Kalamazoo

East Kalamazoo

- A 2 and 3-lanes road with bike lane and shoulder
- The speed limit of 25 mph

Table 12 Normal data distribution in approaching zone in East Kalamazoo

	Distribution	Parameter	Estimate	Lower 95%	Upper 95%
Bike Speed	Normal	Location mu	17.59718	16.83243	18.36193
		Scale sigma	3.84286	3.33476	4.42839
Vehicle Speed	Normal	Location mu	20.86518	20.06966	21.66071
		Scale sigma	3.99755	3.46899	4.60664
Longitude Distance	Normal	Location mu	8.04197	7.6109	8.47304
		Scale sigma	2.16613	1.87972	2.49617

Table 13 Normal data distribution in the passing zone in East Kalamazoo

	Distribution	Parameter	Estimate	Lower 95%	Upper 95%
Bike Speed	Normal	Location mu	17.788	17.00588	18.57012
		Scale sigma	3.93017	3.41052	4.529
Vehicle Speed	Normal	Location mu	21.17883	20.4877	21.86997
		Scale sigma	3.47295	3.01376	4.00212
Longitude Distance	Normal	Location mu	7.28678	7.00003	7.57354
		Scale sigma	1.44094	1.25042	1.6605

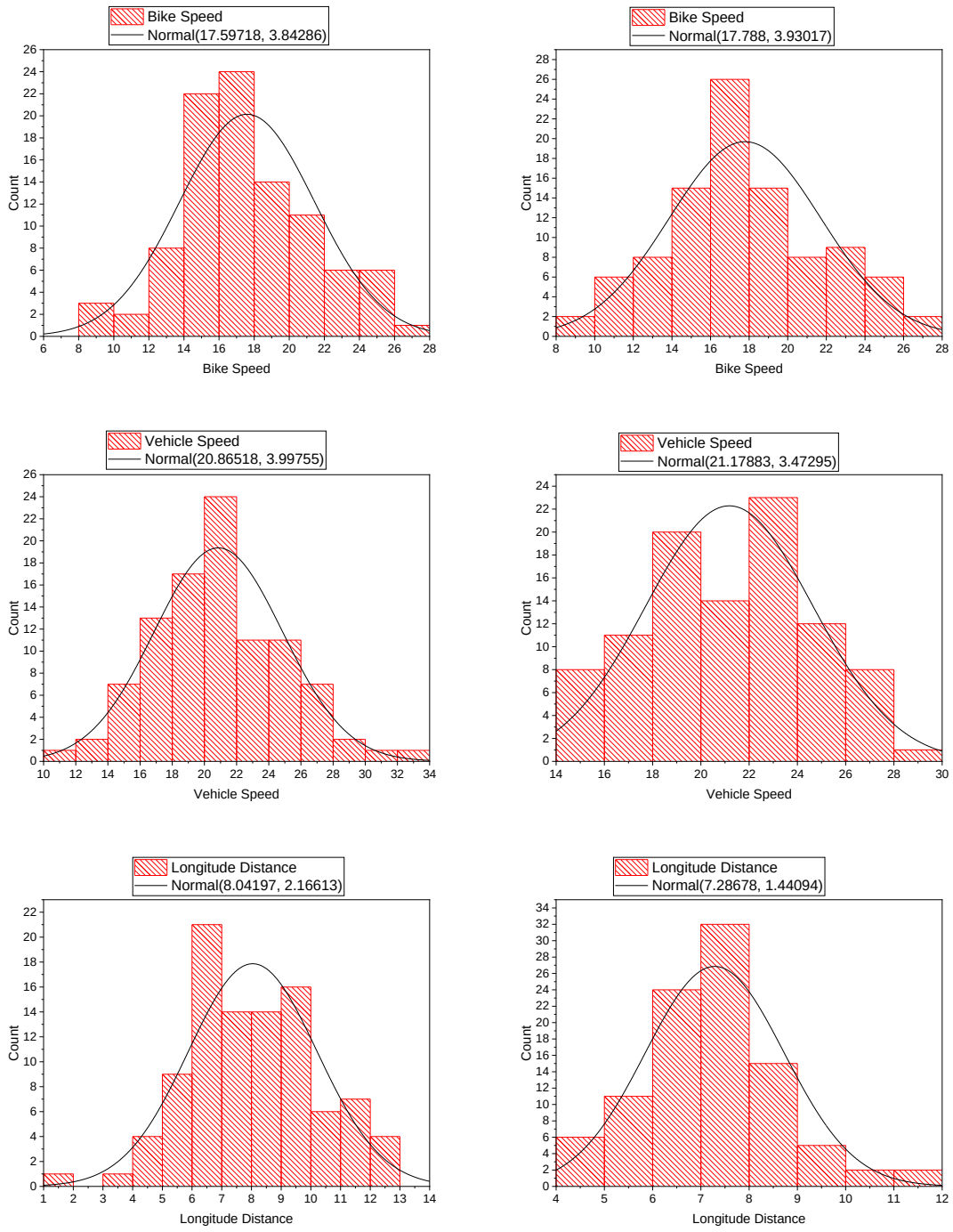

Figure 27 Vehicle, bicycle speed and longitude distance distribution in East Kalamazoo

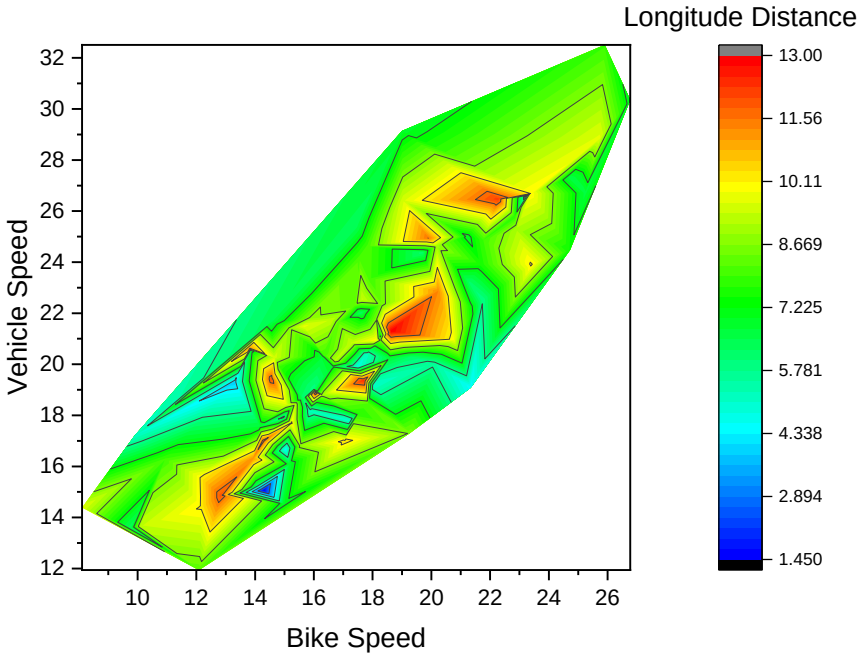

Figure 28 Maneuver analysis in approaching zone in East Kalamazoo

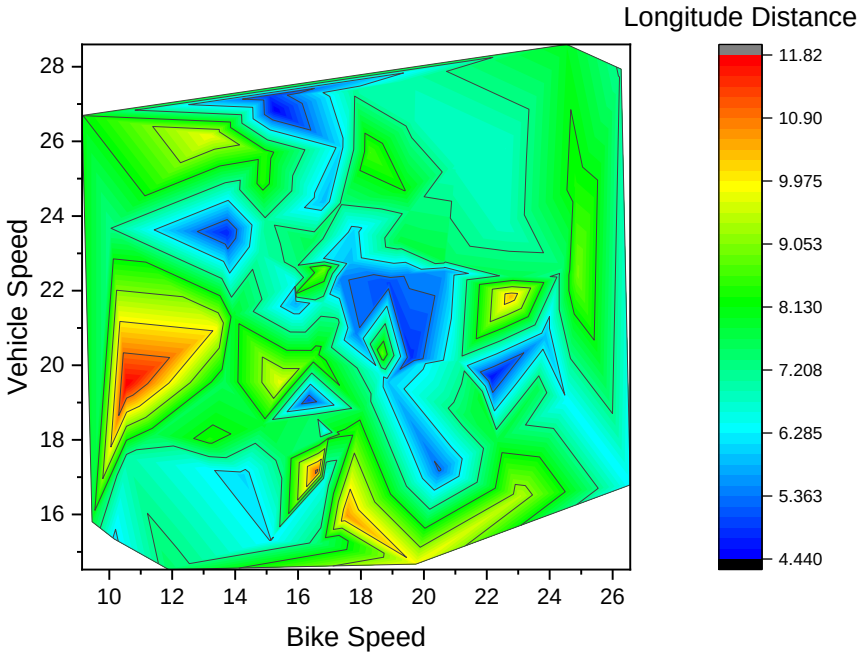

Figure 29 Maneuver analysis in the passing zone in East Kalamazoo

Pleasant Grove Road

- A 2-lane road with a bike lane
- The speed limit of 35 mph

Table 14 Normal data distribution in approaching zone in Pleasant Grove Road

	Distribution	Parameter	Estimate	Lower 95%	Upper 95%
Bike Speed	Normal	Location mu	21.08645	20.21434	21.95857
		Scale sigma	3.53179	2.95968	4.21449
Vehicle Speed	Normal	Location mu	24.72978	23.84012	25.61944
		Scale sigma	3.60285	3.01923	4.29929
Longitude Distance	Normal	Location mu	8.07478	7.65531	8.49425
		Scale sigma	1.69872	1.42355	2.02709

Table 15 Normal data distribution in the passing zone in Pleasant Grove Road

	Distribution	Parameter	Estimate	Lower 95%	Upper 95%
Bike Speed	Normal	Location mu	20.81469	19.95444	21.67494
		Scale sigma	3.48374	2.91941	4.15716
Vehicle Speed	Normal	Location mu	22.36867	21.47852	23.25883
		Scale sigma	3.60486	3.02091	4.30168
Longitude Distance	Normal	Location mu	7.07466	6.6711	7.47822
		Scale sigma	1.6343	1.36956	1.95022

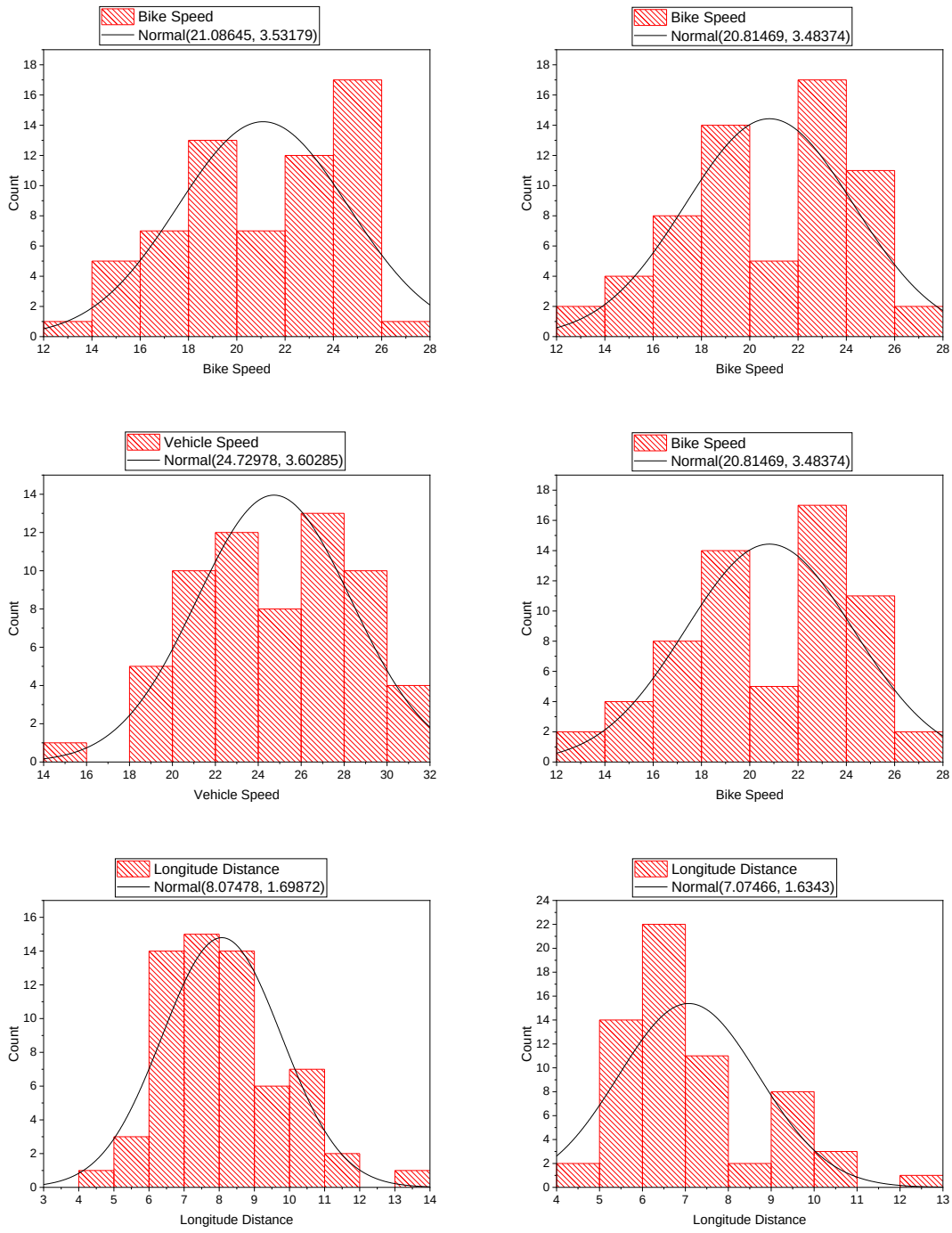

Figure 30 Vehicle, bicycle speed and longitude distance distribution in Pleasant Grove Road

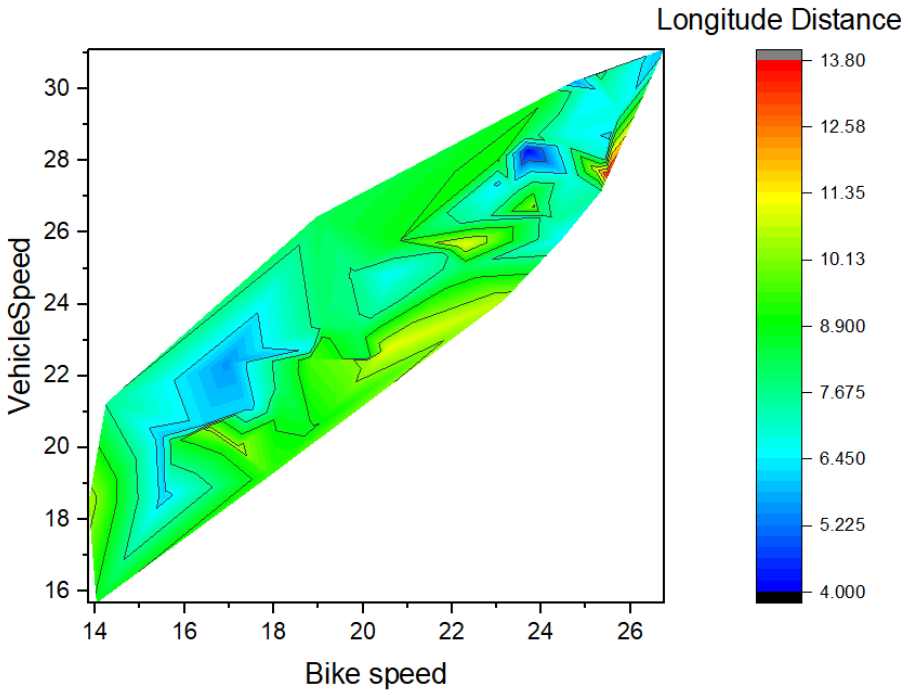

Figure 31 Maneuver analysis in approaching zone in Pleasant Grove Road

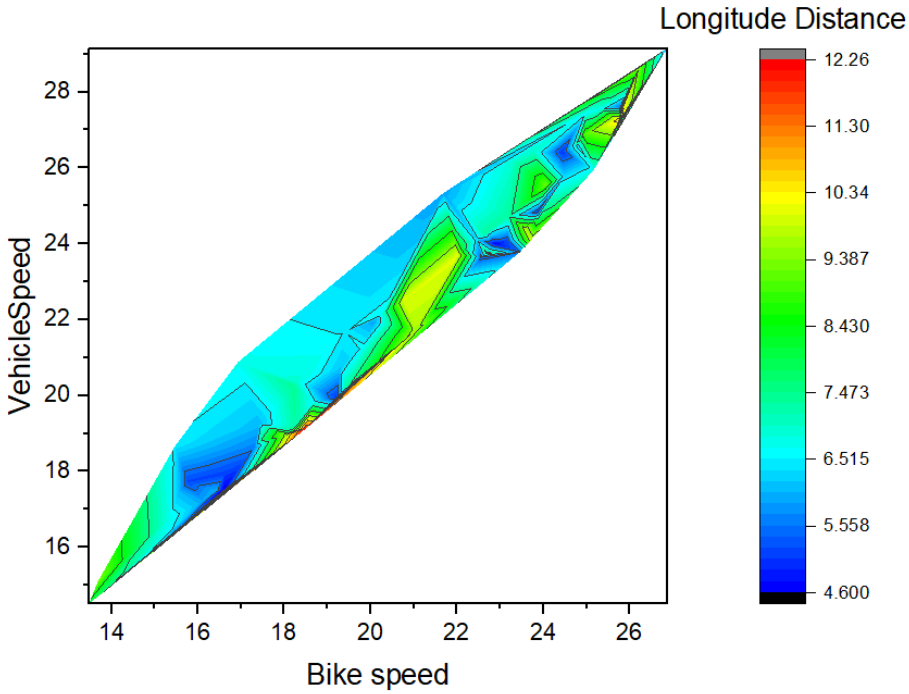

Figure 32 Maneuver analysis in the passing zone in Pleasant Grove Road

Miller Road

- A 3-lane road with a shoulder
- The speed limit of 30 mph

Table 16 Normal data distribution in approaching zone in Miller Road

	Distribution	Parameter	Estimate	Lower 95%	Upper 95%
Bike Speed	Normal	Location mu	19.82188	19.14472	20.49904
		Scale sigma	3.60708	3.15576	4.12294
Vehicle Speed	Normal	Location mu	23.12564	22.41324	23.83804
		Scale sigma	3.79481	3.32	4.33752
Longitude Distance	Normal	Location mu	9.0541	8.5177	9.59049
		Scale sigma	2.85725	2.49975	3.26588

Table 17 Normal data distribution in the passing zone in Miller Road

	Distribution	Parameter	Estimate	Lower 95%	Upper 95%
Bike Speed	Normal	Location mu	19.63575	18.9544	20.31711
		Scale sigma	3.62944	3.17533	4.1485
Vehicle Speed	Normal	Location mu	21.04498	20.38468	21.70528
		Scale sigma	3.51725	3.07717	4.02027
Longitude Distance	Normal	Location mu	8.1272	7.80178	8.45261
		Scale sigma	1.73341	1.51652	1.98131

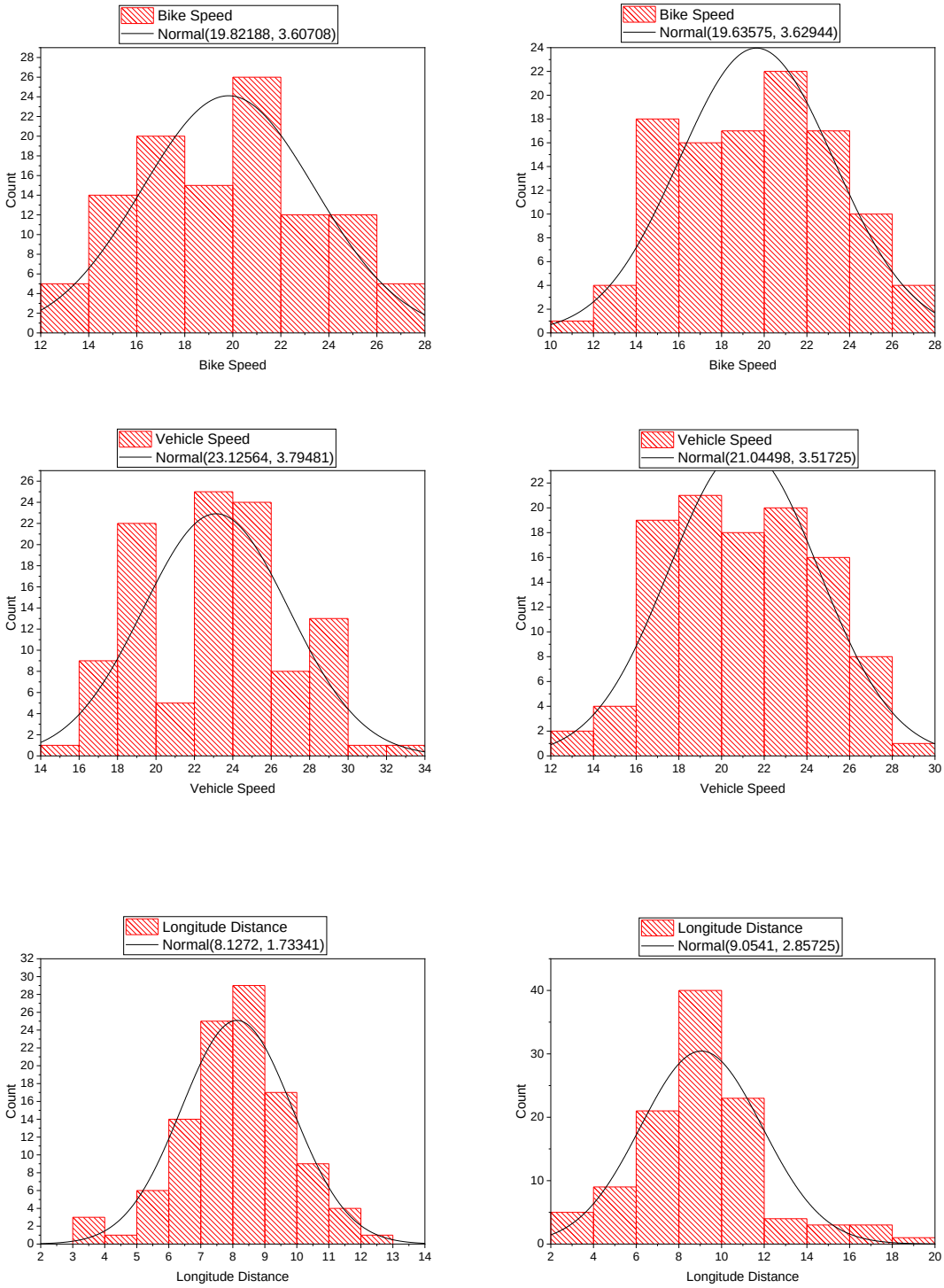

Figure 33 Vehicle, bicycle speed and longitude distance distribution in Miller Road

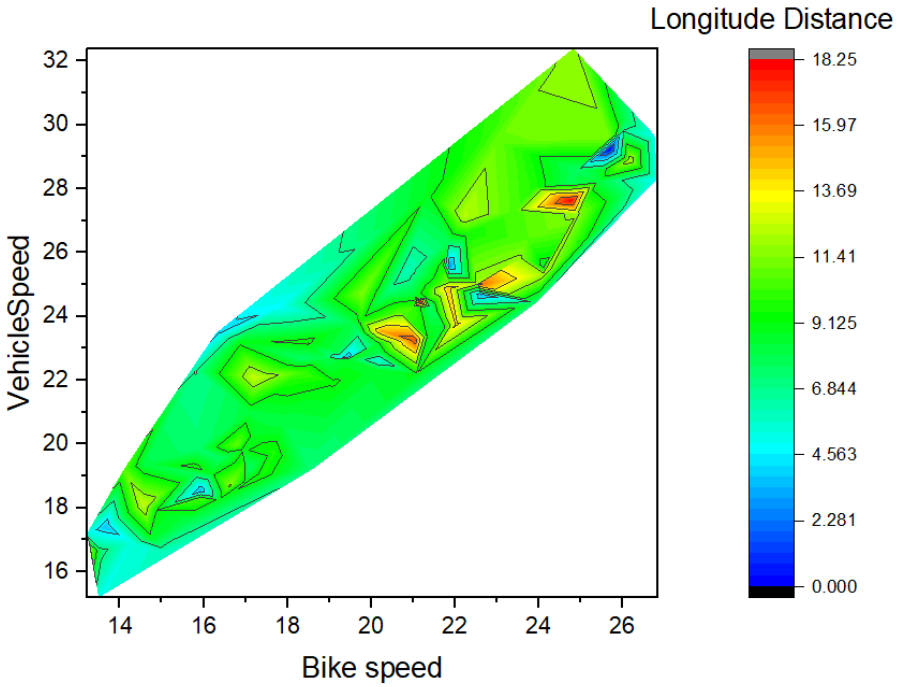

Figure 34 Maneuver analysis in approaching zone in Miller Road

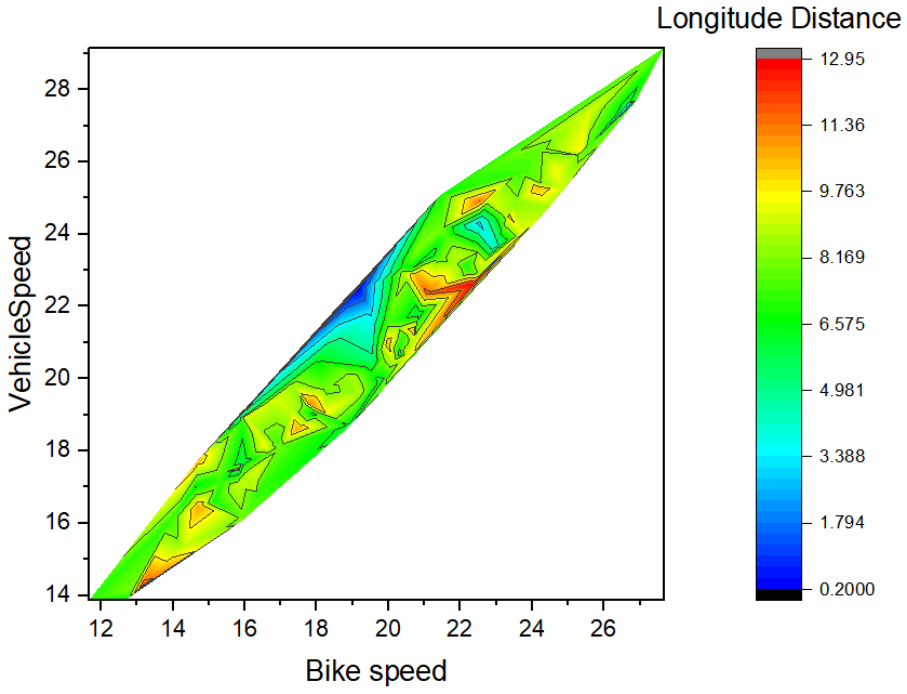

Figure 35 Maneuver analysis in the passing zone in Miller Road

East Cavanaugh Road

- A 2-lane road with no bike lane
- The speed limit of 35 mph

Table 18 Normal data distribution in approaching zone in East Cavanaugh Road

	Distribution	Parameter	Estimate	Lower 95%	Upper 95%
Bike Speed	Normal	Location mu	22.46351	21.49791	23.42911
		Scale sigma	2.87269	2.25274	3.66326
Vehicle Speed	Normal	Location mu	24.9551	23.97825	25.93195
		Scale sigma	2.90615	2.27898	3.70593
Longitude Distance	Normal	Location mu	7.42329	6.63414	8.21243
		Scale sigma	2.34773	1.84107	2.99383

Table 19 Normal data distribution in the passing zone in East Cavanaugh Road

	Distribution	Parameter	Estimate	Lower 95%	Upper 95%
Bike Speed	Normal	Location mu	22.17657	21.14725	23.20588
		Scale sigma	3.06224	2.40138	3.90497
Vehicle Speed	Normal	Location mu	23.62876	22.57183	24.6857
		Scale sigma	3.14441	2.46582	4.00975
Longitude Distance	Normal	Location mu	6.24236	5.65705	6.82767
		Scale sigma	1.74132	1.36552	2.22053

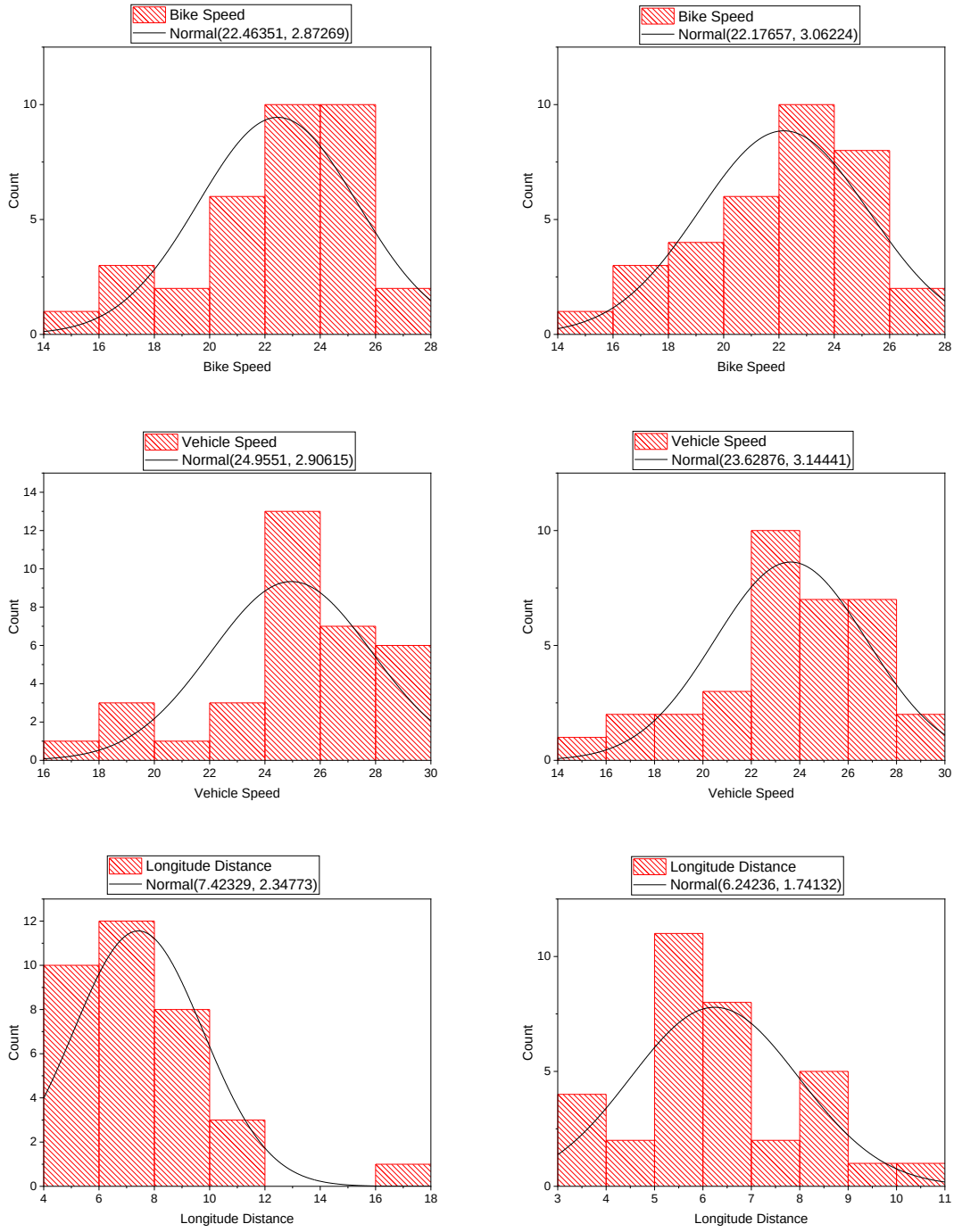

Figure 36 Vehicle, bicycle speed and longitude distance distribution in East Cavanaugh Road

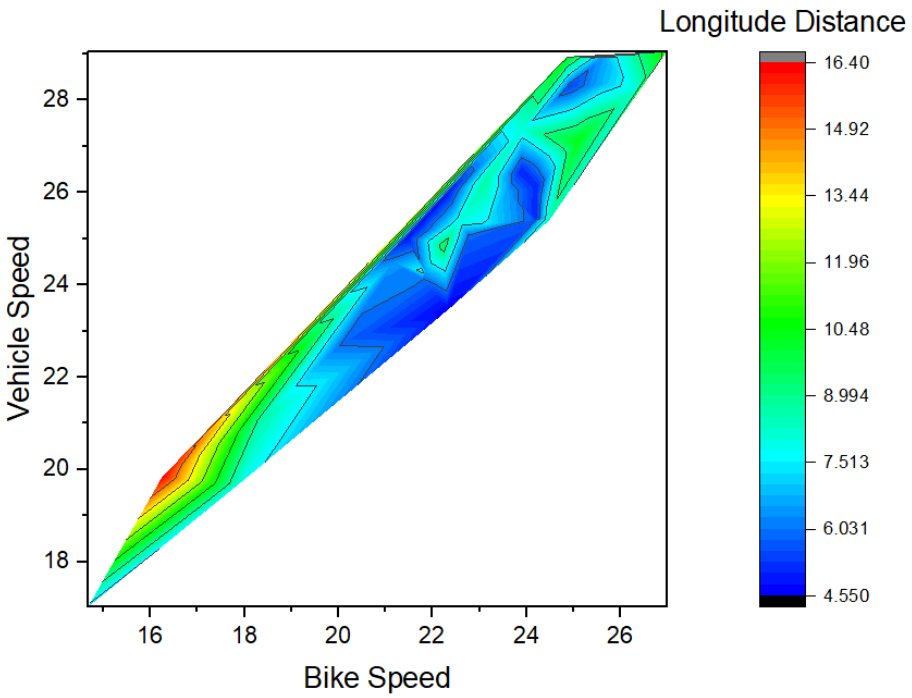

Figure 37 Maneuver analysis in approaching zone in East Cavanaugh Road

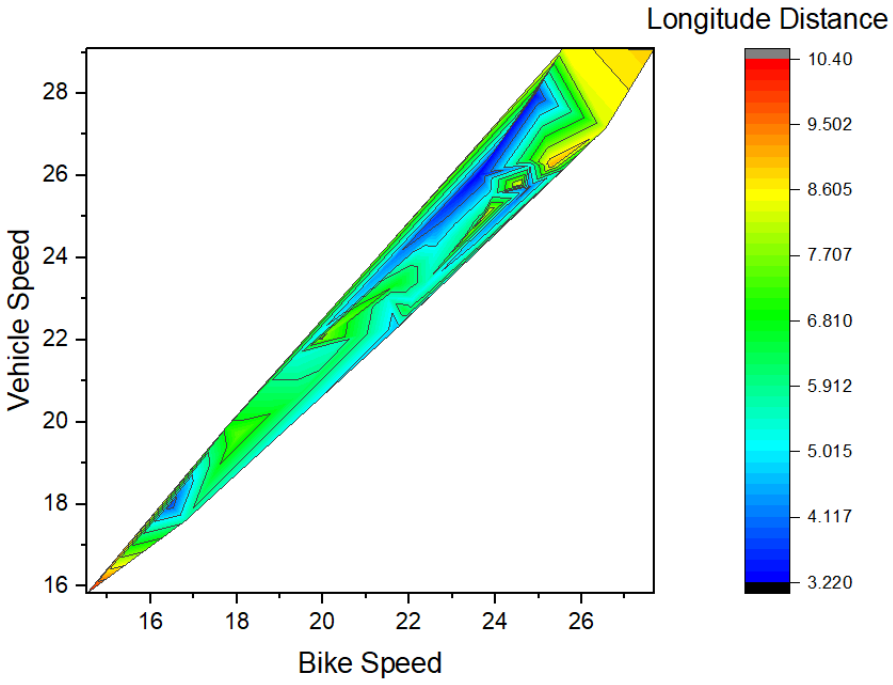

Figure 38 Maneuver analysis in the passing zone in East Cavanaugh Road

Martin Luther King

- A 2 and 3-lane road with bike lane and shoulder
- The speed limit of 25 mph

Table 20 Normal data distribution in the approaching zone in Martin Luther King

	Distribution	Parameter	Estimate	Lower 95%	Upper 95%
Bike Speed	Normal	Location mu	20.35747	19.45312	21.26181
		Scale sigma	3.91518	3.31946	4.6178
Vehicle Speed	Normal	Location mu	22.73843	21.85992	23.61695
		Scale sigma	3.80336	3.22466	4.48592
Longitude Distance	Normal	Location mu	6.8542	6.33076	7.37763
		Scale sigma	2.26609	1.92129	2.67277

Table 21 Normal data distribution in the passing zone in Martin Luther King

	Distribution	Parameter	Estimate	Lower 95%	Upper 95%
Bike Speed	Normal	Location mu	20.29449	19.41899	21.16998
		Scale sigma	3.79027	3.21355	4.47048
Vehicle Speed	Normal	Location mu	22.67545	21.81813	23.53277
		Scale sigma	3.71158	3.14684	4.37767
Longitude Distance	Normal	Location mu	5.34348	4.88571	5.80125
		Scale sigma	1.98182	1.68027	2.33748

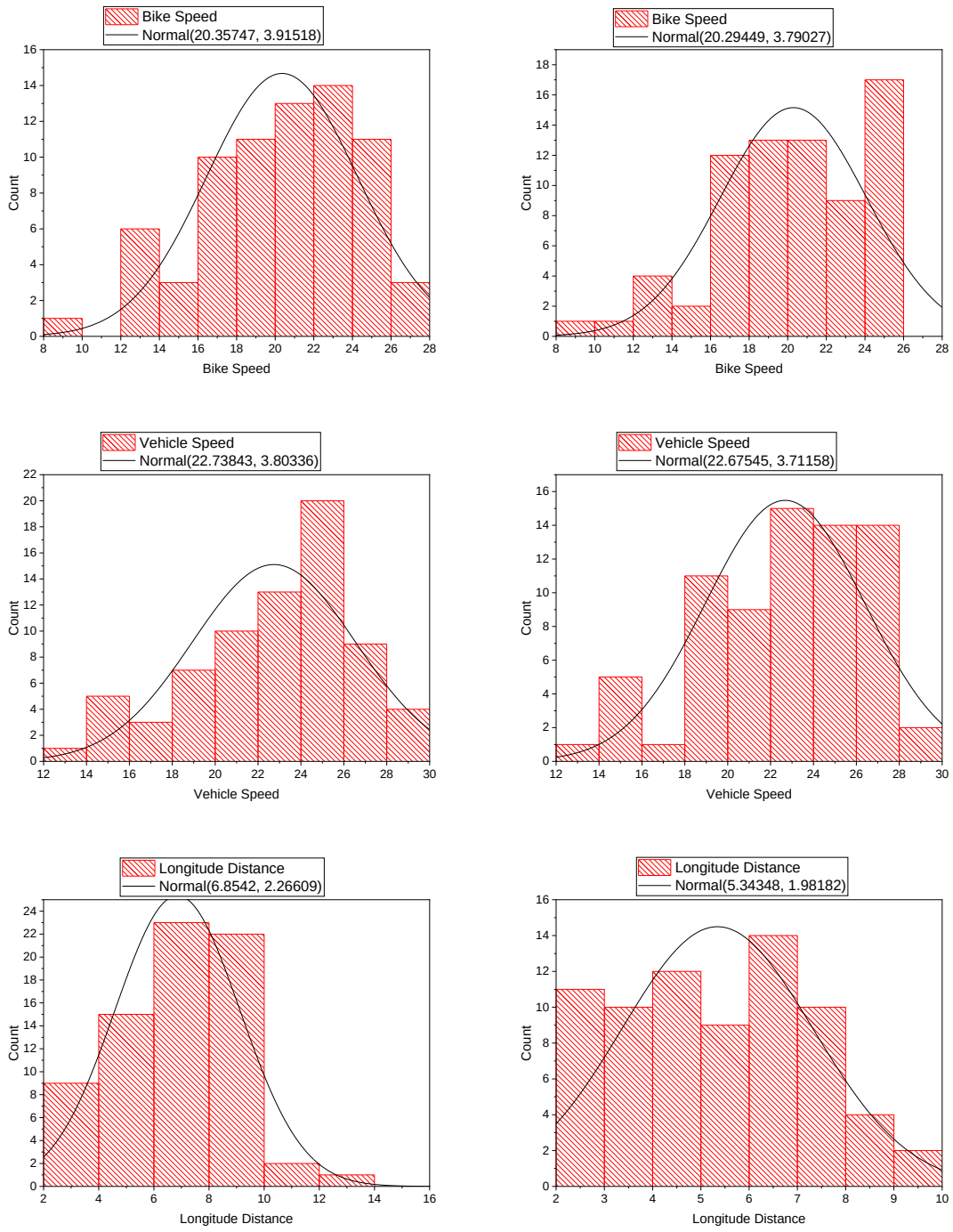

Figure 39 Vehicle, bicycle speed and longitude distance distribution in Martin Luther King

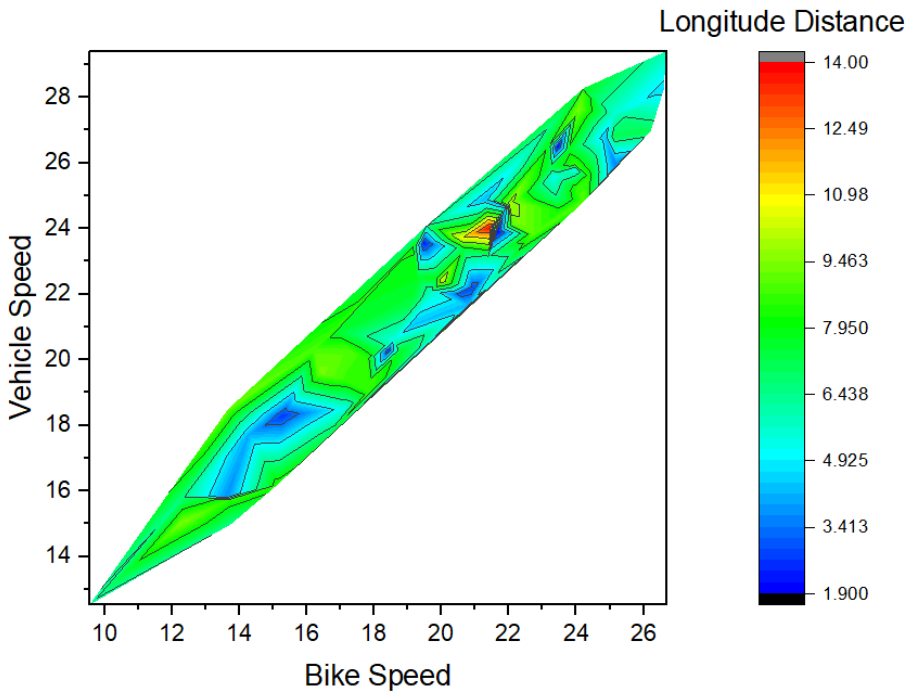

Figure 40 Maneuver analysis in approaching zone in Martin Luther King

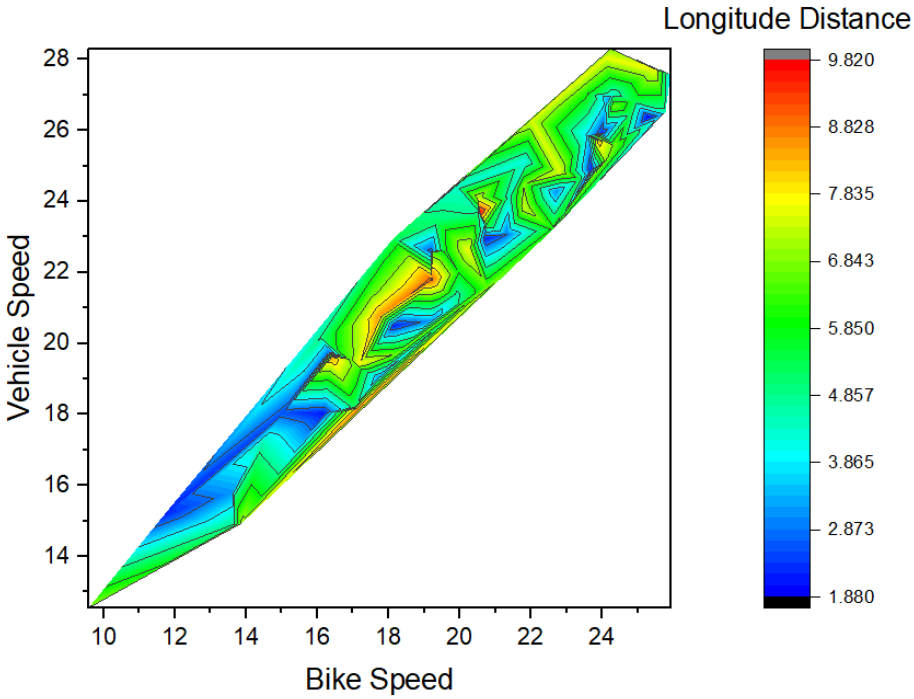

Figure 41 Maneuver analysis in the passing zone in Martin Luther King

Lincoln-Way

A 3-lane road with a bike lane and sharrow

The speed limit of 40 mph

Table 22 Normal data distribution in approaching zone in Lincoln Way

	Distribution	Parameter	Estimate	Lower 95%	Upper 95%
Bike Speed	Normal	Location mu	23.02656	22.48401	23.56911
		Scale sigma	2.29942	1.94249	2.72193
Vehicle Speed	Normal	Location mu	25.60856	25.0686	26.14851
		Scale sigma	2.28841	1.93318	2.7089
Longitude Distance	Normal	Location mu	7.67485	7.28475	8.06496
		Scale sigma	1.65332	1.39668	1.95712

Table 23 Normal data distribution in the passing zone in Lincoln Way

	Distribution	Parameter	Estimate	Lower 95%	Upper 95%
Bike Speed	Normal	Location mu	22.83232	22.28939	23.37525
		Scale sigma	2.30103	1.94385	2.72384
Vehicle Speed	Normal	Location mu	24.21351	23.7004	24.72662
		Scale sigma	2.17464	1.83708	2.57423
Longitude Distance	Normal	Location mu	6.76016	6.44614	7.07418
		Scale sigma	1.33085	1.12427	1.57539

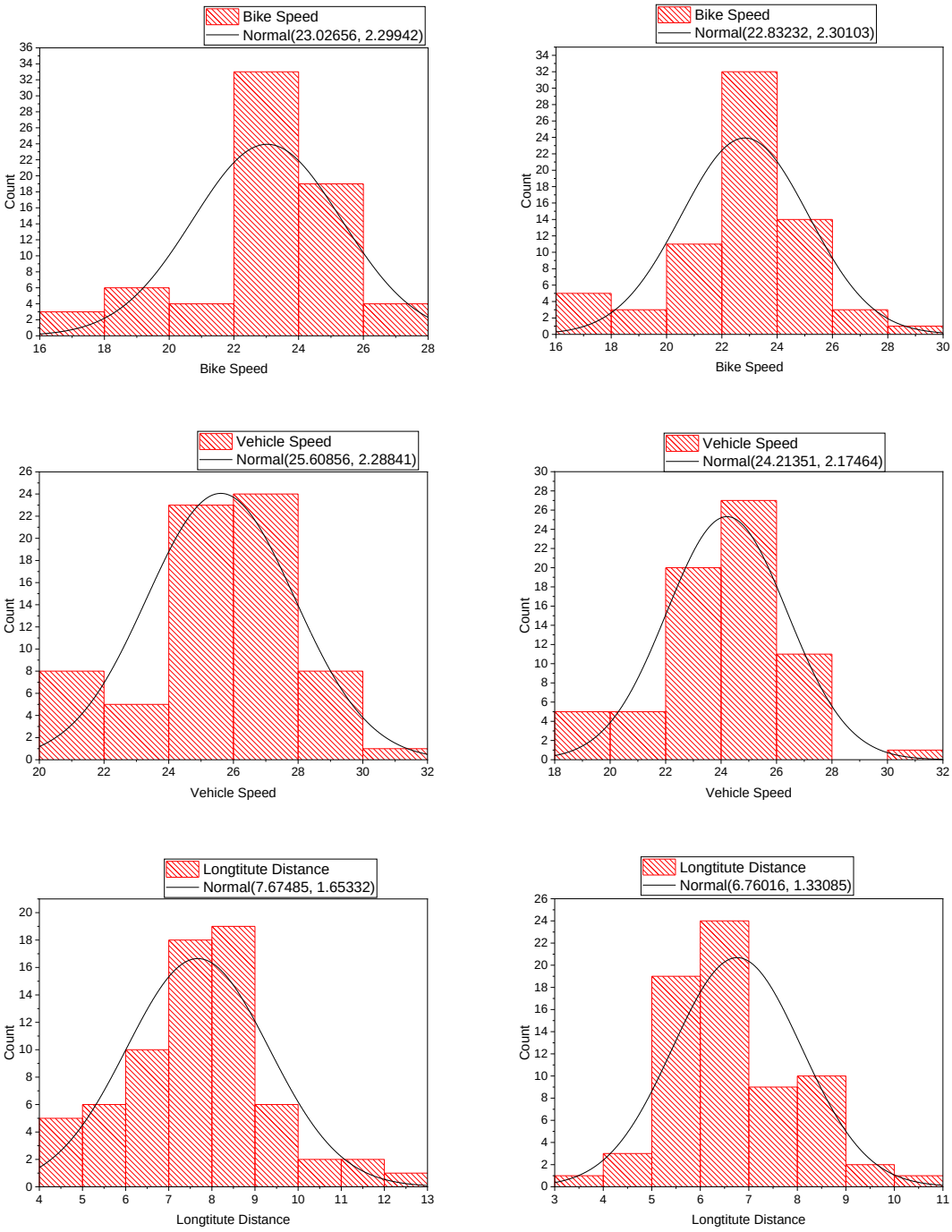

Figure 42 Vehicle, bicycle speed and longitude distance distribution in Lincoln Way

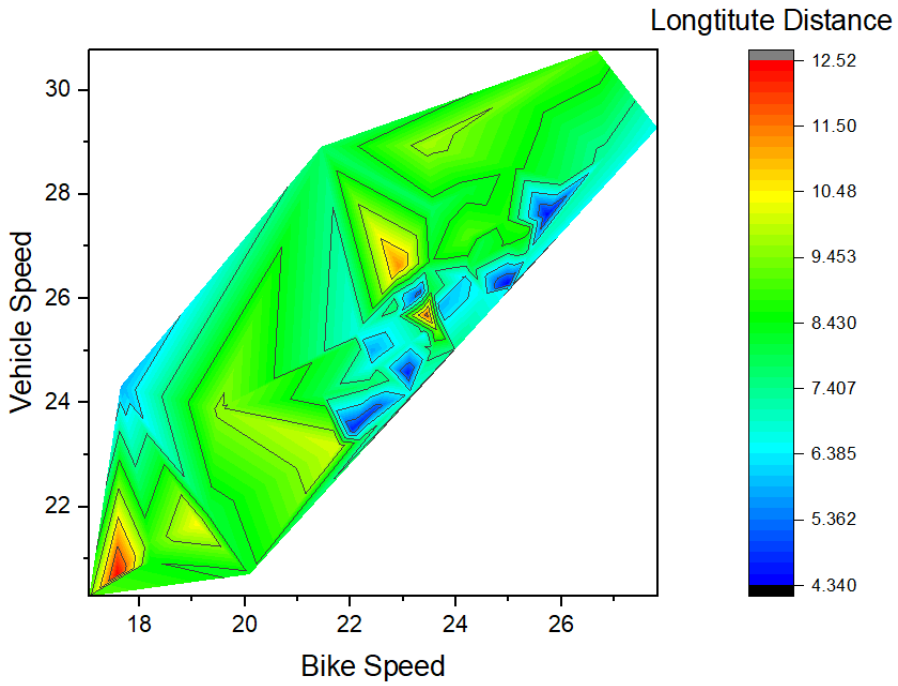

Figure 43 Maneuver analysis in approaching zone in Lincoln Way

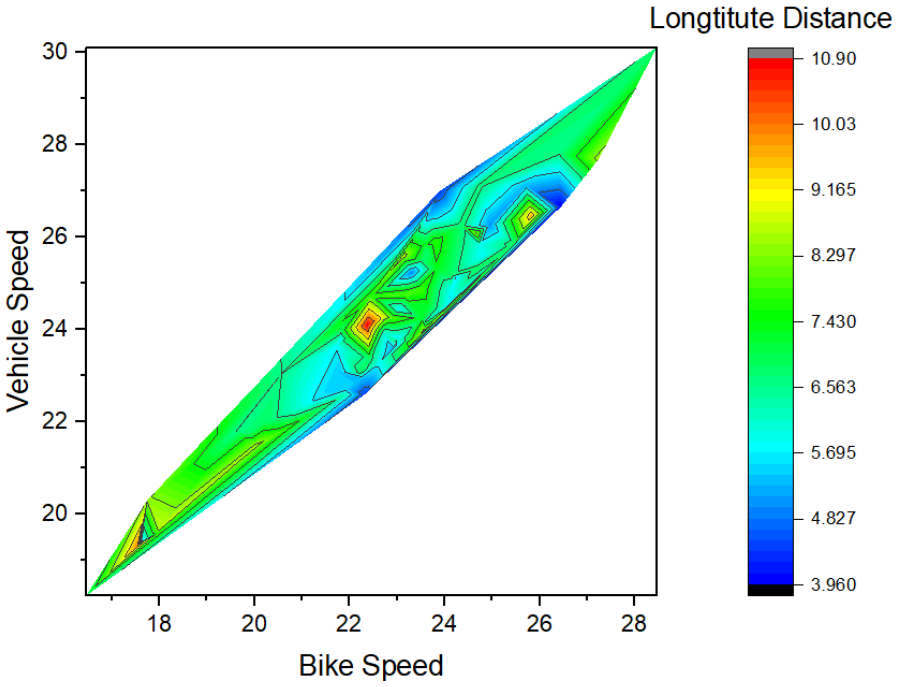

Figure 44 Maneuver analysis in the passing zone in Lincoln Way

Portage Avenue Road

A 2-lane road with a sharrow, and no bike lane

The speed limit of 30 mph

Table 24 Normal data distribution in approaching zone in Portage Avenue Road

	Distribution	Parameter	Estimate	Lower 95%	Upper 95%
Bike Speed	Normal	Location mu	21.77876	21.28358	22.27394
		Scale sigma	3.36126	3.02739	3.73195
Vehicle Speed	Normal	Location mu	24.95991	24.42221	25.49761
		Scale sigma	3.64989	3.28735	4.05241
Longitude Distance	Normal	Location mu	7.21654	6.82455	7.60854
		Scale sigma	2.66082	2.39652	2.95426

Table 25 Normal data distribution in the passing zone in Portage Avenue Road

	Distribution	Parameter	Estimate	Lower 95%	Upper 95%
Bike Speed	Normal	Location mu	21.77876	21.28358	22.27394
		Scale sigma	3.36126	3.02739	3.73195
Vehicle Speed	Normal	Location mu	24.95991	24.42221	25.49761
		Scale sigma	3.64989	3.28735	4.05241
Longitude Distance	Normal	Location mu	7.21654	6.82455	7.60854
		Scale sigma	2.66082	2.39652	2.95426

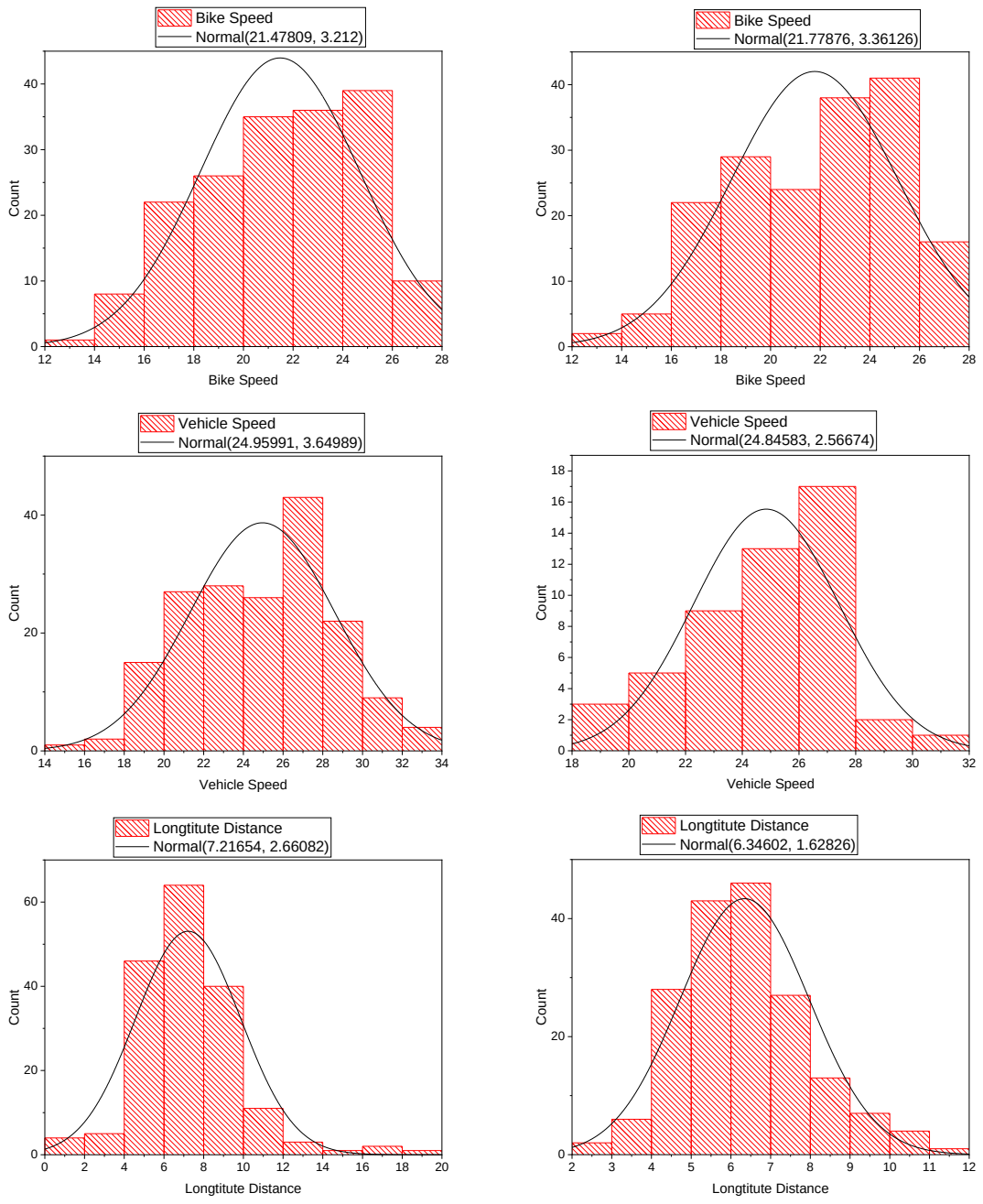

Figure 45 Vehicle, bicycle speed and longitude distance distribution in Portage Avenue Road

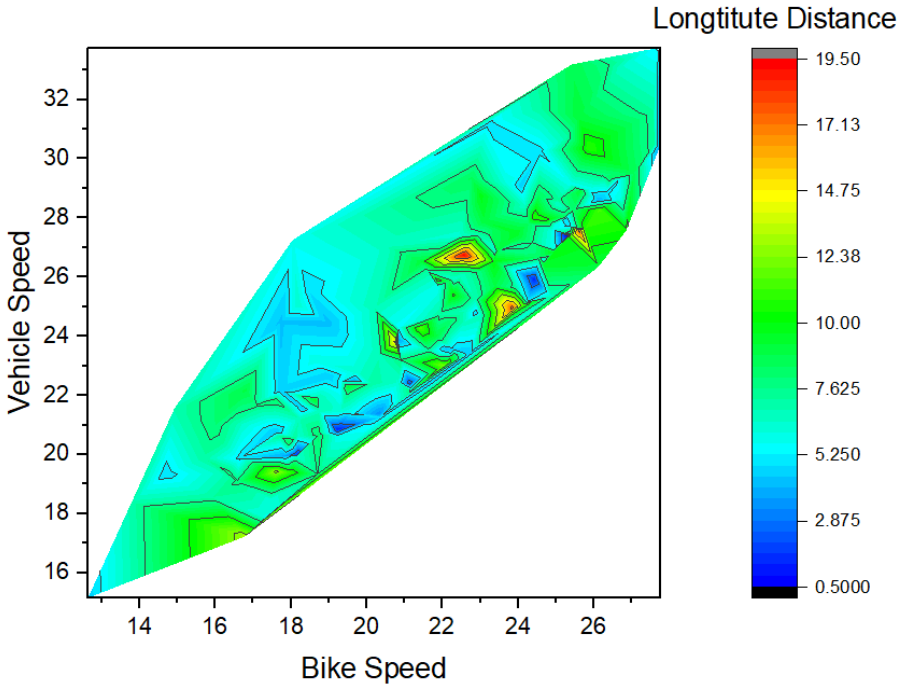

Figure 46 Maneuver analysis in approaching zone in Portage Avenue Road

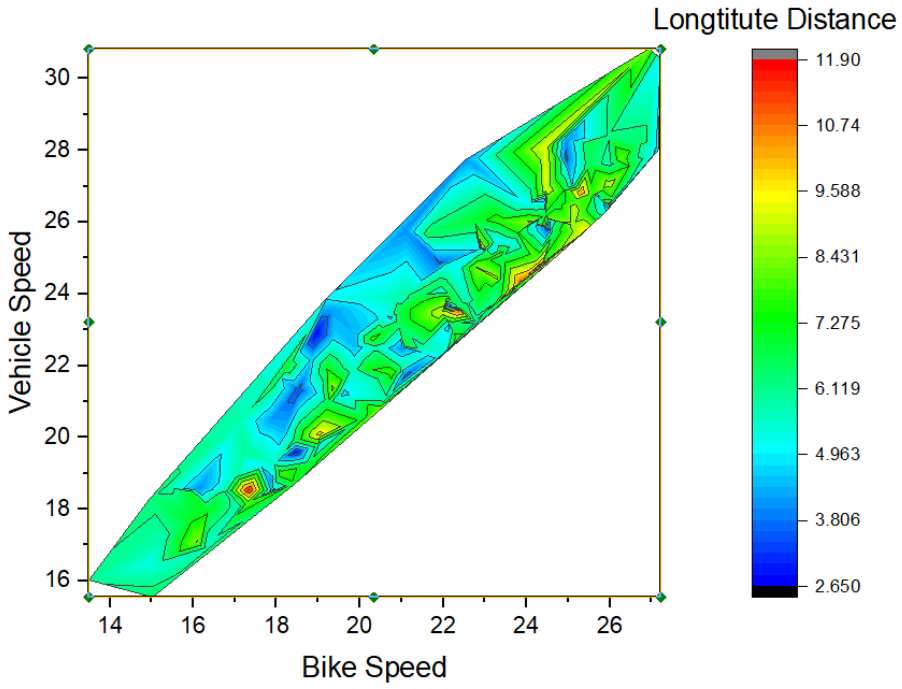

Figure 47 Maneuver analysis in the passing zone in Portage Avenue Road

Twyckenham Drive

A 2-lane road with bike lane and shoulder

The speed limit of 30 mph

Table 26 Normal data distribution in approaching zone in Twyckenham Drive

	Distribution	Parameter	Estimate	Lower 95%	Upper 95%
Bike Speed	Normal	Location mu	21.77876	21.28358	22.27394
		Scale sigma	3.36126	3.02739	3.73195
Vehicle Speed	Normal	Location mu	24.95991	24.42221	25.49761
		Scale sigma	3.64989	3.28735	4.05241
Longitude Distance	Normal	Location mu	7.21654	6.82455	7.60854
		Scale sigma	2.66082	2.39652	2.95426

Table 27 Normal data distribution in the passing zone in Twyckenham Drive

	Distribution	Parameter	Estimate	Lower 95%	Upper 95%
Bike Speed	Normal	Location mu	21.77876	21.28358	22.27394
		Scale sigma	3.36126	3.02739	3.73195
Vehicle Speed	Normal	Location mu	24.95991	24.42221	25.49761
		Scale sigma	3.64989	3.28735	4.05241
Longitude Distance	Normal	Location mu	7.21654	6.82455	7.60854
		Scale sigma	2.66082	2.39652	2.95426

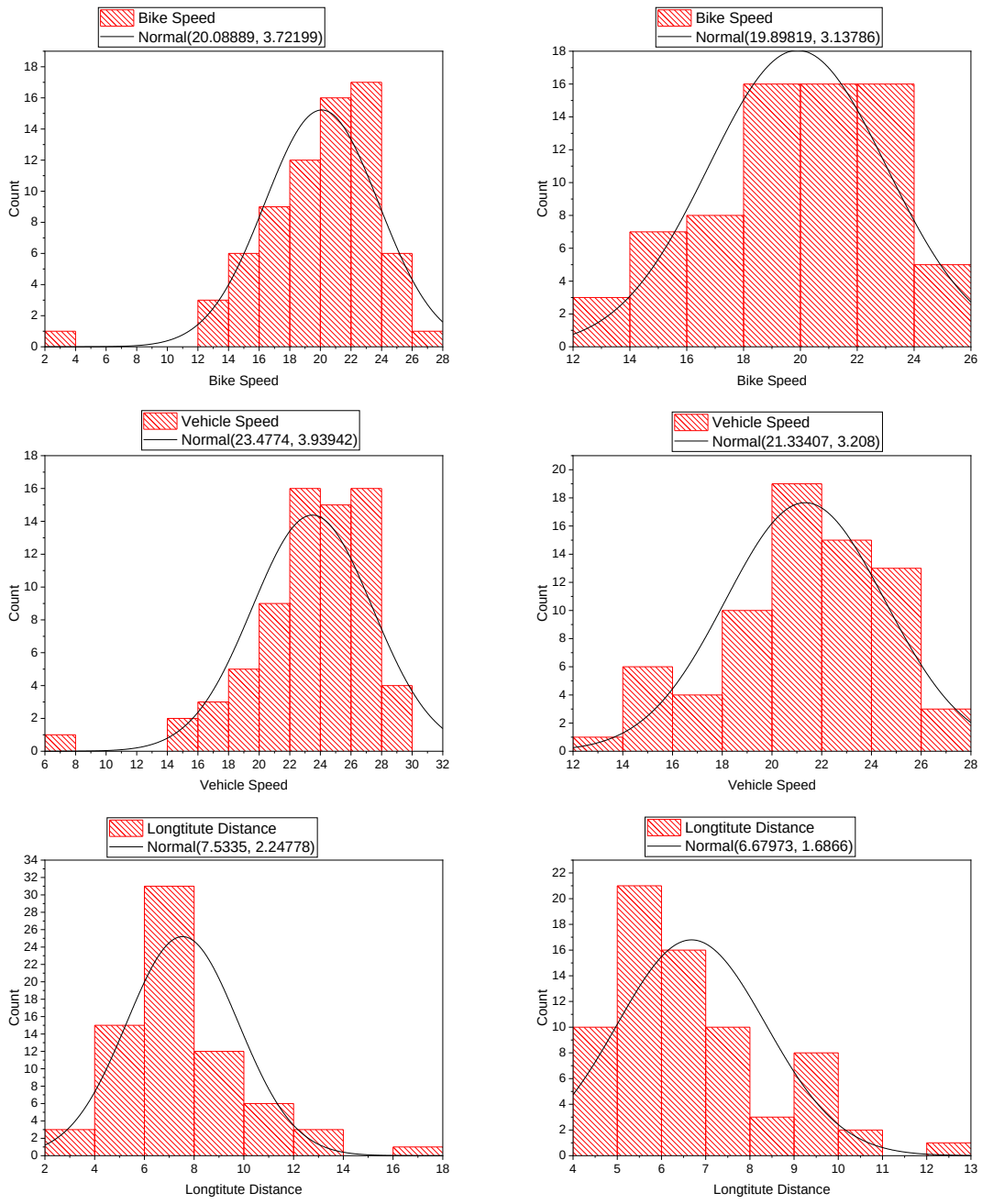

Figure 48 Vehicle, bicycle speed and longitude distance distribution in Twyckenham Drive

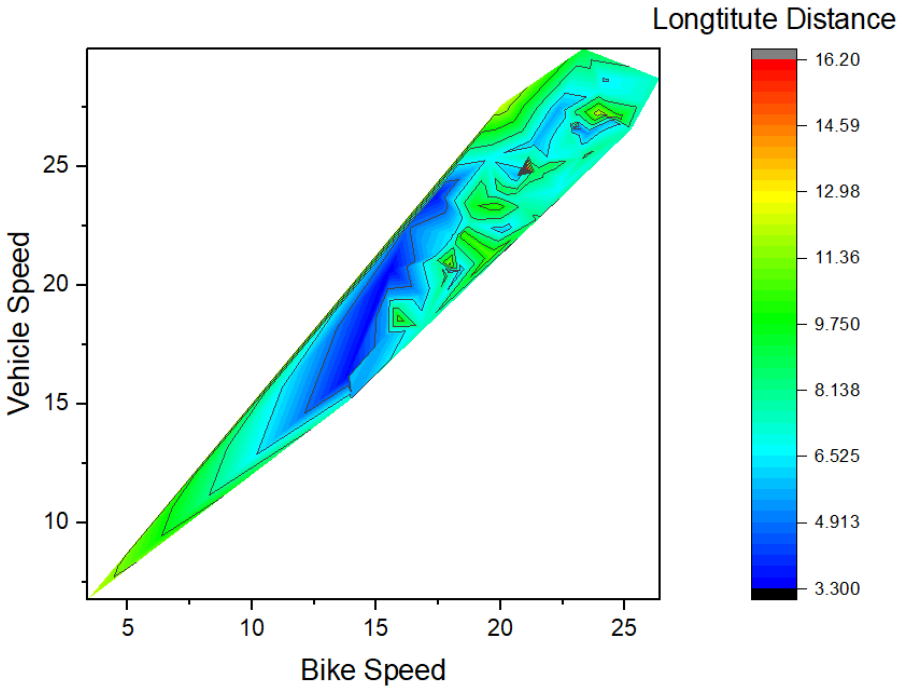

Figure 49 Maneuver analysis in approaching zone in Twyckenham Drive

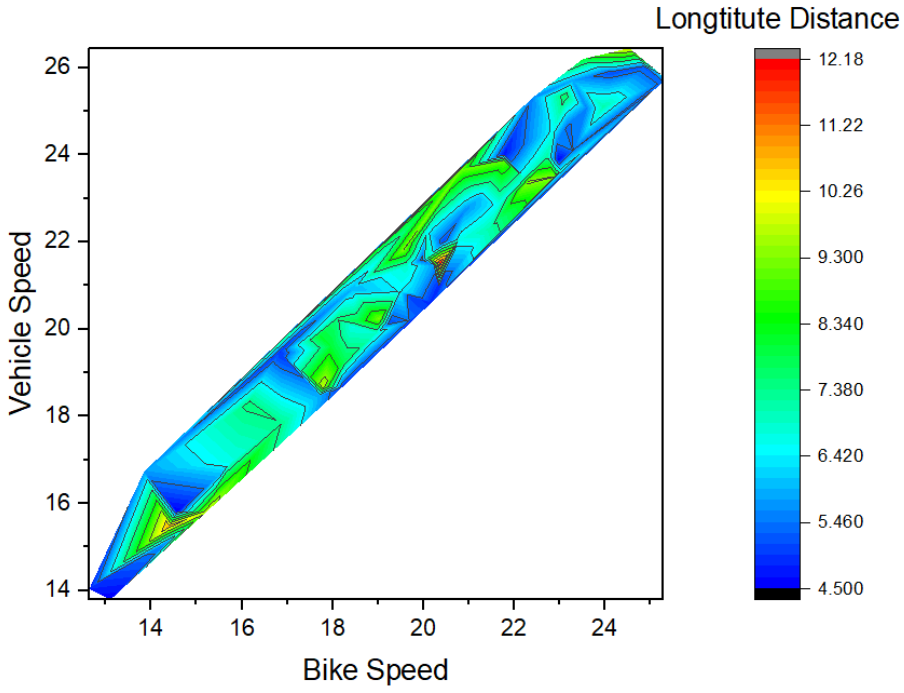

Figure 50 Maneuver analysis in the passing zone in Twyckenham Drive

South Main Street

3-lane road with no bike lane and shoulder,

The speed limit of 30 mph

Table 28 Normal data distribution in approaching zone in South Main Street

	Distribution	Parameter	Estimate	Lower 95%	Upper 95%
Bike Speed	Normal	Location mu	21.77876	21.28358	22.27394
		Scale sigma	3.36126	3.02739	3.73195
Vehicle Speed	Normal	Location mu	24.95991	24.42221	25.49761
		Scale sigma	3.64989	3.28735	4.05241
Longitude Distance	Normal	Location mu	7.21654	6.82455	7.60854
		Scale sigma	2.66082	2.39652	2.95426

Table 29 Normal data distribution in the passing zone in South Main Street

	Distribution	Parameter	Estimate	Lower 95%	Upper 95%
Bike Speed	Normal	Location mu	21.77876	21.28358	22.27394
		Scale sigma	3.36126	3.02739	3.73195
Vehicle Speed	Normal	Location mu	24.95991	24.42221	25.49761
		Scale sigma	3.64989	3.28735	4.05241
Longitude Distance	Normal	Location mu	7.21654	6.82455	7.60854
		Scale sigma	2.66082	2.39652	2.95426

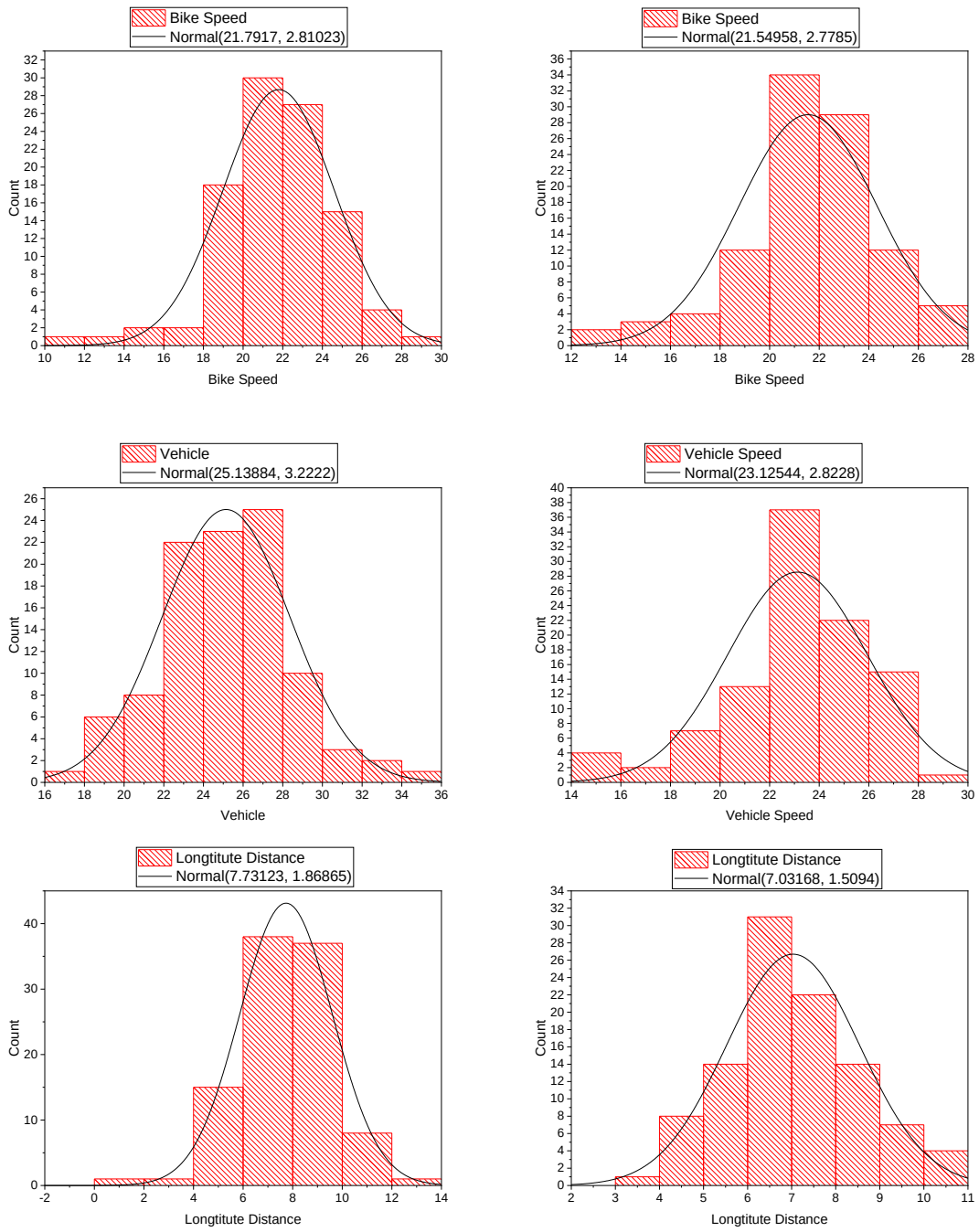

Figure 51 Vehicle, bicycle speed and longitude distance distribution in South Main Street

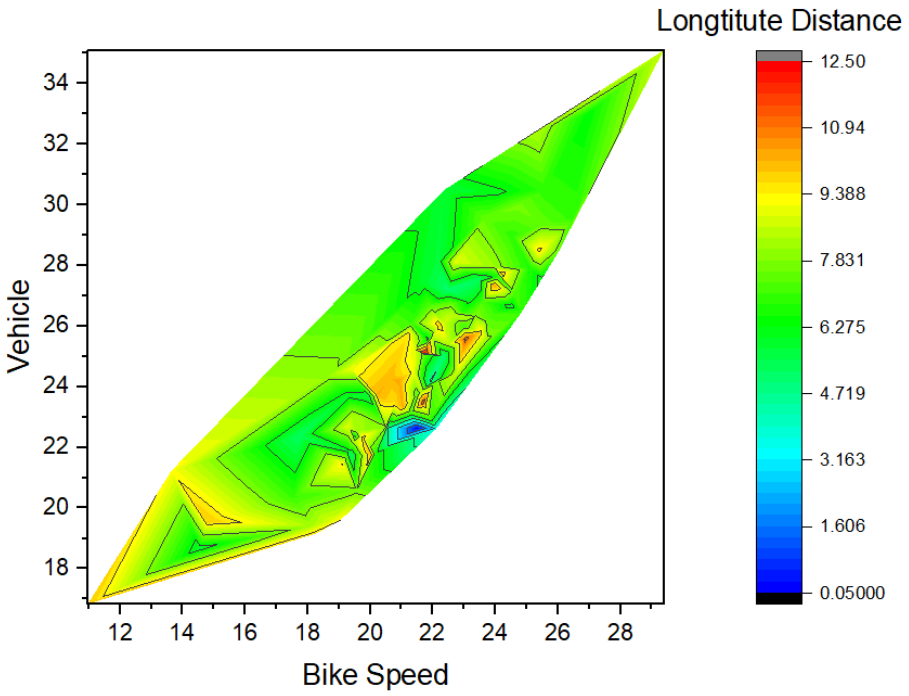

Figure 52 Maneuver analysis in approaching zone in South Main Street

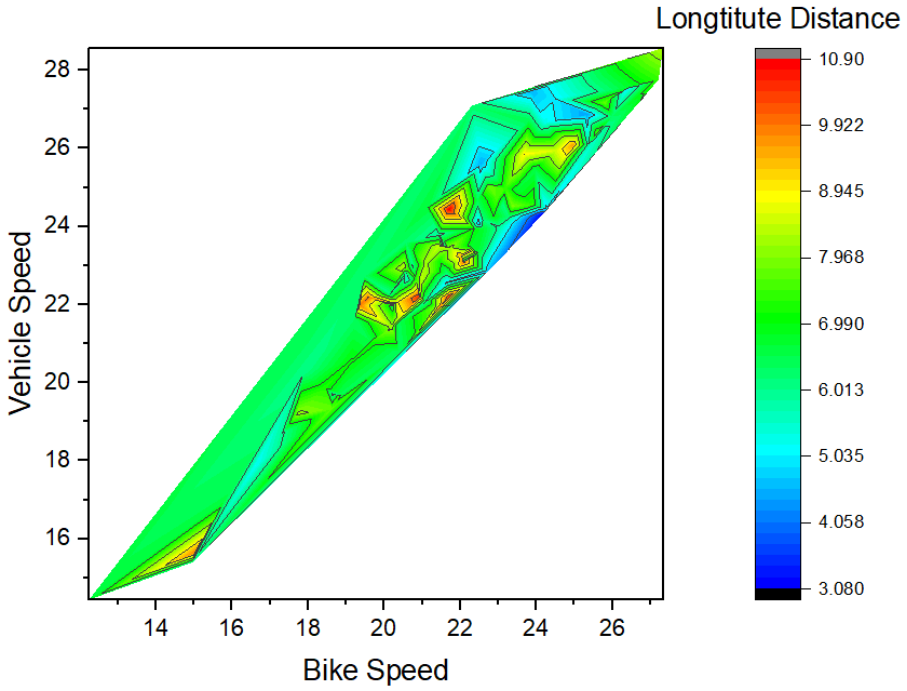

Figure 53 Maneuver analysis in the passing zone in South Main Street

B. Application and Service of Proposed Method: Trajectory Data Overview

The most significant output of the developed algorithm is trajectory extraction. Trajectories were recorded while vehicles were entering and passing the bicyclists. As it was discussed, the LiDAR record the surrounding information. The developed algorithm could extract the locations of the moving objects at certain moments, and this provides the necessary means for studying drivers and bicyclists' behavior and a safer place for both vehicle drivers and bicyclists. Trajectory detection and analysis is one of the most critical applications in smart cities. Kong (2018) mentions that one of the most critical results of trajectory analysis is understanding travel behavior. It was also illustrated that the investigation of travel behavior is complex and involves a verity of variables (Kong, Xiangjie, et al., 2018).

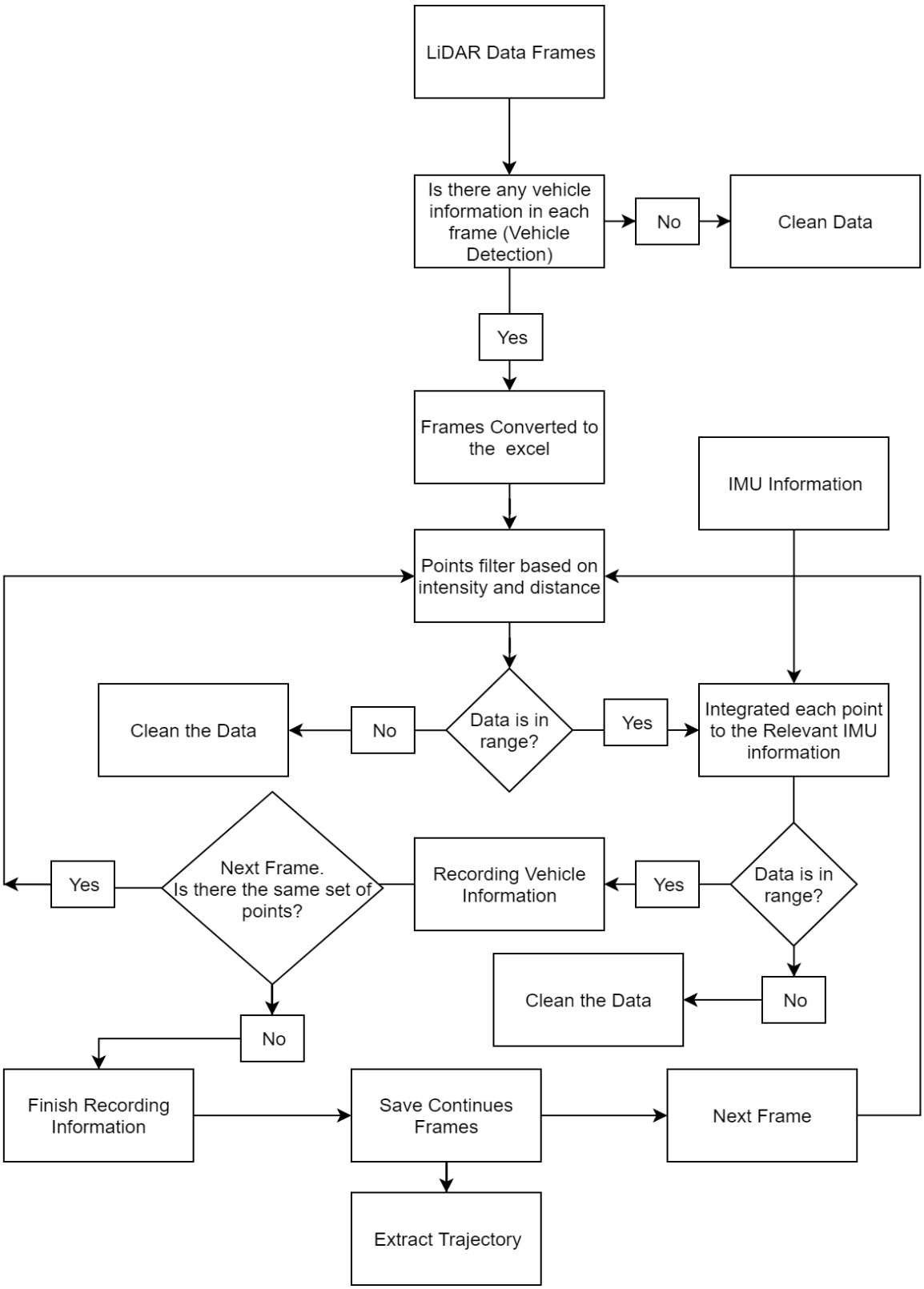

Figure 54 Trajectory extraction

C. Data Processing

Lansing, Michigan trajectories

In Lansing, a total number of 143,174 data frames (10 frames per second) were analyzed (around 239 minutes), and 378 vehicle maneuvers were detected.

The developed algorithm was applied to West and east Kalamazoo Road, Pleasant Grove Road, Cavanaugh Road, and Miler Road. Table 8 shows vehicles and bicycles' passing distance in Lansing. It should be noted that the distance was calculated based on the clearance between the bicycle handles and vehicles. Pleasant Grove Road has a 2-lane road with a bike lane and a speed limit of 35 mph, and its most recent counted Annual Average Daily Traffic (AADT) is 9300 Miller. The road has a 3-lane road with shoulder and speed limit of 30 mph, and its most recent counted Annual Average Daily Traffic (AADT) is 8800. Kalamazoo road has a 2 and 3-lane road with bike lane and shoulder and a speed limit of 25 mph, and it is most recent counted Annual Average Daily Traffic (AADT) is 14000. Cavanaugh road has a 2-lane road with no bike lane, and a speed limit of 35 mph and it is most recent counted Annual Average Daily Traffic (AADT) is 5000. 143,174 data frames and 378 vehicles were analyzed.

The following figures indicate different trajectories for different road types.

Distance Traveled: 9,287

Total Number of Elements in Point Cloud: 90,000,000

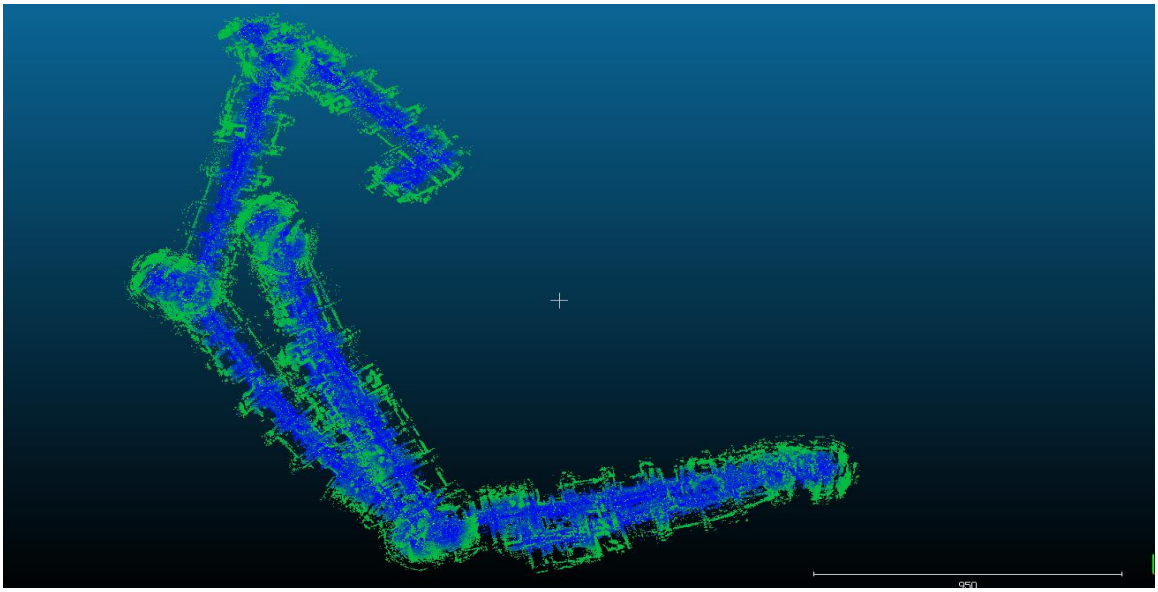

Figure 55 Bicycle trajectory in West Kalamazoo Street

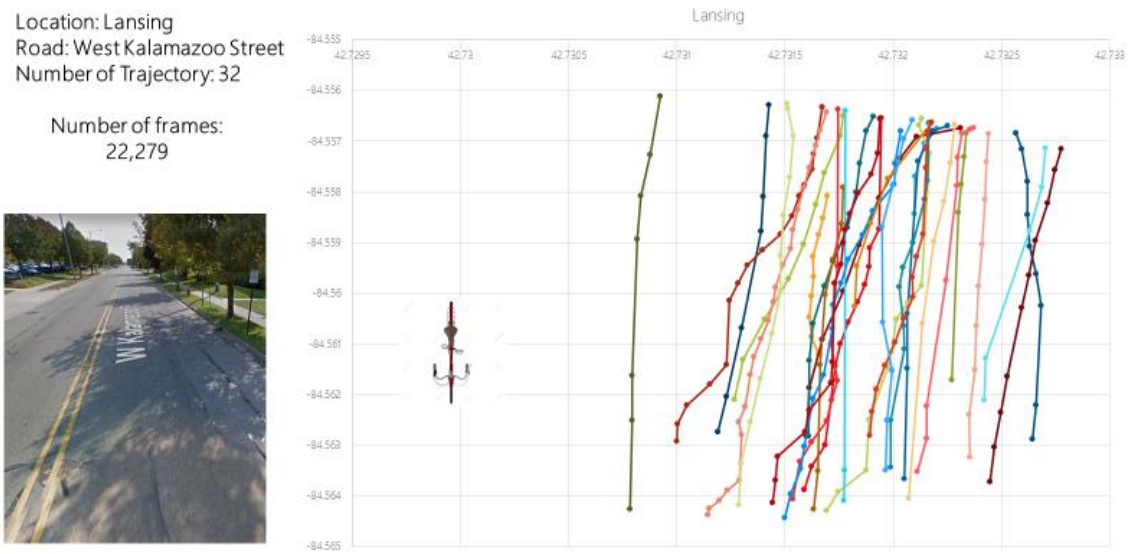

Figure 56 West Kalamazoo Street trajectories

Distance Traveled: 5,493

Total Number of Elements in Point Cloud: 90,000,000

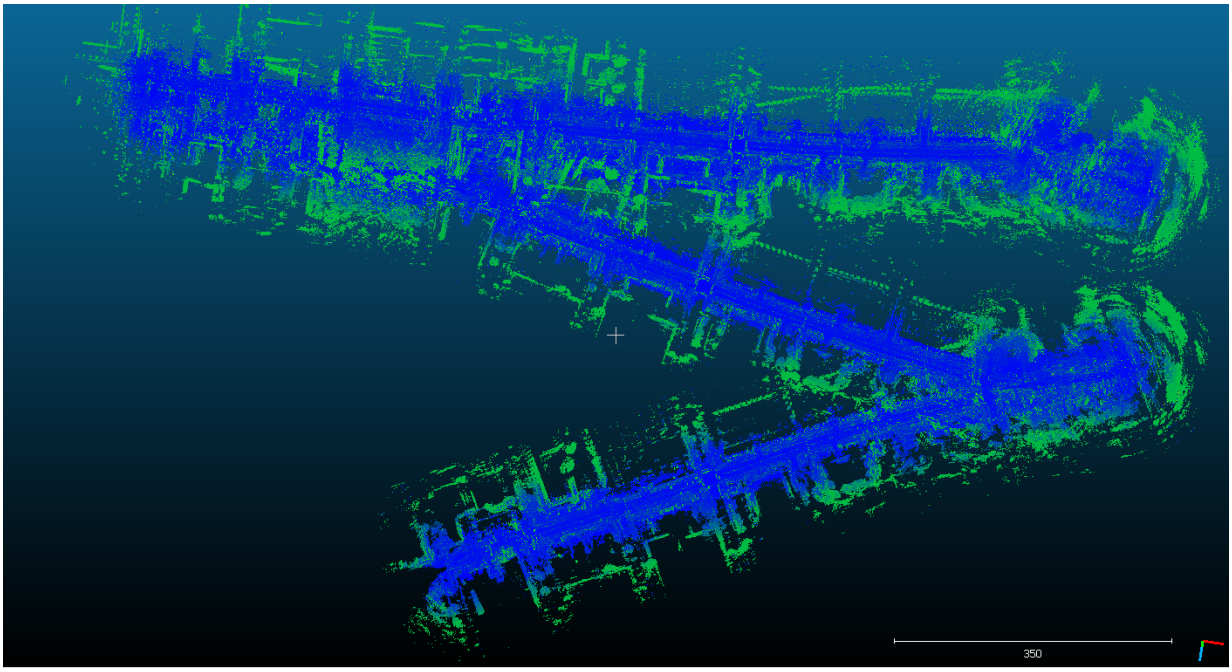

Figure 57 Bicycle trajectory in East Kalamazoo Street

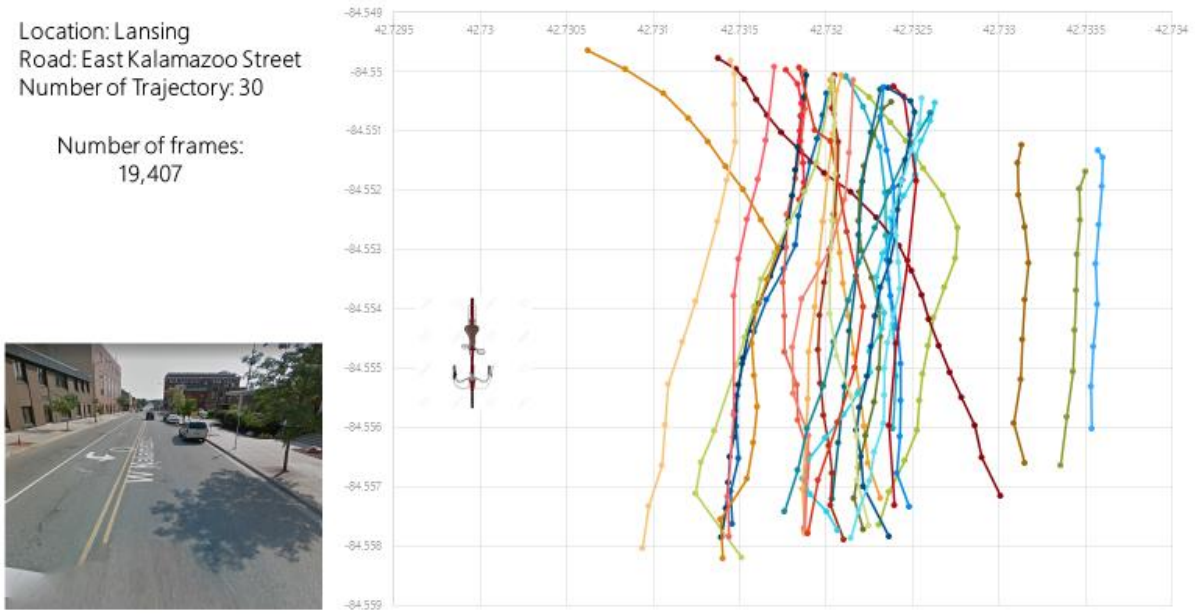

Figure 58 East Kalamazoo Street trajectories

Distance Traveled: 2,301

Total Number of Elements in Point Cloud: 48,824,125

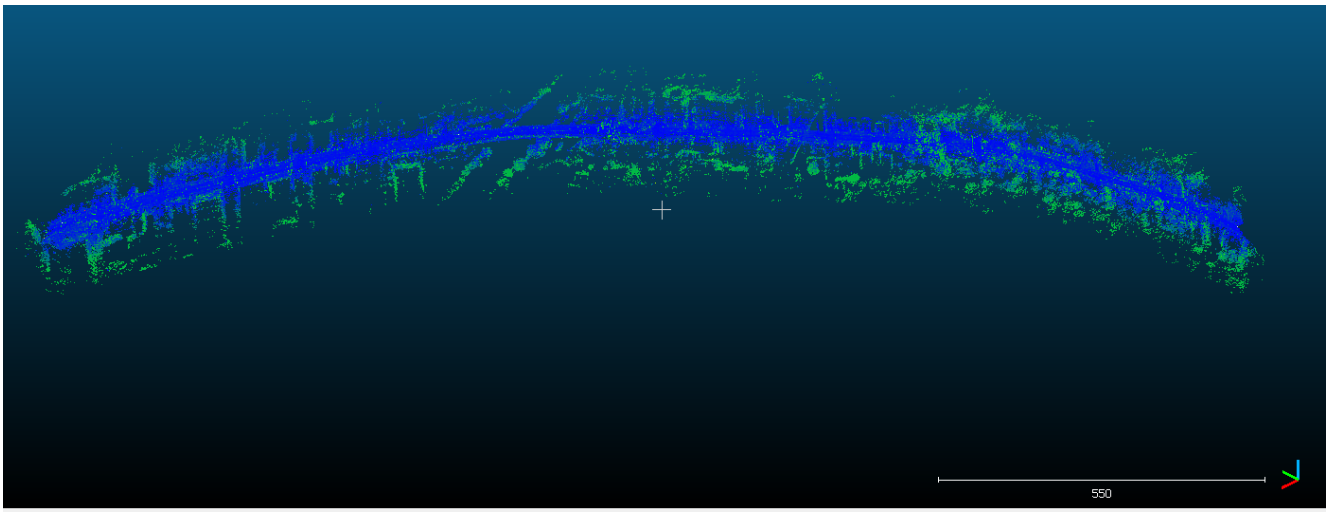

Figure 59 Bicycle trajectory in East Kalamazoo Street

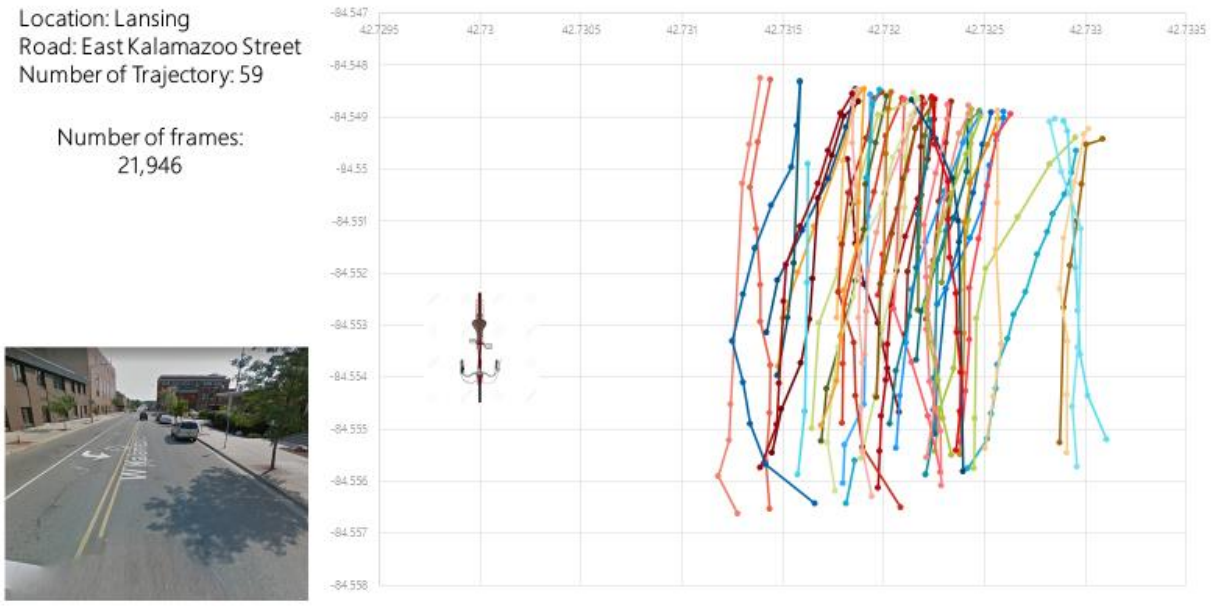

Figure 60 East Kalamazoo Street trajectories

Distance Traveled: 2,595

Total Number of Elements in Point Cloud: 24,135,150

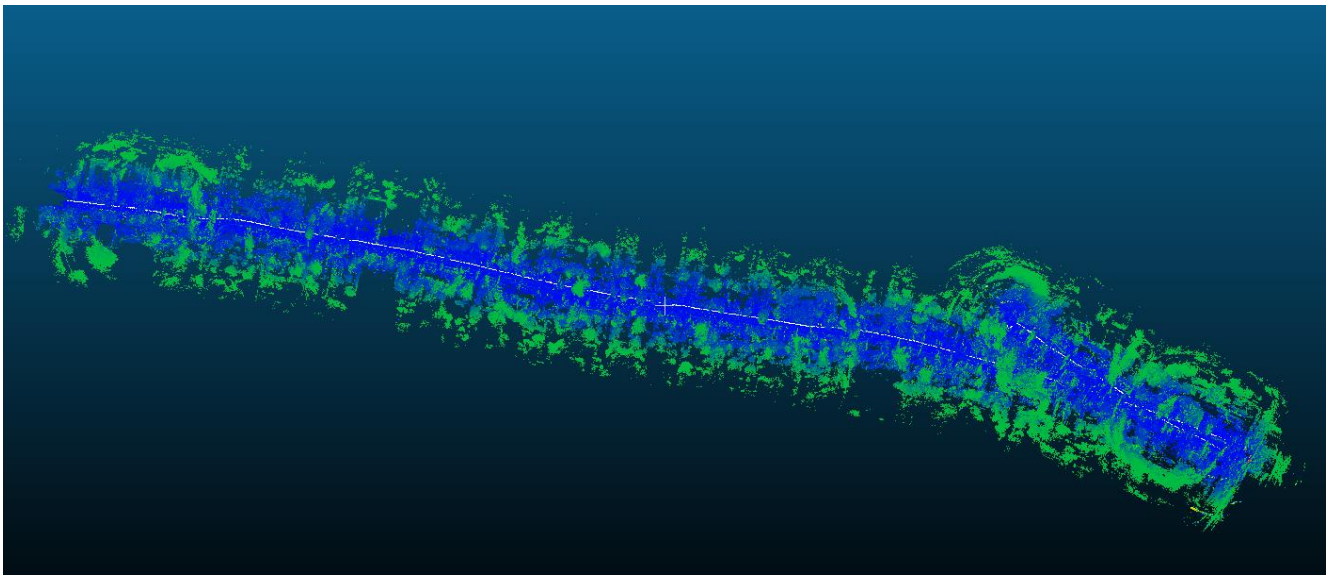

Figure 61 Bicycle trajectory in East Kalamazoo Street

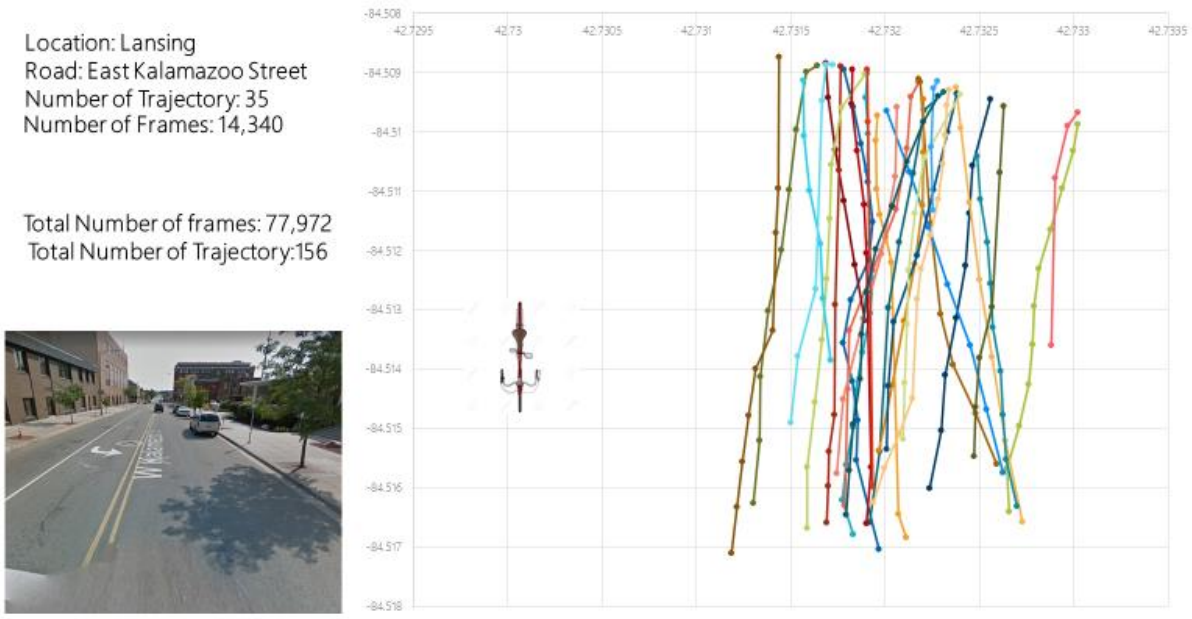

Figure 62 East Kalamazoo Street trajectories

Distance Traveled: 3,100

Total Number of Elements in Point Cloud: 72,327,613

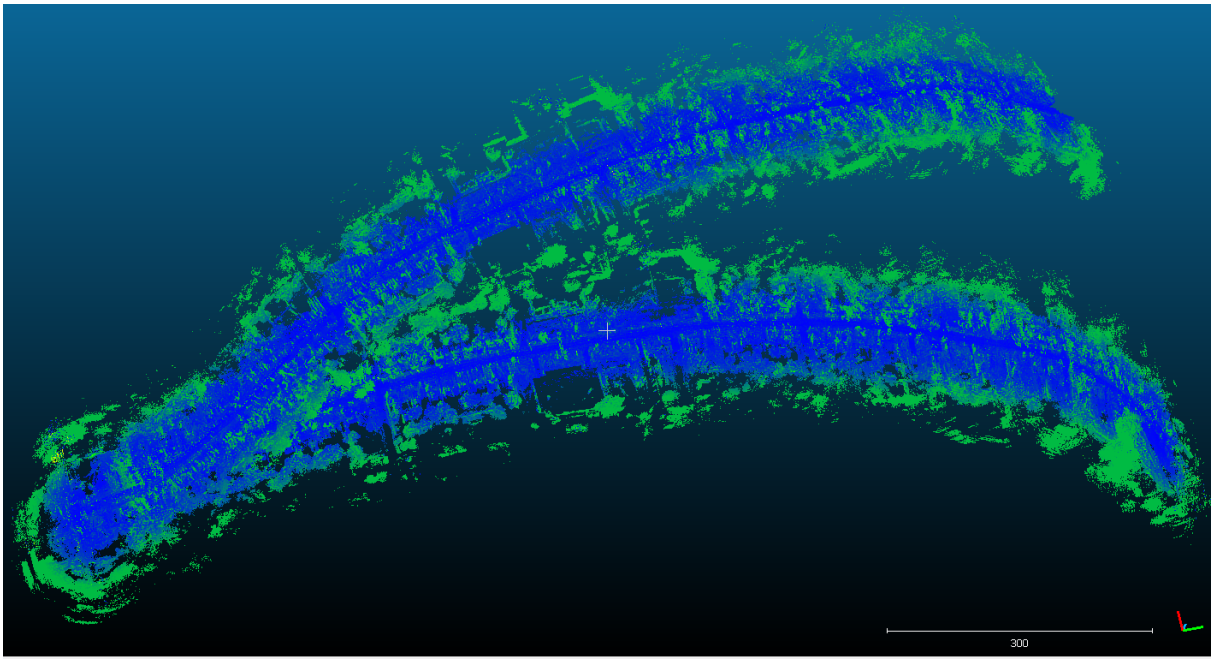

Figure 63 Bicycle trajectory in Pleasant Grove Road

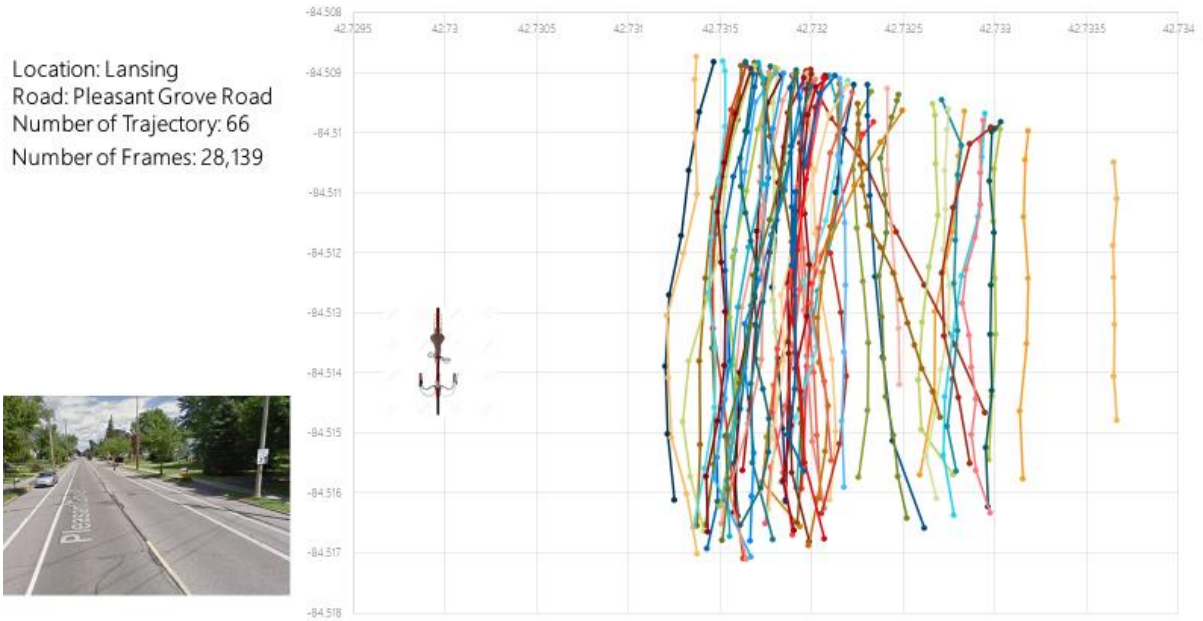

Figure 64 Pleasant Grove Road trajectories

Distance Traveled: 1,134

Total Number of Elements in Point Cloud: 28,016,644

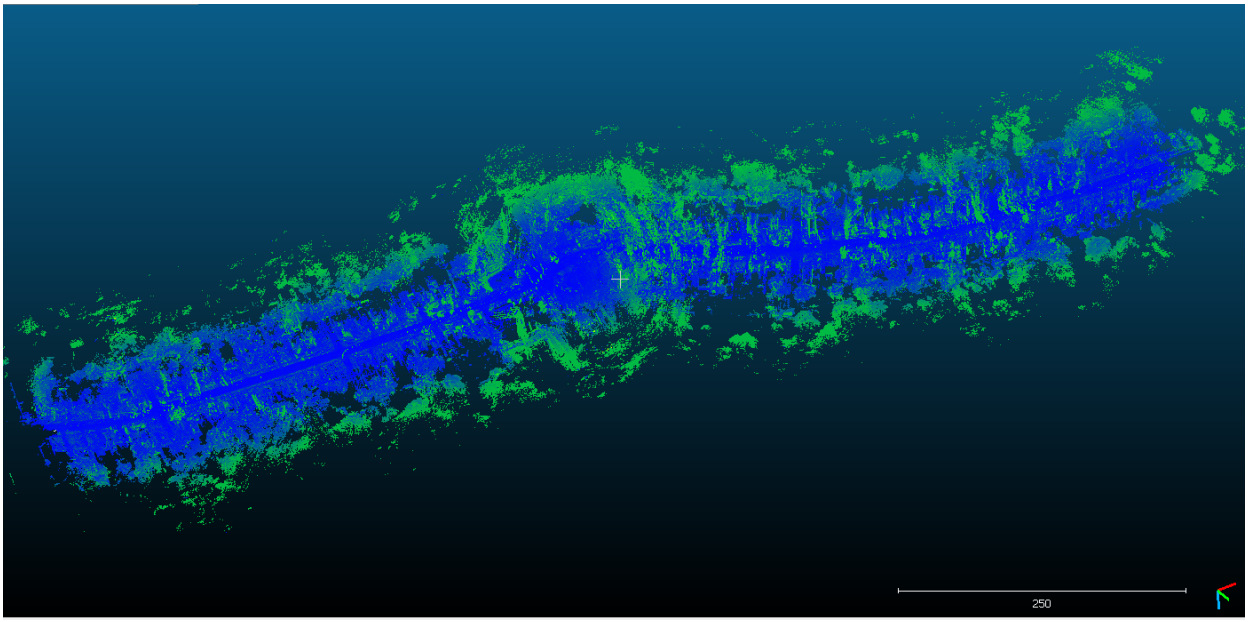

Figure 65 Bicycle trajectory in Cavanaugh Road

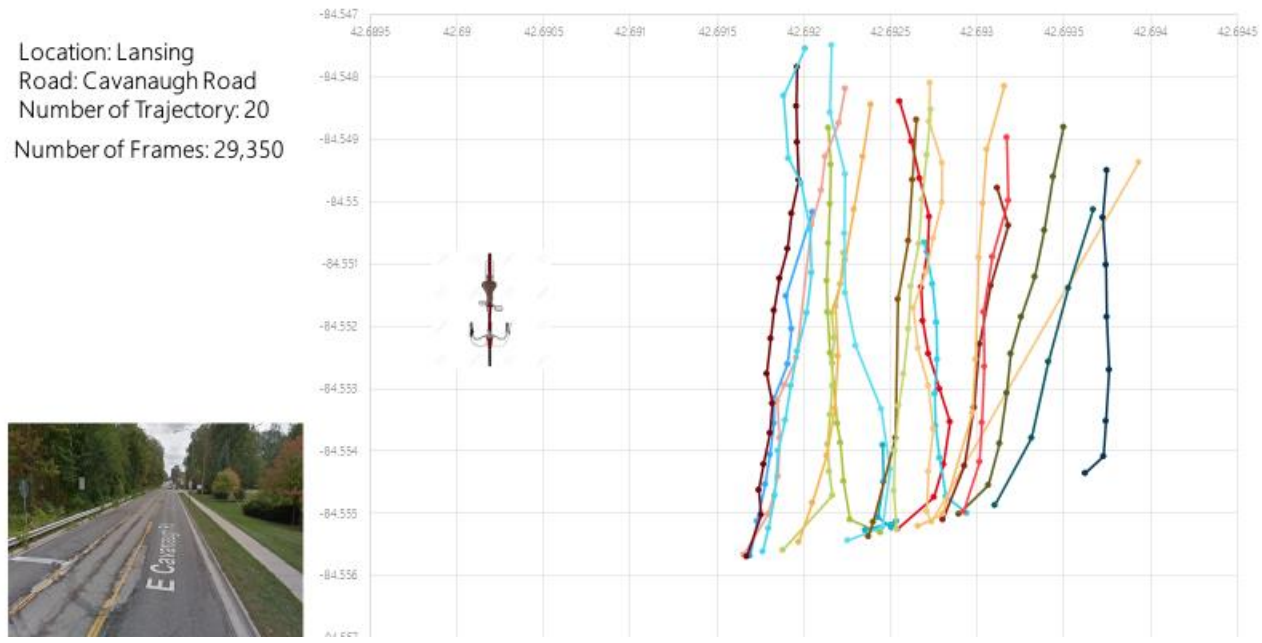

Figure 66 Cavanaugh Road trajectories

Distance Traveled: 5,183

Total Number of Elements in Point Cloud: 90,000,000

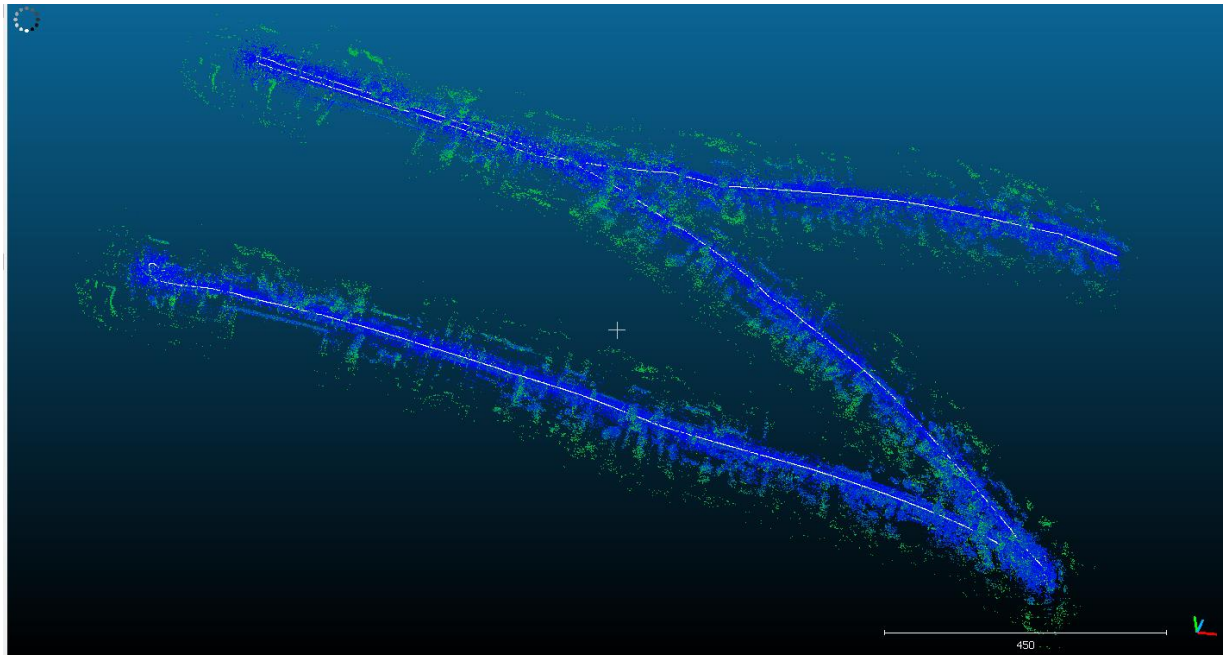

Figure 67 Bicycle trajectory in Miller Road

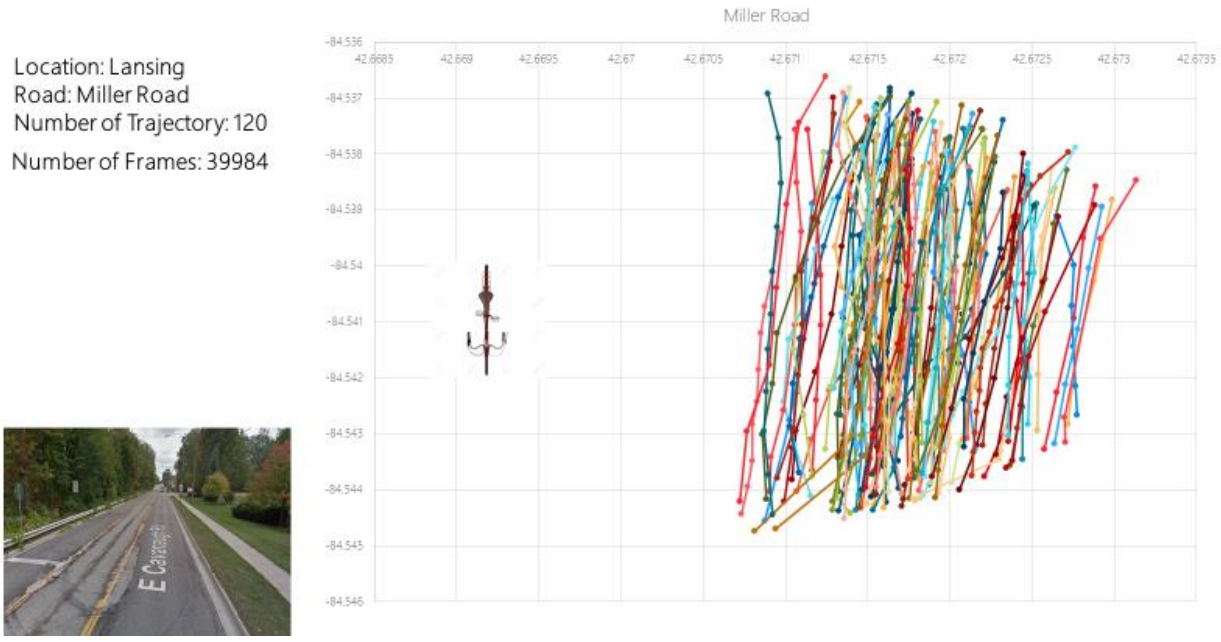

Figure 68 Miller Road trajectories

South Bend, Indiana Trajectories

In South Bend, a total number of 125,548 data frames (10 frames per second) were analyzed (around 209 minutes) for passing distance measurements, and 452 vehicle maneuvers were detected.

The developed algorithm was applied to Lincoln Way, Portage Avenue, Twyckenham Drive, and Main Street. The following figures show vehicles and bicycles' passing distance. The results are shown in Table 10. Table 10 also contains the vehicles and bicycles' passing distance information in Lansing. It should be noted that the distance was calculated based on the clearance between the bicycle handles and vehicles. Lincoln-Way has a 3-lane road with a bike lane and sharrow and a speed limit of 40 mph, and its most recent counted Annual Average Daily Traffic (AADT) is 35000. Portage Avenue has a 2-lane road with a sharrow, and no bike lane and a speed limit of 30 mph, and it's most recent counted Annual Average Daily Traffic (AADT) is 17500. Twyckenham Drive has a 2 lane road with bike lane and shoulder, and a speed limit of 30 mph and it is most recent counted Annual Average Daily Traffic (AADT) is 14500. Main Street has a 3-lane road with no bike lane and shoulder, and a speed limit of 30 mph and it is most recent counted Annual Average Daily Traffic (AADT) is 5000. 125,548 data frames and 452 vehicles were analyzed.

The following figures indicate different trajectories for different road types.

The following figures indicate different trajectories for different road types at different day times.

Distance Traveled: 6,715

Total Number of Elements in Point Cloud: 86,244,499

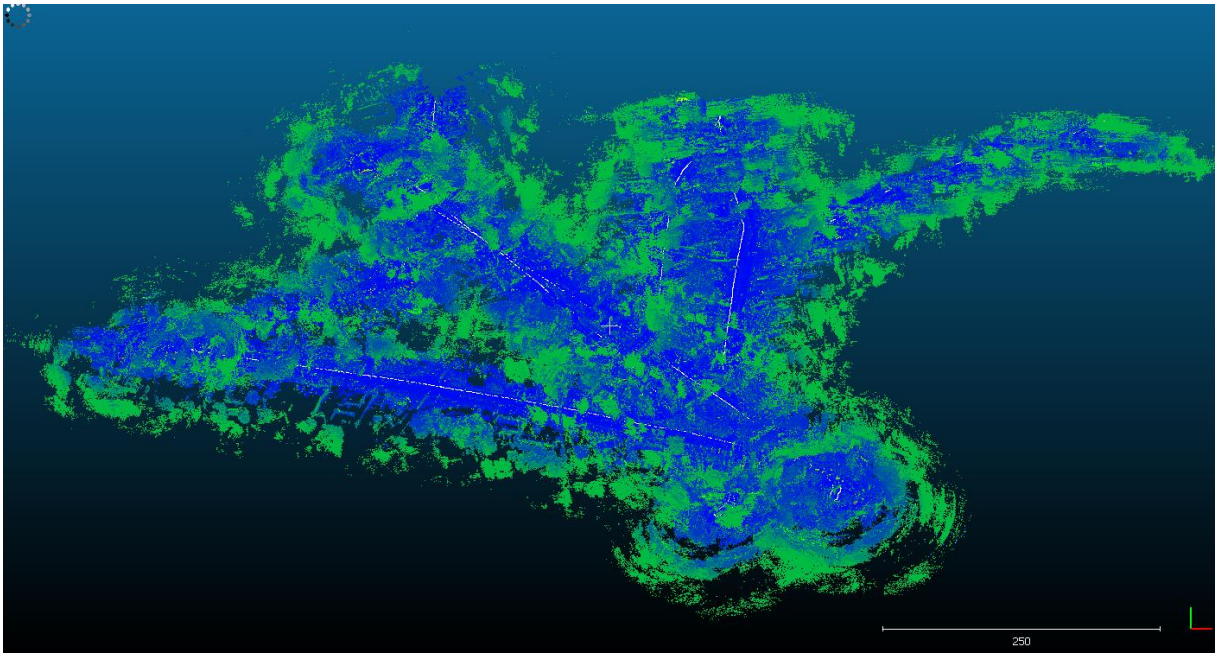

Figure 69 Bicycle trajectory in Lincoln Way

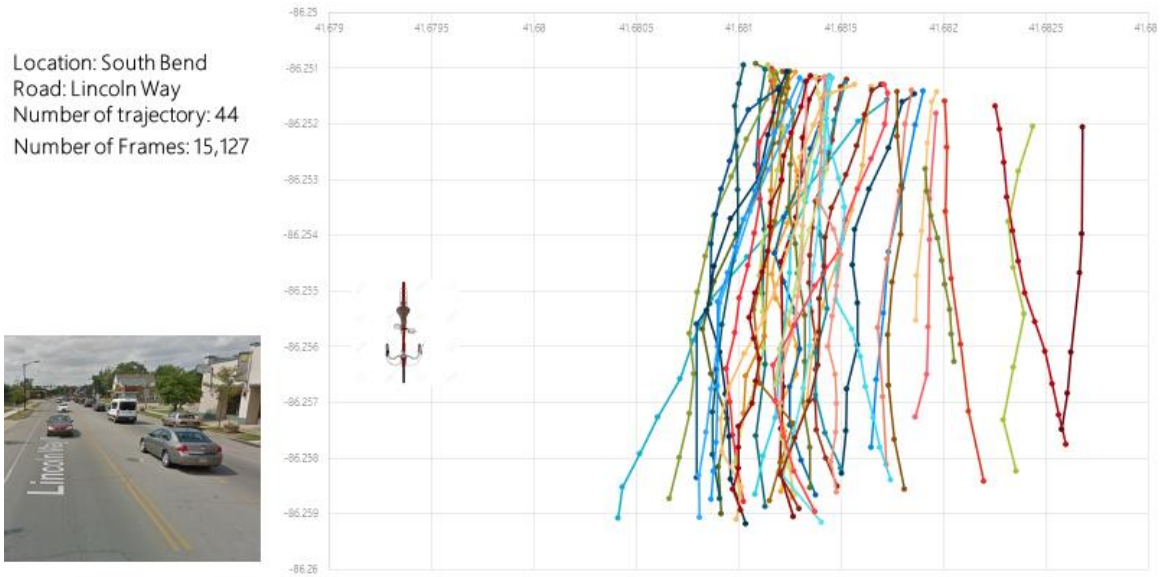

Figure 70 Lincoln-Way trajectories

Distance Traveled: 5,340

Total Number of Elements in PointCloud: 65,870,007

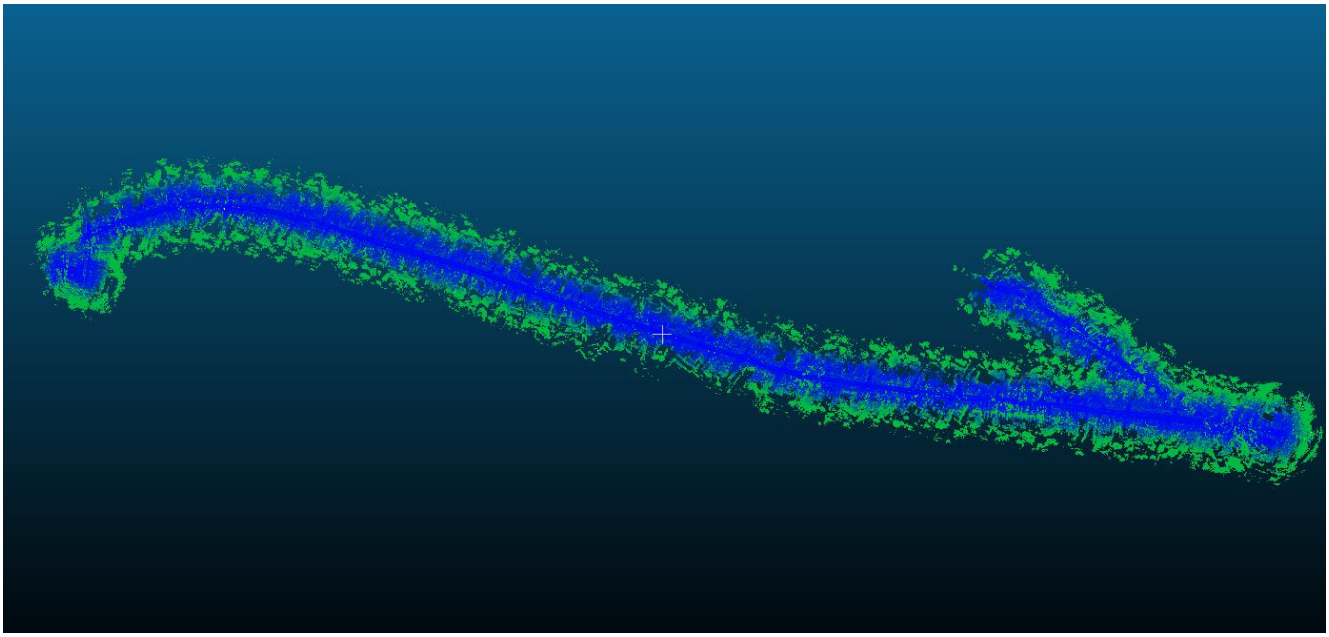

Figure 71 Bicycle trajectory in Lincoln-Way

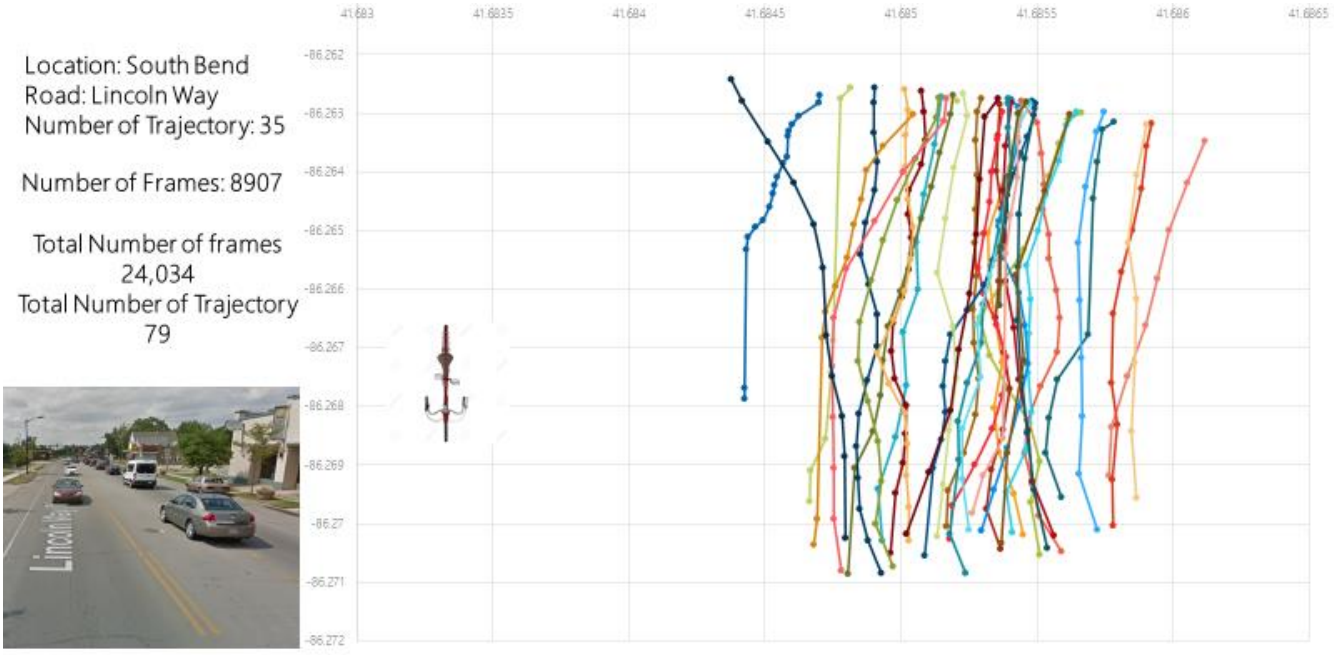

Figure 72 Lincoln-Way trajectories

Distance Traveled: 5,177

Total Number of Elements in Point Cloud: 50,837,941

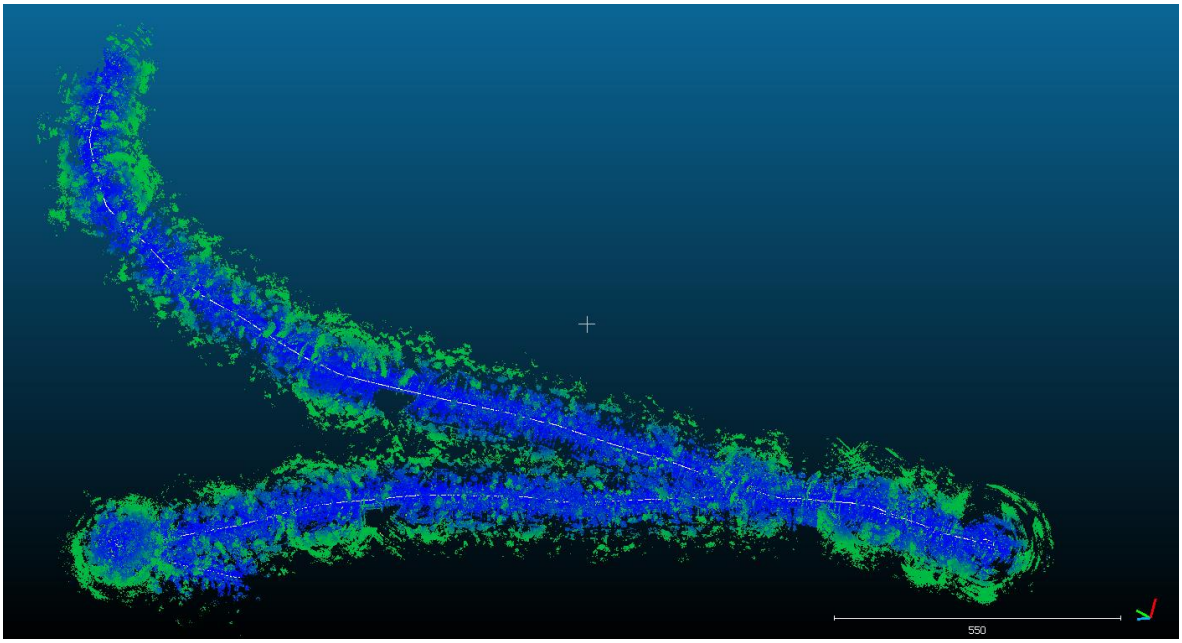

Figure 73 Bicycle trajectory in Portage Ave.

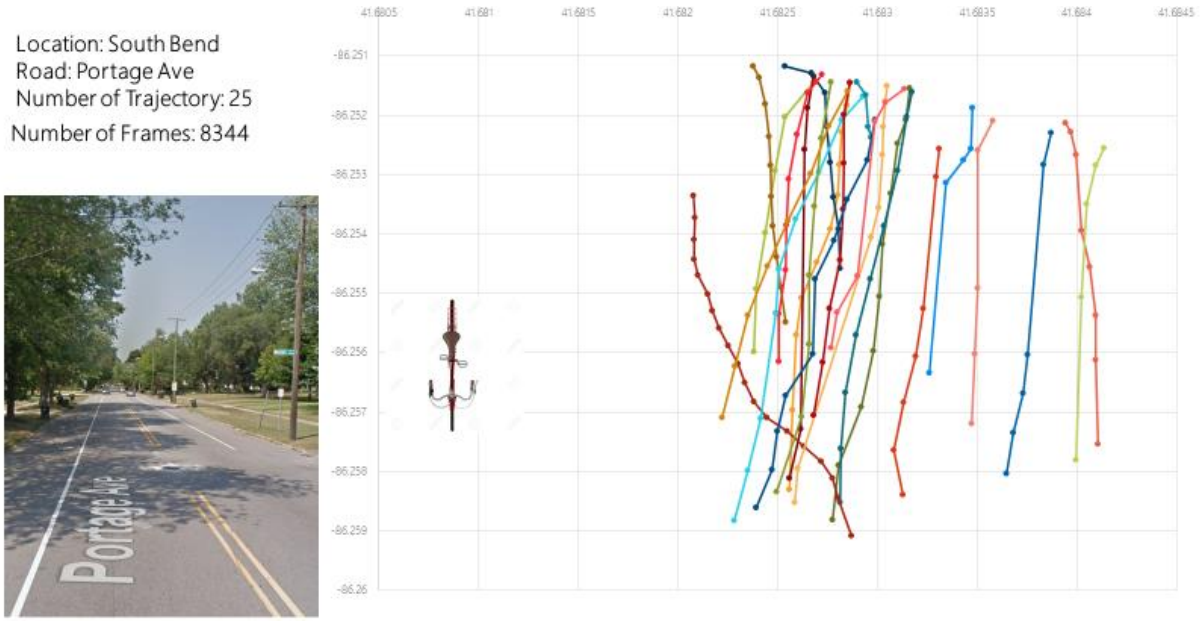

Figure 74 Portage Ave. trajectories

Distance Traveled: 7,082

Total Number of Elements in Point Cloud: 83,133,779

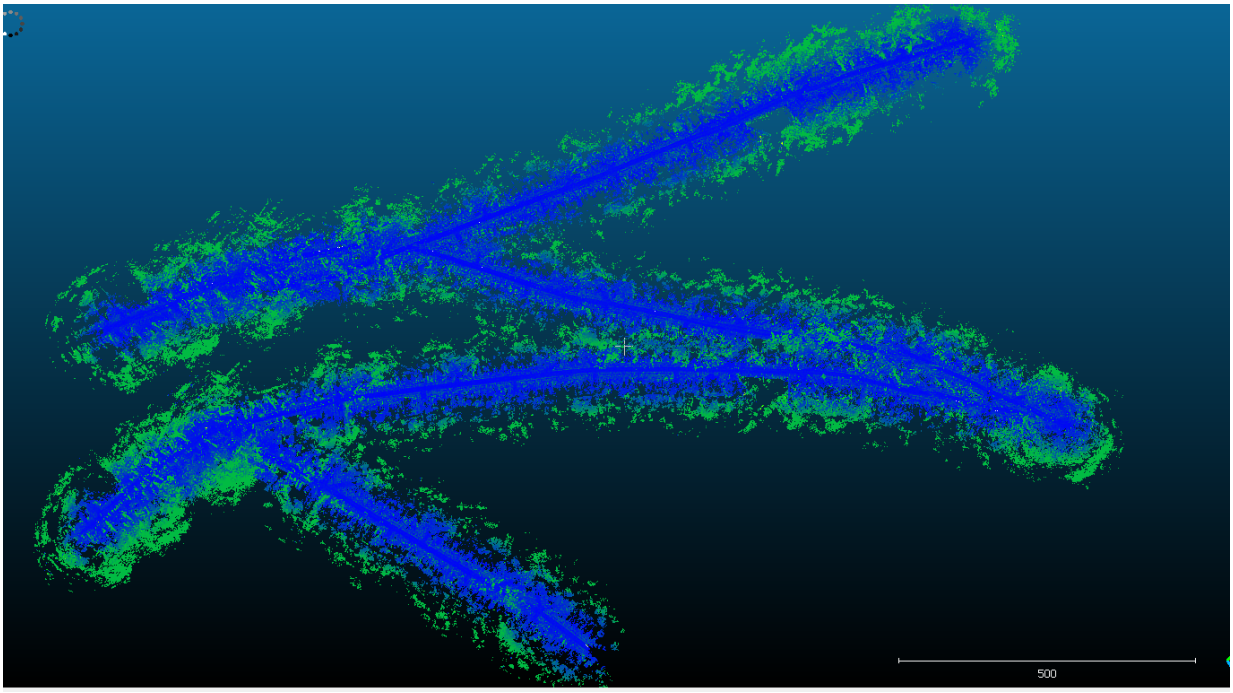

Figure 75 Bicycle trajectory in Portage Ave.

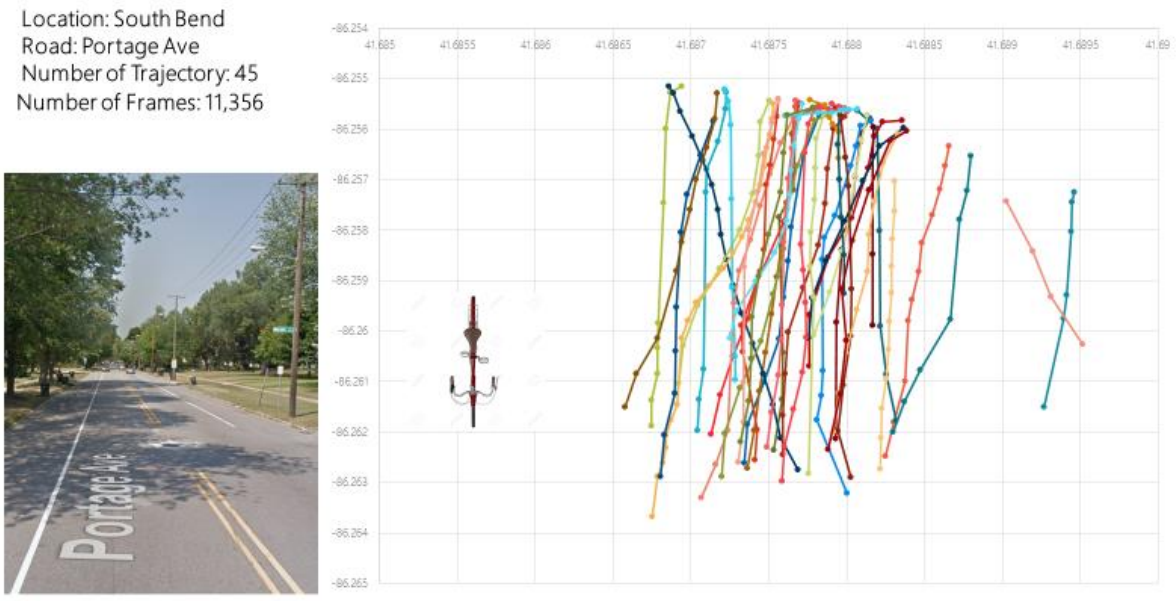

Figure 76 Portage Ave trajectories

Distance Traveled: 6,615

Total Number of Elements in PointCloud: 46,685,681

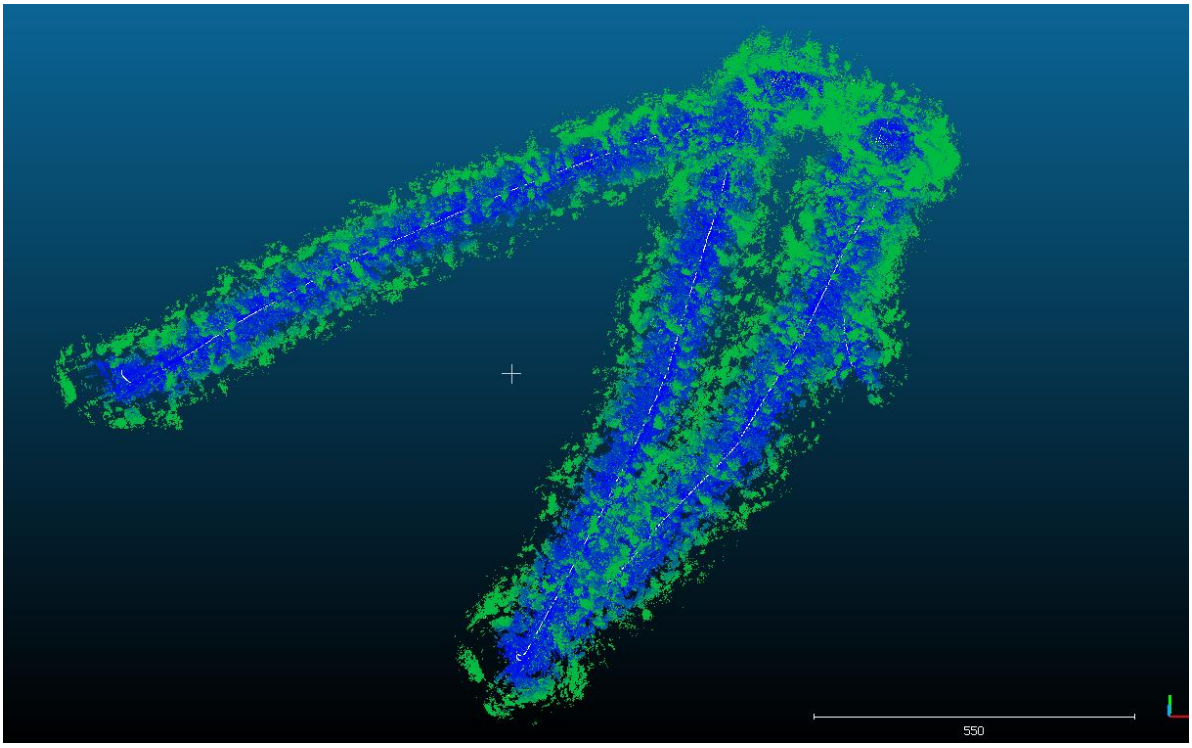

Figure 77 Bicycle trajectory in Portage Ave.

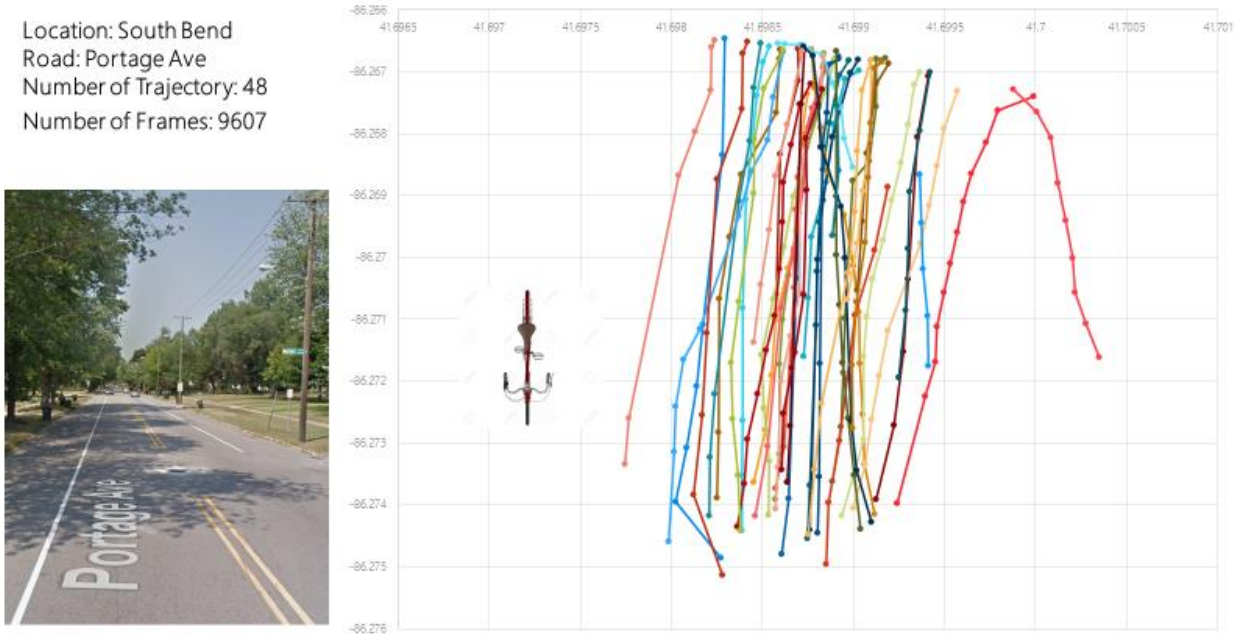

Figure 78 Portage Ave trajectories

Distance Traveled: 3,576

Total Number of Elements in PointCloud: 72,510,989

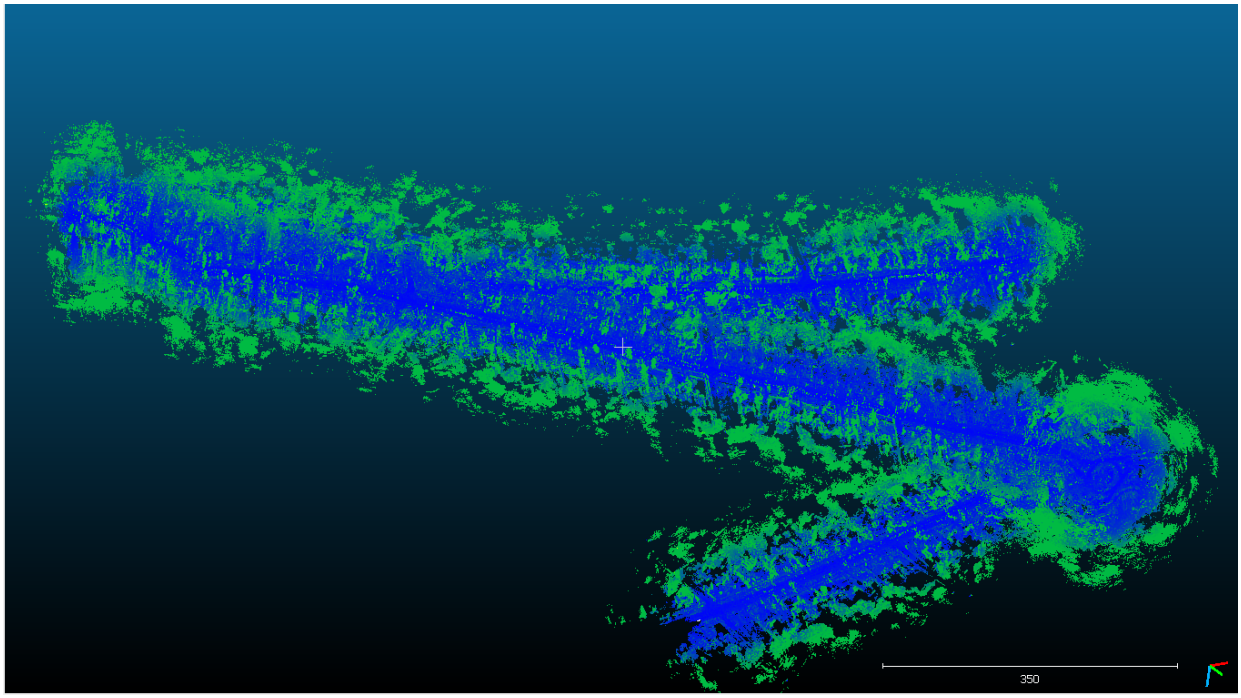

Figure 79 Bicycle trajectory in Portage Ave.

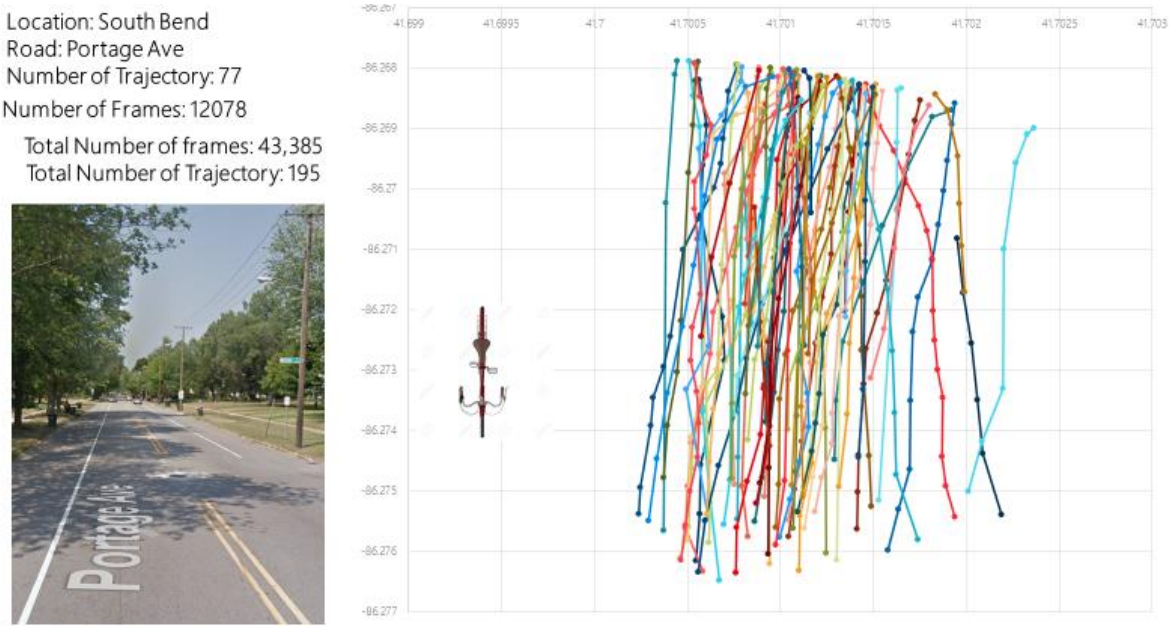

Figure 80 Portage Ave trajectories

Distance Traveled: 2,292

Total Number of Elements in PointCloud: 40,906,033

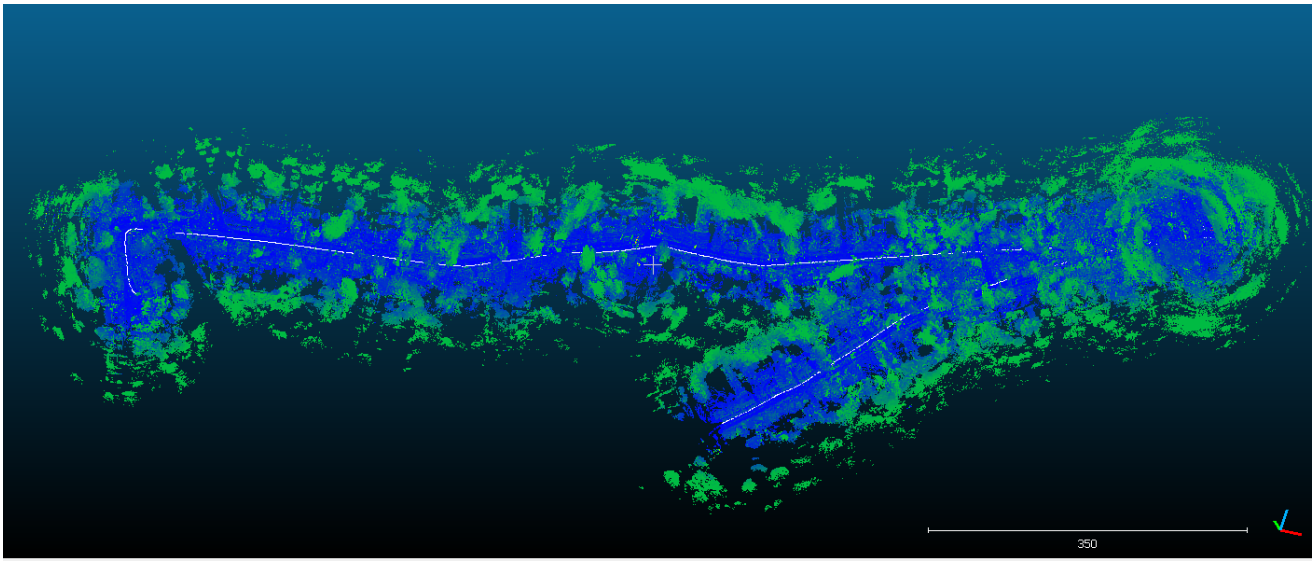

Figure 81 Bicycle trajectory in Twyckenham Drive

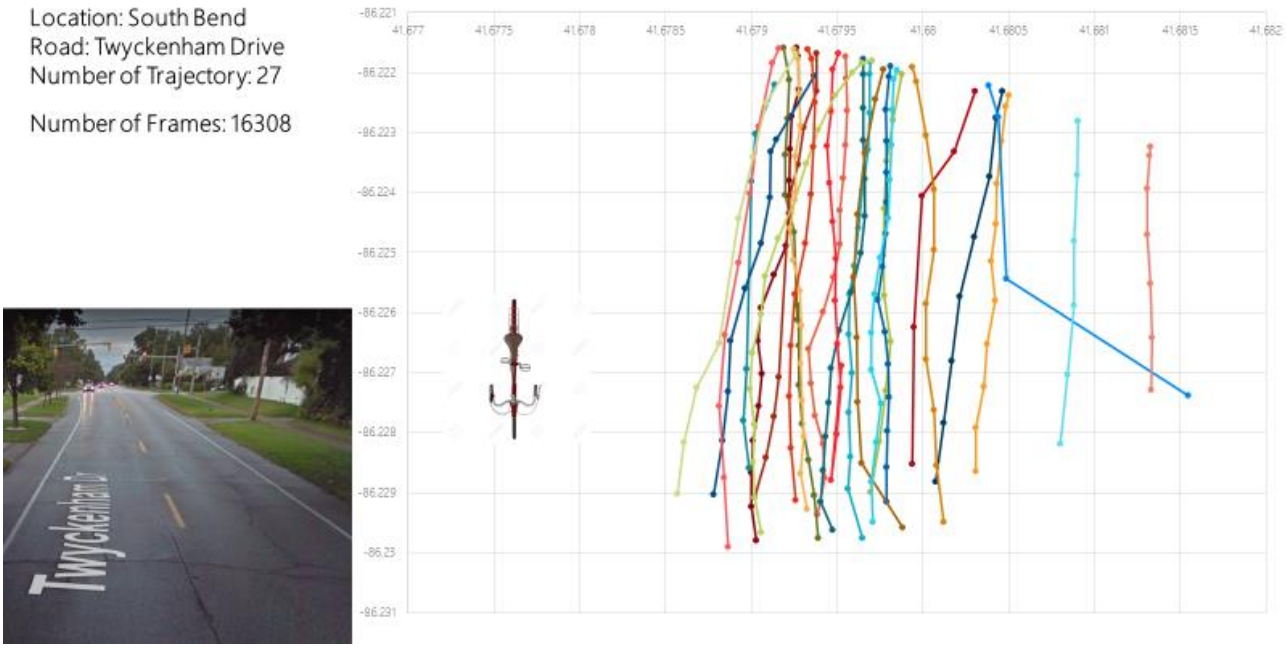

Figure 82 Twyckenham Drive trajectories

Distance Traveled: 5,518

Total Number of Elements in PointCloud: 60,903,632

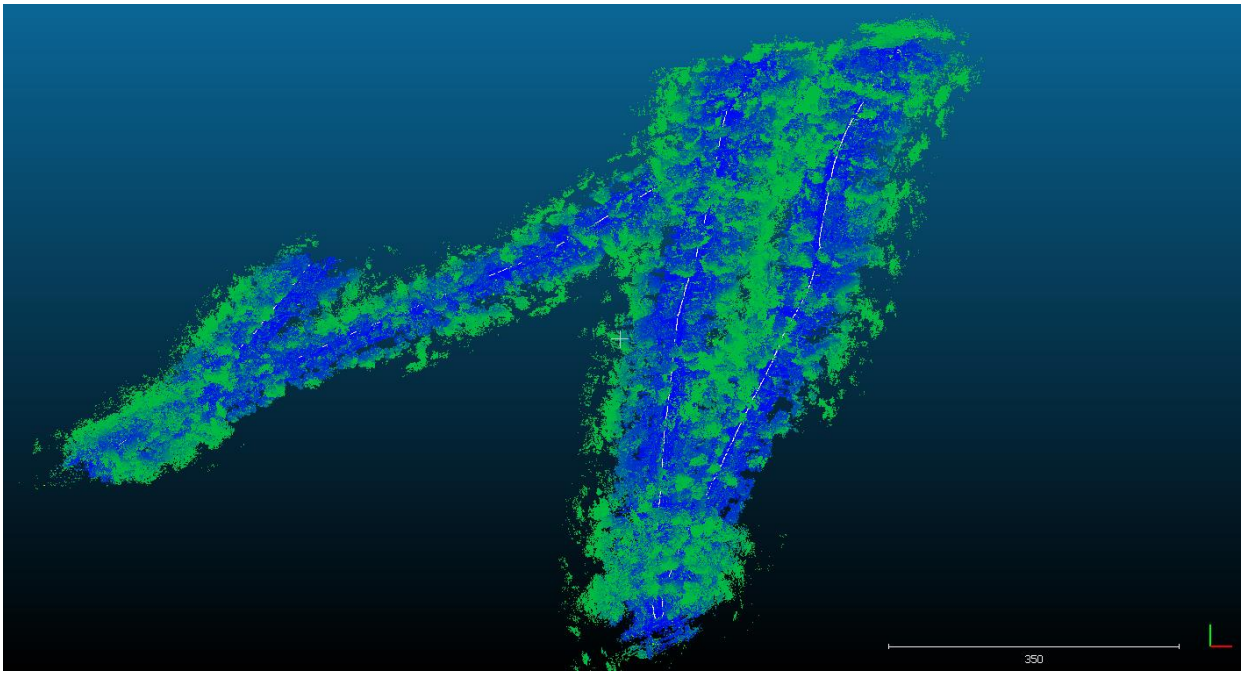

Figure 83 Bicycle trajectory in Twyckenham Drive

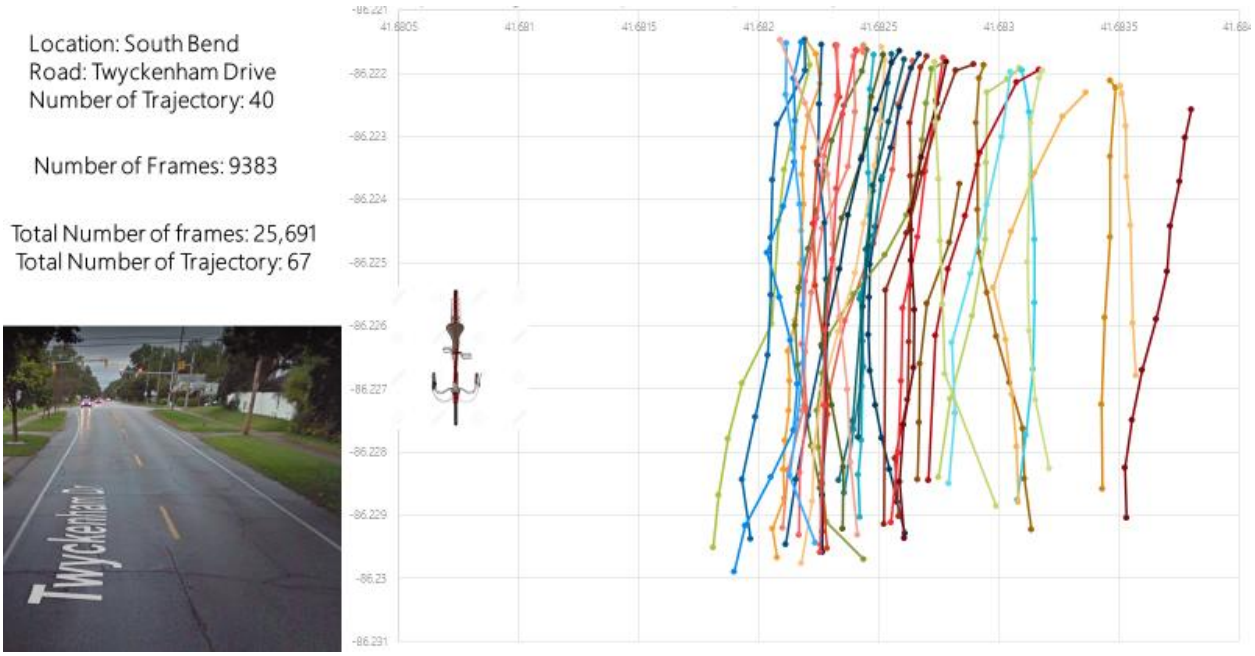

Figure 84 Twyckenham Drive trajectories

Distance Traveled: 4,474

Total Number of Elements in PointCloud: 67,702,547

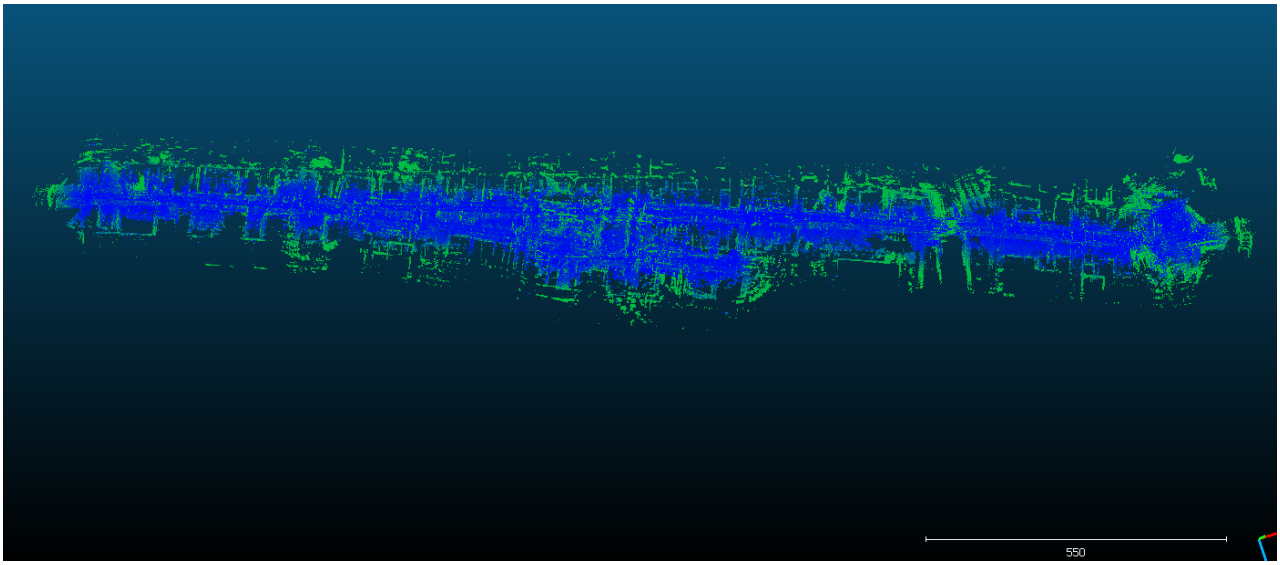

Figure 85 Bicycle trajectory in S. Main Street

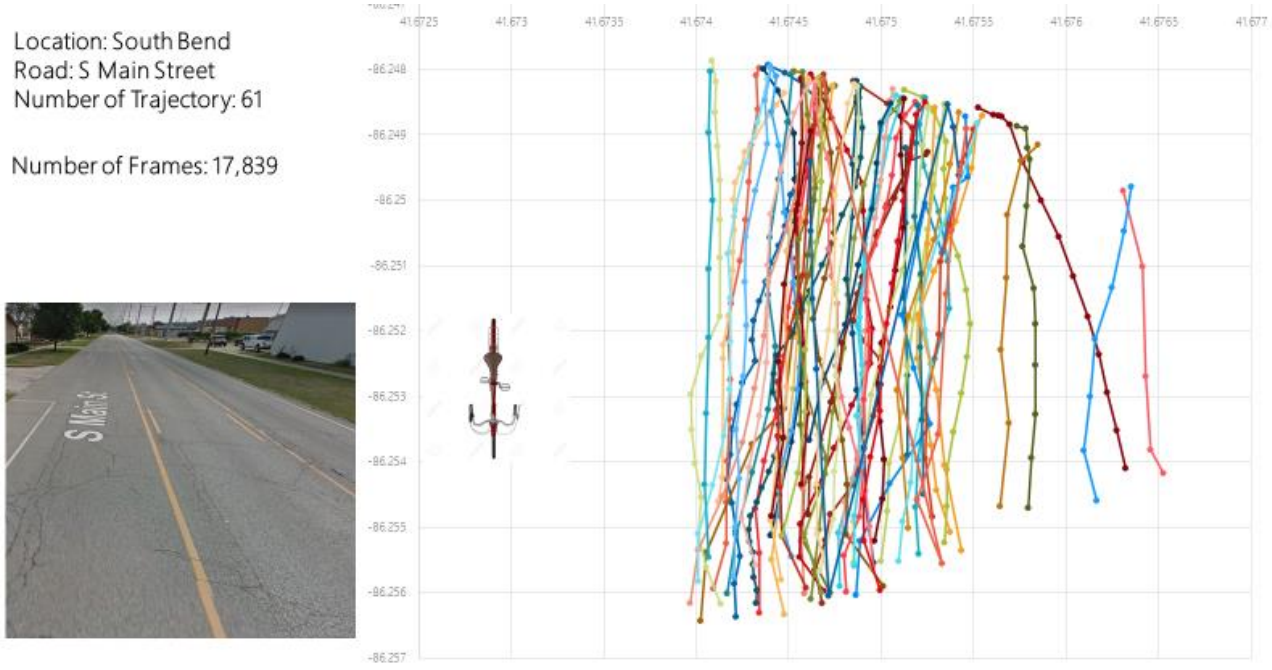

Figure 86 S. Main Street trajectories

Distance Traveled: 4,474

Total Number of Elements in PointCloud: 67,702,547

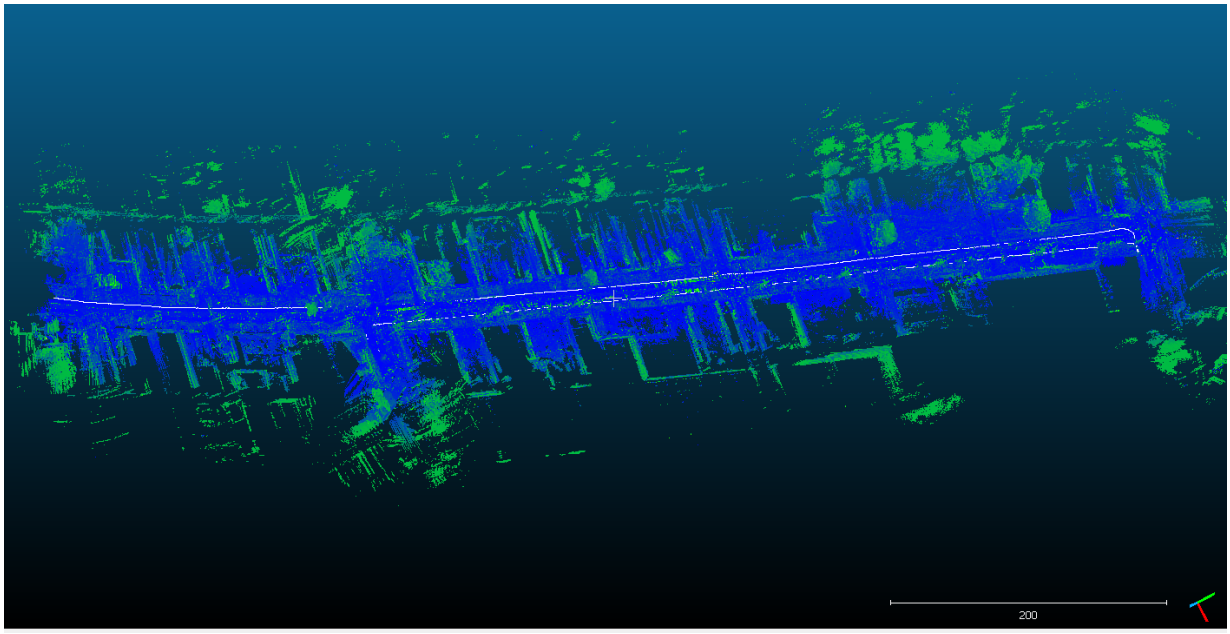

Figure 87 Bicycle trajectory in S Main Street

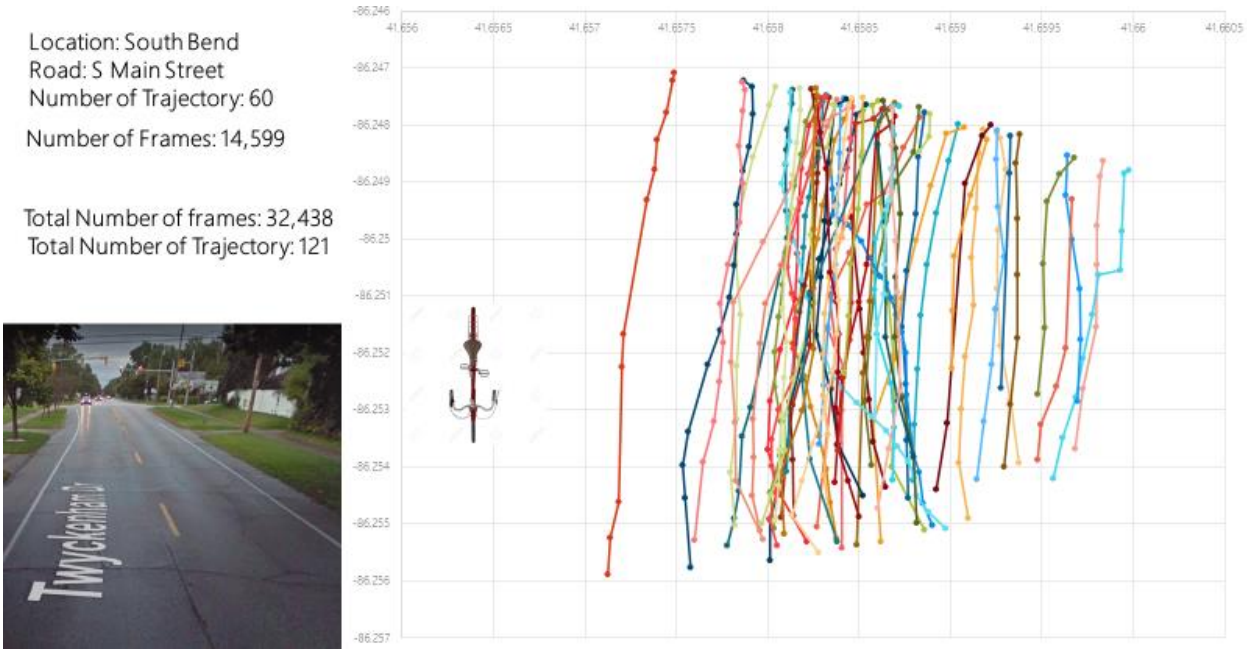

Figure 88 S Main Street trajectories